Published by
NIGERIAN SOCIETY OF PHYSICAL SCIENCES
Available online @ https://journal.nsps.org.ng/index.php/jnsps

J. Nig. Soc. Phys. Sci. 8 (2026) 3261

Journal of the Nigerian Society of Physical Sciences

Complex triple-valued neutrosophic soft sets and their topological framework with AI-driven signal-template analysis

Raed Hatamleh[a], Diana Amin Mohammad Mahmoud[b], Haitham Qawaqneh[c], Hind Y. Saleh[d], Alaa M. Abd El-latif[e], Eman Almuhur[f], Aqeedat Hussain[g], Arif Mehmood[g,*], Cris L. Armada [h,i]

[a]*Department of Mathematics, Faculty of Science, Jadara University, P.O. Box 733, Irbid 21110, Jordan*
[b]*Department of Mathematics, College of Arts and Sciences, Amman Arab University, P.O. Box 2234, Amman 11953, Jordan*
[c]*Department of Basic Science, Al-Zaytoonah University of Jordan, Amman 11733, Jordan*
[d]*Department of Mathematics, College of Education, University of Duhok, Duhok 42001, Iraq*
[e]*Department of Mathematics, College of Science, Northern Border University, Arar 91431, Saudi Arabia*
[f]*Department of Mathematics, Faculty of Science, Applied Science Private University, Amman, Jordan*
[g]*Department of Mathematics, Institute of Numerical Sciences, Gomal University, Dera Ismail Khan 29050, KPK, Pakistan*
[h]*Vietnam National University Ho Chi Minh City, Linh Trung Ward, Thu Duc City, Ho Chi Minh City, Vietnam*
[i]*Department of Applied Mathematics, Faculty of Applied Science, Ho Chi Minh City University of Technology (HCMUT), 268 Ly Thuong Kiet, Ward 14, District 10, Ho Chi Minh City, Vietnam*

Abstract

This research proposes basic operations on complex triple-valued neutrosophic soft sets (CTVNSs) and defines complex triple-valued neutrosophic soft topological spaces (CTVNSTSs) with interior and closure operators. The study also presents an application to signal-template matching using cotangent similarity. Visual comparisons of four signals (S_1–S_4) and four templates (T_1–T_4) show that T_4 is the most similar template, T_2 is the least similar, and T_1 and T_3 are moderately similar. Normalization affects dominance and makes T_1 relevant in some comparisons. Correlation analysis and clustering using principal component analysis and K-means ($K = 2$) identify one cluster (S_1, S_2, and S_3) and one outlier (S_4). These results indicate that cotangent similarity, together with data visualization and normalization, can effectively support the analysis of complex data.

DOI: 10.46481/jnsps.2026.3261

Keywords: Complex triple-valued neutrosophic soft sets, Complex triple-valued neutrosophic soft topology, Cotangent similarity measures Data visualization techniques.

Article History:
Received: 06 January 2026
Received in revised form: 27 April 2026
Accepted for publication: 20 May 2026
Available online: 22 June 2026

Communicated by: B. J. Falaye

1. Introduction

One of the challenges in mathematics, computer science and engineering has been modeling uncertainty. Conventional binary logic cannot very easily reflect the imprecision of reality. To solve this, Zadeh [1] came up with fuzzy set theory where the membership of an element to a set has a degree of membership between 0 and 1 thus formalizing the concept of partial truth. Turksen [2] introduced interval-valued fuzzy sets based on normal forms. Going a step further, Atanassov [3] created intuitionistic fuzzy sets (IFSs), that include a degree of

*Corresponding author Tel. No.: 03335445510;
Email address: mehdaniyal@gmail.com (Arif Mehmood)

membership and a degree of non-membership, whose sum is less than or equal to one, thereby enabling explicit hesitation. Based on this, Atanassov and Gargov [4] proposed interval-valued intuitionistic fuzzy sets (IVIFSs), in which membership and non-membership are interval-valued, which provides more flexibility in modeling incomplete information. Smarandache [5] suggested a more abstract framework in which each element was specified by three independent membership functions: truth (T), indeterminacy (I), and falsity (F), defined on the non-standard interval $]^{-}0, 1^{+}[$. This is an expansion of fuzzy and classical set theories that specifically takes into account the existence of ambiguous, inconsistent, and incomplete data. Lupianez [6] subsequently studied the topology of neutrosophic sets, making neutrosophic topology a new area of point-set topology. To apply to real-world computational problems, Wang *et al.* [7] specified single-valued neutrosophic sets (SVNSs), with T, I, F being ordinary real numbers in [0,1], which allows direct application of neutrosophic theory to engineering and decision-making. This was later generalized by Wang and others [8] to interval neutrosophic sets (INSs) with each element being an interval, with a possibility of uncertainty, indeterminacy, and falsity at the same time. Comparing these sets, Broumi and Smarandache [9] came up with the cosine similarity of INSs and Broumi and Smarandache [10] came up with new measures of distance and similarity, which were tested numerically. Ye [11] added more measures of similarities to INSs and showed how they can be used in multi-criteria decision-making (MCDM). To supplement this, Broumi and Smarandache [12] defined a correlation coefficient of INSs and made comparisons of the results statistically. Majumdar and Samanta [13] concentrated on similarity and entropy of neutrosophic sets, and their connection to information theory and neutrosophic uncertainty.

Chen [14] and Chen *et al.* [15] independently created new methods of fuzzy decision making based on similarity measures and made comparisons between similarity measures respectively, both of which later inspired neutrosophic decision methods. In the meantime, a completely new way of treating uncertainty was launched by Molodtsov [16]: soft set theory that models the universe of discourse by a set of parameters, providing a parameterized description without membership functions. As an extension of Molodtsov's soft set theory, Aktas and Cagman [17] proposed soft groups to analyze group-theoretic structures and Babitha and Sunil [18] defined soft set relations and functions and provided a categorical background. Chen *et al.* [19] observed the significance of reductions in parameterization to prevent redundant parameters and Chen *et al.* [20] extended this to a systematic reduction approach with applications. In decision-making, Cagman and Enginoglu [21] suggested the uni-int decision-making approach that uses soft sets and Feng *et al.* [22] suggested an adjustable approach of fuzzy soft set based decision-making. Lately, Roy and Maji [23] proposed the theory of fuzzy soft set in decision making and Singh and Mantri [24] used soft set in clinical diagnosis which showed that fuzzy soft set has some applications in real world. The hybrid models came up as obvious combinations of the benefits of different paradigms. Ahmad and Kharal [25] defined fuzzy soft sets (FSSs) by an intersection of fuzzy sets and soft sets, and Tripathy et al. [26] added intuitionistic fuzzy soft sets (IFSSs). Maji *et al.* [27] reconsidered also the soft set theory in its entirety, including the fundamental operations. Cagman and Deli [28] presented FP-soft sets (soft sets with fuzzy parameters) and their means, and Cagman and Deli [29] presented products of FP-soft sets of complex aggregations. Deli [30] proposed a considerable integration interval-valued neutrosophic soft sets (IVNSSs), which combine interval neutrosophic sets and soft sets, and an algorithm to make a decision.

The similarity and distance measurement are important in comparison of uncertain sets. Similarity measures of soft sets were defined by Majumdar and Samanta [31] and distance and similarity measures of soft sets with applications were introduced by Kharal [32]. In the case of intuitionistic fuzzy sets, Grzegorzewski [33] suggested distances on Hausdorff metric that subsequently inspired neutrosophic distance measures. Arora *et al.* [34] used neutrosophic sets to the decomposition of relational databases and Arora and Biswas [35] constructed a neutrosophic natural language query system. Aggarwal *et al.* [36] investigated neutrosophic modeling and control of uncertain systems. Cheng and Guo [37] applied the neutrosophic concept of image thresholding, Guo and Cheng [38] applied the concept to image segmentation, and Zhang *et al.* [39] applied the combination of neutrosophic concept and watershed segmentation. Ansari *et al.* [40] suggested neutrosophic medical AI to diagnose in the presence of uncertainty. There were further developments in algebra and topology. Ali *et al.* [41] introduced new operations (restricted union, extended intersection) in soft set theory and Ali [42] refined the correspondence between soft, rough and fuzzy soft sets.

1.1. Literature review

Soft rings were proposed by Acar *et al.* [43], and interval-valued intuitionistic fuzzy soft sets were defined by Jiang *et al.* [44] that possess properties. Similarity measures of the intuitionistic fuzzy soft sets of decision-making were suggested by Cagman [45]. Broumi [46] defined the generalized neutrosophic soft set, and Broumi and Smarandache [47] listed a number of similarity measures of neutrosophic sets. Formally, neutrosophic soft topological spaces were defined by Bera and Mahapatra [48], and neutrosophic soft sets with operation were defined by Maji [49]. Neutrosophic soft relations were studied by Deli and Broumi [50]. Smarandache [51] reconsidered neutrosophy to be a generalization of intuitionistic fuzzy sets.

1.2. Motivation for research

Modern data is becoming more complicated, especially in fields like signal processing, which necessitates analytical frameworks that can deal with ambiguity, uncertainty, and multi-dimensional data. The complex, neutral, and contradicting states prevalent in real-world occurrences are frequently not well captured by traditional set-theoretic models. This disparity calls for the creation of increasingly complicated mathematical

frameworks that can both rigorously support the study of such complex data and model it. The gap between abstract theoretical concepts and their usefulness must also be closed immediately to guarantee that new frameworks are not only theoretically valid but also clearly successful in resolving real-world data analysis issues. The urgent need for a complete tool that combines topological principles and sophisticated set theory to produce a flexible and potent platform for classification and pattern recognition tasks is what drives our study.

1.3. Novelty of the research

Several important contributions to the area are introduced in this study. CTVNS Sets (CTVNSS), a unique structure designed to capture a higher level of complexity and uncertainty in data representation, are the main source of novelty. The building of a complete triple-valued neutrosophic soft topology extends this, providing a strong and innovative mathematical foundation by rigorously defining topological features like interior and closure. Beyond theoretical development, the study shows how to use the cotangent similarity measure (Cot SM) to apply this framework in a novel way to a real-world signal classification challenge. Using a multifaceted graphical framework that integrates 2D Heatmaps, 3D surface plots, spline-smoothed curves, and cluster analysis in a synergistic manner, the analytical methodology itself is novel. In addition to quantifying similarity strengths, our hybrid approach offers a clear visual evaluation of classification reliability. Thus, the research is unique in its comprehensive contribution, including a new theoretical model and validation through an intricate, multifaceted analytical procedure. It also sets a new standard for template-based signal analysis and pattern recognition.

2. Preliminaries

This section exhibits some basic operations that are absolutely necessary for the upcoming sections.

Definition 2.1. *[51] A neutrosophic set $\mathcal{A}$ on the universe of discourse $\mathbb{X}$ is defined as:*

$$\mathcal{A} = \{\langle x, T_{\mathcal{A}}(x), I_{\mathcal{A}}(x), F_{\mathcal{A}}(x)\rangle : x \in \mathbb{X}\},$$

where T, I, F : $\mathbb{X} \longrightarrow]0,1[$ *and* $0 \le T_A(x) + I_A(x) + F_A(x) \le 3$.

Definition 2.2. *[16] Let $\mathbb{X}$ be an initial universe, $\acute{\mathcal{E}}$ be a set of all parameters, and $P(\mathbb{X})$ denote the power set of $\mathbb{X}$. A pair $(\tilde{\mathcal{F}}, \acute{\mathcal{E}})$ is called a soft set on $\mathbb{X}$, where $\tilde{\mathcal{F}}$ is the mapping given by $\tilde{\mathcal{F}} : \acute{\mathcal{E}} \longrightarrow P(\mathbb{X})$. In other words, the soft set is a parameterized family of subsets of the set $\mathbb{X}$. For $\mathfrak{e} \in \acute{\mathcal{E}}$, $\tilde{\mathcal{F}}(\mathfrak{e})$ can be considered as the set of $\mathfrak{e}$-elements of the soft set $(\tilde{\mathcal{F}}, \acute{\mathcal{E}})$, or as the set of $\mathfrak{e}$-approximate elements of the soft set, i.e.*

$$(\tilde{\mathcal{F}}, \acute{\mathcal{E}}) = \{(\mathfrak{e}, \mathcal{F}(\mathfrak{e})) : \mathfrak{e} \in \acute{\mathcal{E}}, \mathcal{F} : \acute{\mathcal{E}} \longrightarrow P(\mathbb{X})\}.$$

First, the neutrosophic soft set was defined by Maji [49] and later modified by Deli and Broumi [50] as follows:

Definition 2.3. *Let $\mathbb{X}$ be an initial universe, $\acute{\mathcal{E}}$ be a set of all parameters. Let $P(\mathbb{X})$ denote the set of all neutrosophic sets of $\mathbb{X}$. Then, a soft neutrosophic set $(\tilde{\mathcal{F}}, \acute{\mathcal{E}})$ over $\mathbb{X}$ is a set defined by a set valued function $\tilde{\mathcal{F}}$ representing a mapping $\tilde{\mathcal{F}} : \acute{\mathcal{E}} \longrightarrow P(\mathbb{X})$ where $\tilde{\mathcal{F}}$ is called an approximate function of the soft neutrosophic set $(\tilde{\mathcal{F}}, \acute{\mathcal{E}})$. In other words, the neutrosophic soft set is a parameterized family of some elements of the set $P(\mathbb{X})$ and therefore can be written as a set of ordered pairs,*

$$(\tilde{\mathcal{F}}, \acute{\mathcal{E}}) = \{(\mathfrak{e}, \langle x, T_{\tilde{\mathcal{F}}(\mathfrak{e})}(x), I_{\tilde{\mathcal{F}}(\mathfrak{e})}(x), F_{\tilde{\mathcal{F}}(\mathfrak{e})}(x)\rangle : x \in \mathbb{X}) : \mathfrak{e} \in \acute{\mathcal{E}}\},$$

where $T_{\tilde{\mathcal{F}}(\mathfrak{e})}(x), I_{\tilde{\mathcal{F}}(\mathfrak{e})}(x), F_{\tilde{\mathcal{F}}(\mathfrak{e})}(x) \in [0,1]$, respectively, called the truth-membership, indeterminacy-membership, and falsity-membership of $\tilde{\mathcal{F}}(\mathfrak{e})$. Since supremum of each T, I, F *is* 1 *so the inequality* $0 \le T_{\tilde{\mathcal{F}}(\mathfrak{e})}(x) + I_{\tilde{\mathcal{F}}(\mathfrak{e})}(x) + F_{\tilde{\mathcal{F}}(\mathfrak{e})}(x) \le 3$ *is obvious.*

Definition 2.4. *[48] Let $(\tilde{\mathcal{F}}, \acute{\mathcal{E}})$ be a CTVNS set over the universe set $\mathbb{X}$. The complement of $(\tilde{\mathcal{F}}, \acute{\mathcal{E}})$ is denoted by $(\tilde{\mathcal{F}}, \acute{\mathcal{E}})^c$ and is defined by:*

$$(\tilde{\mathcal{F}}, \acute{\mathcal{E}})^c = \{(\mathfrak{e}, \langle x, F_{\tilde{\mathcal{F}}(\mathfrak{e})}(x), 1 - I_{\tilde{\mathcal{F}}(\mathfrak{e})}(x), T_{\tilde{\mathcal{F}}(\mathfrak{e})}(x)\rangle : x \in \mathbb{X}) : \mathfrak{e} \in \acute{\mathcal{E}}\}.$$

It is obvious that, $((\tilde{\mathcal{F}}, \acute{\mathcal{E}})^c)^c = (\tilde{\mathcal{F}}, \acute{\mathcal{E}})$.

Definition 2.5. *[49] Let $(\tilde{\mathcal{F}}, \acute{\mathcal{E}})$ and $(\tilde{\mathcal{G}}, \acute{\mathcal{E}})$ be two neutrosophic soft sets over the universe set $\mathbb{X}$. $(\tilde{\mathcal{F}}, \acute{\mathcal{E}})$ is said to be neutrosophic soft subset of $(\tilde{\mathcal{G}}, \acute{\mathcal{E}})$ if $T_{\tilde{\mathcal{F}}(\mathfrak{e})}(x) \le T_{\tilde{\mathcal{G}}(\mathfrak{e})}(x), I_{\tilde{\mathcal{F}}(\mathfrak{e})}(x) \le I_{\tilde{\mathcal{G}}(\mathfrak{e})}(x), F_{\tilde{\mathcal{F}}(\mathfrak{e})}(x) \ge F_{\tilde{\mathcal{G}}(\mathfrak{e})}(x)$, for all $\mathfrak{e} \in \acute{\mathcal{E}}$, for all $x \in \mathbb{X}$. It is denoted by $(\tilde{\mathcal{F}}, \acute{\mathcal{E}}) \subseteq (\tilde{\mathcal{G}}, \acute{\mathcal{E}})$. $(\tilde{\mathcal{F}}, \acute{\mathcal{E}})$ is said to be neutrosophic soft set equal to $(\tilde{\mathcal{G}}, \acute{\mathcal{E}})$ if $(\tilde{\mathcal{F}}, \acute{\mathcal{E}})$ is neutrosophic soft subset of $(\tilde{\mathcal{G}}, \acute{\mathcal{E}})$ and $(\tilde{\mathcal{G}}, \acute{\mathcal{E}})$ is neutrosophic soft subset of $(\tilde{\mathcal{F}}, \acute{\mathcal{E}})$. It is denoted by $(\tilde{\mathcal{F}}, \acute{\mathcal{E}}) = (\tilde{\mathcal{G}}, \acute{\mathcal{E}})$.*

Definition 2.6. *[61] Let $\mathcal{E}$ be the set of parameters and $\mathcal{M}$ be the key set. Let $P(\mathcal{M})$ represent the power set of $\mathcal{M}$. Then, a QPNS set $(\tilde{\mathcal{F}}, \acute{\mathcal{E}})$ over $\mathcal{M}$ is a mapping $\tilde{F} : \mathcal{E} \to P(\mathcal{M})$, where $\tilde{F}$ is the function of the QPNS set $(\tilde{\mathcal{F}}, \acute{\mathcal{E}})$. Symbolically,*

$$(\tilde{\mathcal{F}}, \acute{\mathcal{E}}) = \left\{\left(\mathfrak{e}, \left\langle \begin{matrix} s, AbT_{\tilde{\mathcal{F}}(\mathfrak{e})}(s), ReT_{\tilde{\mathcal{F}}(\mathfrak{e})}(s), \\ ReF_{\tilde{\mathcal{F}}(\mathfrak{e})}(s), AbF_{\tilde{\mathcal{F}}(\mathfrak{e})}(s) \end{matrix} \right\rangle\right) : s \in \mathcal{M}, \mathfrak{e} \in \acute{\mathcal{E}}\right\}.$$

Here, $AbT_{\tilde{\mathcal{F}}(\mathfrak{e})}(s)$, $ReT_{\tilde{\mathcal{F}}(\mathfrak{e})}(s)$, $ReF_{\tilde{\mathcal{F}}(\mathfrak{e})}(s)$, and $AbF_{\tilde{\mathcal{F}}(\mathfrak{e})}(s)$ belong to the interval $[0,1]$. Respectively, these functions are called the absolute true membership, relative true membership, relative false membership, and absolute false-membership functions of $\tilde{\mathcal{F}}(\mathfrak{e})$. Since the supremum of each function is 1 and the infimum is 0, the following inequality holds:

$$0 \le AbT_{\tilde{\mathcal{F}}(\mathfrak{e})}(s) + ReT_{\tilde{\mathcal{F}}(\mathfrak{e})}(s) + ReF_{\tilde{\mathcal{F}}(\mathfrak{e})}(s) + AbF_{\tilde{\mathcal{F}}(\mathfrak{e})}(s) \le 4.$$

Definition 2.7. *[61] Let $(\tilde{\mathcal{F}}, \acute{\mathcal{E}})$ be a QPNS set over the key set $\mathcal{M}$. Then, the complement of $(\tilde{\mathcal{F}}, \acute{\mathcal{E}})$ is denoted by $(\tilde{\mathcal{F}}, \acute{\mathcal{E}})^c$ and is defined as follows:*

$$(\tilde{\mathcal{F}}, \acute{\mathcal{E}})^c = \left\{\left(\mathfrak{e}, \left\langle \begin{matrix} s, AbF_{\tilde{\mathcal{F}}(\mathfrak{e})}(s), ReF_{\tilde{\mathcal{F}}(\mathfrak{e})}(s), \\ ReT_{\tilde{\mathcal{F}}(\mathfrak{e})}(s), AbT_{\tilde{\mathcal{F}}(\mathfrak{e})}(s) \end{matrix} \right\rangle\right) : s \in \mathcal{M}, e \in \acute{\mathcal{E}}\right\}.$$

It follows that $\left((\tilde{\mathcal{F}}, \acute{\mathcal{E}})^c\right)^c = (\tilde{\mathcal{F}}, \acute{\mathcal{E}})$.

Definition 2.8. *[61] Let $(\tilde{\mathcal{F}},\acute{\mathcal{E}})$ and $(\tilde{\mathcal{G}},\acute{\mathcal{E}})$ be two QPNS sets over the key set $\mathcal{M}$. Then, $(\tilde{\mathcal{F}},\acute{\mathcal{E}})\subseteq(\tilde{\mathcal{G}},\acute{\mathcal{E}})$ if*

$$AbT_{\tilde{\mathcal{F}}(\mathfrak{e})}(\mathrm{s})\le AbT_{\tilde{\mathcal{G}}(\mathfrak{e})}(\mathrm{s}),$$
$$ReT_{\tilde{\mathcal{F}}(\mathfrak{e})}(\mathrm{s})\le ReT_{\tilde{\mathcal{G}}(\mathfrak{e})}(\mathrm{s}),$$
$$ReF_{\tilde{\mathcal{F}}(\mathfrak{e})}(\mathrm{s})\ge ReF_{\tilde{\mathcal{G}}(\mathfrak{e})}(\mathrm{s}),$$
$$AbF_{\tilde{\mathcal{F}}(\mathfrak{e})}(\mathrm{s})\ge AbF_{\tilde{\mathcal{G}}(\mathfrak{e})}(\mathrm{s}),$$

for all $\mathfrak{e}\in\acute{\mathcal{E}}$ and $\mathrm{s}\in\mathcal{M}$. If $(\tilde{\mathcal{F}},\acute{\mathcal{E}})\subseteq(\tilde{\mathcal{G}},\acute{\mathcal{E}})$ and $(\tilde{\mathcal{F}},\acute{\mathcal{E}})\supseteq(\tilde{\mathcal{G}},\acute{\mathcal{E}})$, then $(\tilde{\mathcal{F}},\acute{\mathcal{E}})=(\tilde{\mathcal{G}},\acute{\mathcal{E}})$.

Definition 2.9. *[61] Let $(\tilde{\mathcal{F}},\acute{\mathcal{E}})$ and $(\tilde{\mathcal{G}},\acute{\mathcal{E}})$ be two QPNS sets over the key set $\mathcal{M}$ such that $(\tilde{\mathcal{F}},\acute{\mathcal{E}})\neq(\tilde{\mathcal{G}},\acute{\mathcal{E}})$. Then their union is denoted by $(\tilde{\mathcal{F}},\acute{\mathcal{E}})\Cup(\tilde{\mathcal{G}},\acute{\mathcal{E}})=(\tilde{\mathcal{H}},\acute{\mathcal{E}})$ and is defined as:*

$$(\tilde{\mathcal{H}},\acute{\mathcal{E}})=\left\{\left(\mathfrak{e},\left\langle\begin{matrix}\mathrm{s},AbT_{\tilde{H}(\mathfrak{e})}(\mathrm{s}),ReT_{\tilde{\mathcal{H}}(\mathfrak{e})}(\mathrm{s}),\\ ReF_{\tilde{\mathcal{H}}(\mathfrak{e})}(\mathrm{s}),AbF_{\tilde{\mathcal{H}}(\mathfrak{e})}(\mathrm{s})\end{matrix}\right\rangle\right):\mathrm{s}\in\mathcal{M},\mathfrak{e}\in\acute{\mathcal{E}}\right\},$$

where

$$AbT_{\tilde{\mathcal{H}}(\mathfrak{e})}(\mathrm{s})=\max\left\{AbT_{\tilde{\mathcal{F}}(\mathfrak{e})}(\mathrm{s}),AbT_{\tilde{\mathcal{G}}(\mathfrak{e})}(\mathrm{s})\right\},$$
$$ReT_{\tilde{\mathcal{H}}(\mathfrak{e})}(\mathrm{s})=\max\left\{ReT_{\tilde{\mathcal{F}}(\mathfrak{e})}(\mathrm{s}),ReT_{\tilde{\mathcal{G}}(\mathfrak{e})}(\mathrm{s})\right\},$$
$$ReF_{\tilde{\mathcal{H}}(\mathfrak{e})}(\mathrm{s})=\min\left\{ReF_{\tilde{\mathcal{F}}(\mathfrak{e})}(\mathrm{s}),ReF_{\tilde{\mathcal{G}}(\mathfrak{e})}(\mathrm{s})\right\},$$
$$AbF_{\tilde{\mathcal{H}}(\mathfrak{e})}(\mathrm{s})=\min\left\{AbF_{\tilde{\mathcal{F}}(\mathfrak{e})}(\mathrm{s}),AbF_{\tilde{\mathcal{G}}(\mathfrak{e})}(\mathrm{s})\right\}.$$

Definition 2.10. *[61] Let $(\tilde{\mathcal{F}},\acute{\mathcal{E}})$ and $(\tilde{\mathcal{G}},\acute{\mathcal{E}})$ be two QPNS sets over the key set $\mathcal{M}$ such that $(\tilde{\mathcal{F}},\acute{\mathcal{E}})\neq(\tilde{\mathcal{G}},\acute{\mathcal{E}})$. Then their intersection is denoted by $(\tilde{\mathcal{F}},\acute{\mathcal{E}})\Cap(\tilde{\mathcal{G}},\acute{\mathcal{E}})=(\tilde{\mathcal{H}},\acute{\mathcal{E}})$ and is defined as:*

$$(\tilde{\mathcal{H}},\acute{\mathcal{E}})=\left\{\left(\mathfrak{e},\left\langle\begin{matrix}\mathrm{s},AbT_{\tilde{\mathcal{H}}(\mathfrak{e})}(\mathrm{s}),ReT_{\tilde{\mathcal{H}}(\mathfrak{e})}(\mathrm{s}),\\ ReF_{\tilde{\mathcal{H}}(\mathfrak{e})}(\mathrm{s}),AbF_{\tilde{\mathcal{H}}(\mathfrak{e})}(\mathrm{s})\end{matrix}\right\rangle\right):\mathrm{s}\in\mathcal{M},\mathfrak{e}\in\acute{\mathcal{E}}\right\},$$

where

$$AbT_{\tilde{\mathcal{H}}(\mathfrak{e})}(\mathrm{s})=\min\left\{AbT_{\tilde{\mathcal{F}}(\mathfrak{e})}(\mathrm{s}),AbT_{\tilde{\mathcal{G}}(\mathfrak{e})}(\mathrm{s})\right\},$$
$$ReT_{\tilde{\mathcal{H}}(\mathfrak{e})}(\mathrm{s})=\min\left\{ReT_{\tilde{\mathcal{F}}(\mathfrak{e})}(\mathrm{s}),ReT_{\tilde{\mathcal{G}}(\mathfrak{e})}(\mathrm{s})\right\},$$
$$ReF_{\tilde{\mathcal{H}}(\mathfrak{e})}(\mathrm{s})=\max\left\{ReF_{\tilde{\mathcal{F}}(\mathfrak{e})}(\mathrm{s}),ReF_{\tilde{\mathcal{G}}(\mathfrak{e})}(\mathrm{s})\right\},$$
$$AbF_{\tilde{\mathcal{H}}(\mathfrak{e})}(\mathrm{s})=\max\left\{AbF_{\tilde{\mathcal{F}}(\mathfrak{e})}(\mathrm{s}),AbF_{\tilde{\mathcal{G}}(\mathfrak{e})}(\mathrm{s})\right\}.$$

Definition 2.11. *[61] Let $(\tilde{\mathcal{F}},\acute{\mathcal{E}})$ and $(\tilde{\mathcal{G}},\acute{\mathcal{E}})$ be two QPNS sets over the key set $\mathcal{M}$ such that $(\tilde{\mathcal{F}},\acute{\mathcal{E}})\neq(\tilde{\mathcal{G}},\acute{\mathcal{E}})$. Then, their difference is denoted by $(\tilde{\mathcal{H}},\acute{\mathcal{E}})=(\tilde{\mathcal{F}},\acute{\mathcal{E}})\setminus(\tilde{\mathcal{G}},\acute{\mathcal{E}})$ and is defined as:*

$$(\tilde{\mathcal{H}},\acute{\mathcal{E}})=(\tilde{\mathcal{F}},\acute{\mathcal{E}})\Cap(\tilde{\mathcal{G}},\acute{\mathcal{E}})^{c},$$

such that

$$(\tilde{\mathcal{H}},\acute{\mathcal{E}})=\left\{\left(\mathfrak{e},\left\langle\begin{matrix}\mathrm{s},AbT_{\tilde{\mathcal{H}}(\mathfrak{e})}(\mathrm{s}),ReT_{\tilde{\mathcal{H}}(\mathfrak{e})}(\mathrm{s}),\\ ReF_{\tilde{\mathcal{H}}(\mathfrak{e})}(\mathrm{s}),AbF_{\tilde{\mathcal{H}}(\mathfrak{e})}(\mathrm{s})\end{matrix}\right\rangle\right):\mathrm{s}\in\mathcal{M},\mathfrak{e}\in\acute{\mathcal{E}}\right\},$$

where

$$AbT_{\tilde{\mathcal{H}}(\mathfrak{e})}(\mathrm{s})=\min\left\{AbT_{\tilde{\mathcal{F}}(\mathfrak{e})}(\mathrm{s}),AbF_{\tilde{\mathcal{G}}(\mathfrak{e})}(\mathrm{s})\right\},$$
$$ReT_{\tilde{\mathcal{H}}(\mathfrak{e})}(\mathrm{s})=\min\left\{ReT_{\tilde{\mathcal{F}}(\mathfrak{e})}(\mathrm{s}),ReF_{\tilde{\mathcal{G}}(\mathfrak{e})}(\mathrm{s})\right\},$$
$$ReF_{\tilde{\mathcal{H}}(\mathfrak{e})}(\mathrm{s})=\max\left\{ReF_{\tilde{\mathcal{F}}(\mathfrak{e})}(\mathrm{s}),ReT_{\tilde{\mathcal{G}}(\mathfrak{e})}(\mathrm{s})\right\},$$
$$AbF_{\tilde{\mathcal{H}}(\mathfrak{e})}(\mathrm{s})=\max\left\{AbF_{\tilde{\mathcal{F}}(\mathfrak{e})}(\mathrm{s}),AbT_{\tilde{\mathcal{G}}(\mathfrak{e})}(\mathrm{s})\right\}.$$

Definition 2.12. *[61] Let $\{(\tilde{\mathcal{F}}_i,\acute{\mathcal{E}}):i\in I\}$ be a family of QPNS sets over the key set $\mathcal{M}$. Then, the union and intersection of this family are defined as follows:*

$$\bigcup_{i\in I}(\tilde{\mathcal{F}}_i,\acute{\mathcal{E}})=\left\{\left(\mathfrak{e},\left\langle\begin{matrix}\mathrm{s},\sup\limits_{i\in I}AbT_{\tilde{\mathcal{F}}_{i(\mathfrak{e})}}(\mathrm{s}),\sup\limits_{i\in I}ReT_{\tilde{\mathcal{F}}_{i(\mathfrak{e})}}(\mathrm{s}),\\ \inf\limits_{i\in I}ReF_{\tilde{\mathcal{F}}_{i(\mathfrak{e})}}(\mathrm{s}),\inf\limits_{i\in I}AbF_{\tilde{\mathcal{F}}_{i(\mathfrak{e})}}(\mathrm{s})\end{matrix}\right\rangle\right):\mathrm{s}\in\mathcal{M},\mathfrak{e}\in\acute{\mathcal{E}}\right\},$$

$$\bigcap_{i\in I}(\tilde{\mathcal{F}}_i,\acute{\mathcal{E}})=\left\{\left(\mathfrak{e},\left\langle\begin{matrix}\mathrm{s},\inf\limits_{i\in I}AbT_{\tilde{\mathcal{F}}_{i(\mathfrak{e})}}(\mathrm{s}),\\ \inf\limits_{i\in I}ReT_{\tilde{\mathcal{F}}_{i(\mathfrak{e})}}(\mathrm{s}),\sup\limits_{i\in I}ReF_{\tilde{\mathcal{F}}_{i(\mathfrak{e})}}(\mathrm{s}),\\ \sup\limits_{i\in I}AbF_{\tilde{\mathcal{F}}_{i(\mathfrak{e})}}(\mathrm{s})\end{matrix}\right\rangle\right):\mathrm{s}\in\mathcal{M},\mathfrak{e}\in\acute{\mathcal{E}}\right\}.$$

3. Some operations on complex triple-valued neutrosophic soft sets

This section exhibits the newly defined operations of union, intersection, difference, AND, and OR on CTVNS sets which are indispensable for the upcoming sections.

Definition 3.1. *Let $\mathcal{E}$ be the set of parameters and $\mathbb{X}$ be the key set. Let $P(\mathbb{X})$ represent the power set of $\mathbb{X}$. Then, a CTVNS set $(\tilde{\mathcal{F}},\acute{\mathcal{E}})$ over $\mathbb{X}$ is a mapping $\tilde{\mathcal{F}}:\mathcal{E}\to P(\mathbb{X})$, where $\tilde{\mathcal{F}}$ is the function of the CTVNS set $(\tilde{\mathcal{F}},\acute{\mathcal{E}})$. Symbolically,*

$$(\tilde{\mathcal{F}},\acute{\mathcal{E}})=\left\{\left(\mathfrak{e},\left\langle\begin{matrix}\mathrm{x},T_{\tilde{\mathcal{F}}(\mathfrak{e})}(\mathrm{x}),RT_{\tilde{\mathcal{F}}(\mathfrak{e})}(\mathrm{x}),C_{\tilde{\mathcal{F}}(\mathfrak{e})}(\mathrm{x}),\\ RF_{\tilde{\mathcal{F}}(\mathfrak{e})}(\mathrm{x}),F_{\tilde{\mathcal{F}}(\mathfrak{e})}(\mathrm{x})\end{matrix}\right\rangle\right):\mathrm{x}\in\mathbb{X},\mathfrak{e}\in\acute{\mathcal{E}}\right\},$$

where $T_{\tilde{\mathcal{F}}(\mathfrak{e})}(\mathrm{x})$, $RT_{\tilde{\mathcal{F}}(\mathfrak{e})}(\mathrm{x})$, $C_{\tilde{\mathcal{F}}(\mathfrak{e})}(\mathrm{x})$, $RF_{\tilde{\mathcal{F}}(\mathfrak{e})}(\mathrm{x})$ and $F_{\tilde{\mathcal{F}}(\mathfrak{e})}(\mathrm{x})$ are such that

$$T_{\tilde{\mathcal{F}}(\mathfrak{e})}(\mathrm{x})=p_{\acute{\mathcal{E}}}(\mathrm{x})e^{i\mu_{\acute{\mathcal{E}}}(\mathrm{x})},\quad RT_{\tilde{\mathcal{F}}(\mathfrak{e})}(\mathrm{x})=q_{\acute{\mathcal{E}}}(\mathrm{x})e^{i\vartheta_{\acute{\mathcal{E}}}(\mathrm{x})},$$
$$C_{\tilde{\mathcal{F}}(\mathfrak{e})}(\mathrm{x})=r_{\acute{\mathcal{E}}}(\mathrm{x})e^{i\omega_{\acute{\mathcal{E}}}(\mathrm{x})},\quad RF_{\tilde{\mathcal{F}}(\mathfrak{e})}(\mathrm{x})=s_{\acute{\mathcal{E}}}(\mathrm{x})e^{i\sigma_{\acute{\mathcal{E}}}(\mathrm{x})},$$
$$F_{\tilde{\mathcal{F}}(\mathfrak{e})}(\mathrm{x})=t_{\acute{\mathcal{E}}}(\mathrm{x})e^{i\rho_{\acute{\mathcal{E}}}(\mathrm{x})},$$

$p_{\acute{\mathcal{E}}}(\mathrm{x})$, $q_{\acute{\mathcal{E}}}(\mathrm{x})$, $r_{\acute{\mathcal{E}}}(\mathrm{x})$, $s_{\acute{\mathcal{E}}}(\mathrm{x})$, $t_{\acute{\mathcal{E}}}(\mathrm{x})\in[0,1]$ and $\mu_{\acute{\mathcal{E}}}(\mathrm{x})$, $\vartheta_{\acute{\mathcal{E}}}(\mathrm{x})$, $\omega_{\acute{\mathcal{E}}}(\mathrm{x})$, $\sigma_{\acute{\mathcal{E}}}(\mathrm{x})$, $\rho_{\acute{\mathcal{E}}}(\mathrm{x})\in[0,2\pi]$, such that the condition $0\le p_{\acute{\mathcal{E}}}(\mathrm{x})+q_{\acute{\mathcal{E}}}(\mathrm{x})+r_{\acute{\mathcal{E}}}(\mathrm{x})+s_{\acute{\mathcal{E}}}(\mathrm{x})+t_{\acute{\mathcal{E}}}(\mathrm{x})\le 5$ is satisfied.

Definition 3.2. *Let $(\tilde{\mathcal{F}}_1,\acute{\mathcal{E}})$ and $(\tilde{\mathcal{F}}_2,\acute{\mathcal{E}})$ be two CTVNS sets over the universe set $\mathbb{X}$. Then their union is represented by $(\tilde{\mathcal{F}}_1,\acute{\mathcal{E}})\Cup(\tilde{\mathcal{F}}_2,\acute{\mathcal{E}})=(\tilde{\mathcal{F}}_3,\acute{\mathcal{E}})$ is defined by:*

$$(\tilde{\mathcal{F}}_3,\acute{\mathcal{E}})=\left\{\left(\mathfrak{e},\left\langle\begin{matrix}\mathrm{x},\mathrm{T}_{\tilde{\mathcal{F}}_3(\mathfrak{e})}(\mathrm{x}),\mathrm{RT}_{\tilde{\mathcal{F}}_3(\mathfrak{e})}(\mathrm{x}),\mathrm{C}_{\tilde{\mathcal{F}}_3(\mathfrak{e})}(\mathrm{x}),\\ \mathrm{RF}_{\tilde{\mathcal{F}}_3(\mathfrak{e})}(\mathrm{x}),\mathrm{F}_{\tilde{\mathcal{F}}_3(\mathfrak{e})}(\mathrm{x})\end{matrix}\right\rangle:\mathrm{x}\in\mathbb{X}\right):\mathfrak{e}\in\acute{\mathcal{E}}\right\},$$

where

$$\mathrm{T}_{\tilde{\mathcal{F}}_3(\mathfrak{e})}(\mathrm{x})=\max\{\mathrm{T}_{\tilde{\mathcal{F}}_1(\mathfrak{e})}(\mathrm{x}),\mathrm{T}_{\tilde{\mathcal{F}}_2(\mathfrak{e})}(\mathrm{x})\},$$
$$\mathrm{RT}_{\tilde{\mathcal{F}}_3(\mathfrak{e})}(\mathrm{x})=\max\{\mathrm{RT}_{\tilde{\mathcal{F}}_1(\mathfrak{e})}(\mathrm{x}),\mathrm{RT}_{\tilde{\mathcal{F}}_2(\mathfrak{e})}(\mathrm{x})\},$$
$$\mathrm{C}_{\tilde{\mathcal{F}}_3(\mathfrak{e})}(\mathrm{x})=\max\{\mathrm{C}_{\tilde{\mathcal{F}}_1(\mathfrak{e})}(\mathrm{x}),\mathrm{C}_{\tilde{\mathcal{F}}_2(\mathfrak{e})}(\mathrm{x})\},$$
$$\mathrm{RF}_{\tilde{\mathcal{F}}_3(\mathfrak{e})}(\mathrm{x})=\min\{\mathrm{RF}_{\tilde{\mathcal{F}}_1(\mathfrak{e})}(\mathrm{x}),\mathrm{RF}_{\tilde{\mathcal{F}}_2(\mathfrak{e})}(\mathrm{x})\},$$
$$\mathrm{F}_{\tilde{\mathcal{F}}_3(\mathfrak{e})}(\mathrm{x})=\min\{\mathrm{F}_{\tilde{\mathcal{F}}_1(\mathfrak{e})}(\mathrm{x}),\mathrm{F}_{\tilde{\mathcal{F}}_2(\mathfrak{e})}(\mathrm{x})\}.$$

Definition 3.3. *Let $(\tilde{\mathcal{F}}_1, \acute{\mathcal{E}})$ and $(\tilde{\mathcal{F}}_2, \acute{\mathcal{E}})$ be two CTVNS sets over the universe set $\mathbb{X}$. Then their intersection is represented by $(\tilde{\mathcal{F}}_1, \acute{\mathcal{E}}) \Cap (\tilde{\mathcal{F}}_2, \acute{\mathcal{E}}) = (\tilde{\mathcal{F}}_3, \acute{\mathcal{E}})$ is defined by:*

$$(\tilde{\mathcal{F}}_3, \acute{\mathcal{E}}) = \left\{\left(\mathfrak{e}, \left\langle \begin{matrix} \mathrm{x}, \mathrm{T}_{\tilde{\mathcal{F}}_3(\mathfrak{e})}(\mathrm{x}), \mathrm{RT}_{\tilde{\mathcal{F}}_3(\mathfrak{e})}(\mathrm{x}), \mathrm{C}_{\tilde{\mathcal{F}}_3(\mathfrak{e})}(\mathrm{x}), \\ \mathrm{RF}_{\tilde{\mathcal{F}}_3(\mathfrak{e})}(\mathrm{x}), \mathrm{F}_{\tilde{\mathcal{F}}_3(\mathfrak{e})}(\mathrm{x}) \end{matrix} \right\rangle : \mathrm{x} \in \mathbb{X}\right) : \mathfrak{e} \in \acute{\mathcal{E}}\right\},$$

where

$$\begin{aligned} \mathrm{T}_{\tilde{\mathcal{F}}_3(\mathfrak{e})}(\mathrm{x}) &= \min\{\mathrm{T}_{\tilde{\mathcal{F}}_1(\mathfrak{e})}(\mathrm{x}), \mathrm{T}_{\tilde{\mathcal{F}}_2(\mathfrak{e})}(\mathrm{x})\}, \\ \mathrm{RT}_{\tilde{\mathcal{F}}_3(\mathfrak{e})}(\mathrm{x}) &= \min\{\mathrm{RT}_{\tilde{\mathcal{F}}_1(\mathfrak{e})}(\mathrm{x}), \mathrm{RT}_{\tilde{\mathcal{F}}_2(\mathfrak{e})}(\mathrm{x})\}, \\ \mathrm{C}_{\tilde{\mathcal{F}}_3(\mathfrak{e})}(\mathrm{x}) &= \min\{\mathrm{C}_{\tilde{\mathcal{F}}_1(\mathfrak{e})}(\mathrm{x}), \mathrm{C}_{\tilde{\mathcal{F}}_2(\mathfrak{e})}(\mathrm{x})\}, \\ \mathrm{RF}_{\tilde{\mathcal{F}}_3(\mathfrak{e})}(\mathrm{x}) &= \max\{\mathrm{RF}_{\tilde{\mathcal{F}}_1(\mathfrak{e})}(\mathrm{x}), \mathrm{RF}_{\tilde{\mathcal{F}}_2(\mathfrak{e})}(\mathrm{x})\}, \\ \mathrm{F}_{\tilde{\mathcal{F}}_3(\mathfrak{e})}(\mathrm{x}) &= \max\{\mathrm{F}_{\tilde{\mathcal{F}}_1(\mathfrak{e})}(\mathrm{x}), \mathrm{F}_{\tilde{\mathcal{F}}_2(\mathfrak{e})}(\mathrm{x})\}. \end{aligned}$$

Definition 3.4. *Let $(\tilde{\mathcal{F}}, \acute{\mathcal{E}})$ be a CTVNS set over the universe set $\mathbb{X}$. The complement of $(\tilde{\mathcal{F}}, \acute{\mathcal{E}})$ is denoted by $(\tilde{\mathcal{F}}, \acute{\mathcal{E}})^c$ and is defined by:*

$$(\tilde{\mathcal{F}}, \acute{\mathcal{E}})^c = \left\{\left(\mathfrak{e}, \left\langle \begin{matrix} \mathrm{x}, F_{\tilde{\mathcal{F}}(\mathfrak{e})}(\mathrm{x}), RF_{\tilde{\mathcal{F}}(\mathfrak{e})}(\mathrm{x}), 1 - C_{\tilde{\mathcal{F}}(\mathfrak{e})}(\mathrm{x}), \\ RT_{\tilde{\mathcal{F}}(\mathfrak{e})}(\mathrm{x}), T_{\tilde{\mathcal{F}}(\mathfrak{e})}(\mathrm{x}) \end{matrix} \right\rangle\right) : \mathrm{x} \in \mathbb{X}, \mathfrak{e} \in \acute{\mathcal{E}}\right\}.$$

It is obvious that, $((\tilde{\mathcal{F}}, \acute{\mathcal{E}})^c)^c = (\tilde{\mathcal{F}}, \acute{\mathcal{E}})$.

Definition 3.5. *Let $(\tilde{\mathcal{F}}_1, \acute{\mathcal{E}})$ and $(\tilde{\mathcal{F}}_2, \acute{\mathcal{E}})$ be two CTVNS sets over the universe set $\mathbb{X}$. Then, $(\tilde{\mathcal{F}}_1, \acute{\mathcal{E}})$ difference $(\tilde{\mathcal{F}}_2, \acute{\mathcal{E}})$ operation on them is denoted by $(\tilde{\mathcal{F}}_1, \acute{\mathcal{E}}) \setminus (\tilde{\mathcal{F}}_2, \acute{\mathcal{E}}) = (\tilde{\mathcal{F}}_3, \acute{\mathcal{E}})$ and is defined by $(\tilde{\mathcal{F}}_3, \acute{\mathcal{E}}) = (\tilde{\mathcal{F}}_1, \acute{\mathcal{E}}) \Cap (\tilde{\mathcal{F}}_2, \acute{\mathcal{E}})^c$ as follows:*

$$(\tilde{\mathcal{F}}_3, \acute{\mathcal{E}}) = \left\{\left(\mathfrak{e}, \left\langle \begin{matrix} \mathrm{x}, \mathrm{T}_{\tilde{\mathcal{F}}_3(\mathfrak{e})}(\mathrm{x}), \mathrm{RT}_{\tilde{\mathcal{F}}_3(\mathfrak{e})}(\mathrm{x}), \mathrm{C}_{\tilde{\mathcal{F}}_3(\mathfrak{e})}(\mathrm{x}), \\ \mathrm{RF}_{\tilde{\mathcal{F}}_3(\mathfrak{e})}(\mathrm{x}), \mathrm{F}_{\tilde{\mathcal{F}}_3(\mathfrak{e})}(\mathrm{x}) \end{matrix} \right\rangle : \mathrm{x} \in \mathbb{X}\right) : \mathfrak{e} \in \acute{\mathcal{E}}\right\},$$

where

$$\begin{aligned} \mathrm{T}_{\tilde{\mathcal{F}}_3(\mathfrak{e})}(\mathrm{x}) &= \min\{\mathrm{T}_{\tilde{\mathcal{F}}_1(\mathfrak{e})}(\mathrm{x}), \mathrm{F}_{\tilde{\mathcal{F}}_2(\mathfrak{e})}(\mathrm{x})\}, \\ \mathrm{RT}_{\tilde{\mathcal{F}}_3(\mathfrak{e})}(\mathrm{x}) &= \min\{\mathrm{RT}_{\tilde{\mathcal{F}}_1(\mathfrak{e})}(\mathrm{x}), \mathrm{RF}_{\tilde{\mathcal{F}}_2(\mathfrak{e})}(\mathrm{x})\}, \\ \mathrm{C}_{\tilde{\mathcal{F}}_3(\mathfrak{e})}(\mathrm{x}) &= \min\{\mathrm{C}_{\tilde{\mathcal{F}}_1(\mathfrak{e})}(\mathrm{x}), \mathrm{C}_{\tilde{\mathcal{F}}_2(\mathfrak{e})}(\mathrm{x})\}, \\ \mathrm{RF}_{\tilde{\mathcal{F}}_3(\mathfrak{e})}(\mathrm{x}) &= \max\{\mathrm{RF}_{\tilde{\mathcal{F}}_1(\mathfrak{e})}(\mathrm{x}), \mathrm{RT}_{\tilde{\mathcal{F}}_2(\mathfrak{e})}(\mathrm{x})\}, \\ \mathrm{F}_{\tilde{\mathcal{F}}_3(\mathfrak{e})}(\mathrm{x}) &= \max\{\mathrm{F}_{\tilde{\mathcal{F}}_1(\mathfrak{e})}(\mathrm{x}), \mathrm{T}_{\tilde{\mathcal{F}}_2(\mathfrak{e})}(\mathrm{x})\}. \end{aligned}$$

Definition 3.6. *Let $\{(\tilde{\mathcal{F}}_i, \acute{\mathcal{E}}) : i \in I\}$ be a family of CTVNS sets over the universe set $\mathbb{X}$. Then,*

$$\bigcup_{i\in I}(\tilde{\mathcal{F}}_i, \acute{\mathcal{E}}) = \left\{\left(\begin{matrix} \mathrm{x}, \sup\limits_{i\in I} \mathrm{T}_{\tilde{\mathcal{F}}_{i(\mathfrak{e})}}(\mathrm{x}), \\ \mathfrak{e}, \langle \sup\limits_{i\in I} \mathrm{RT}_{\tilde{\mathcal{F}}_{i(\mathfrak{e})}}(\mathrm{x}), \sup\limits_{i\in I} \mathrm{C}_{\tilde{\mathcal{F}}_{i(\mathfrak{e})}}(\mathrm{x}), \rangle : \mathrm{x} \in \mathbb{X} \\ \inf\limits_{i\in I} \mathrm{RF}_{\tilde{\mathcal{F}}_{i(\mathfrak{e})}}(\mathrm{x}), \inf\limits_{i\in I} \mathrm{F}_{\tilde{\mathcal{F}}_{i(\mathfrak{e})}}(\mathrm{x}) \end{matrix}\right) : \mathfrak{e} \in \acute{\mathcal{E}}\right\},$$

$$\bigcap_{i\in I}(\tilde{\mathcal{F}}_i, \acute{\mathcal{E}}) = \left\{\left(\begin{matrix} \mathrm{x}, \inf\limits_{i\in I} \mathrm{T}_{\tilde{\mathcal{F}}_{i(\mathfrak{e})}}(\mathrm{x}), \\ \mathfrak{e}, \langle \inf\limits_{i\in I} \mathrm{RT}_{\tilde{\mathcal{F}}_{i(\mathfrak{e})}}(\mathrm{x}), \inf\limits_{i\in I} \mathrm{C}_{\tilde{\mathcal{F}}_{i(\mathfrak{e})}}(\mathrm{x}), \rangle : \mathrm{x} \in \mathbb{X} \\ \sup\limits_{i\in I} \mathrm{RF}_{\tilde{\mathcal{F}}_{i(\mathfrak{e})}}(\mathrm{x}), \sup\limits_{i\in I} \mathrm{F}_{\tilde{\mathcal{F}}_{i(\mathfrak{e})}}(\mathrm{x}) \end{matrix}\right) : \mathfrak{e} \in \acute{\mathcal{E}}\right\}.$$

Definition 3.7. *Let $(\tilde{\mathcal{F}}_1, \acute{\mathcal{E}})$ and $(\tilde{\mathcal{F}}_2, \acute{\mathcal{E}})$ be two CTVNS sets over the universe set $\mathbb{X}$. Then, the AND operation on them is denoted by $(\tilde{\mathcal{F}}_1, \acute{\mathcal{E}}) \wedge (\tilde{\mathcal{F}}_2, \acute{\mathcal{E}}) = (\tilde{\mathcal{F}}_3, \acute{\mathcal{E}} \times \acute{\mathcal{E}})$ and is defined by:*

$$(\tilde{\mathcal{F}}_3, \acute{\mathcal{E}} \times \acute{\mathcal{E}}) = \left\{\left((\mathfrak{e}_1, \mathfrak{e}_2), \langle \mathrm{x}, \mathrm{T}_{\tilde{\mathcal{F}}_3(\mathfrak{e}_1,\mathfrak{e}_2)}(\mathrm{x}), \mathrm{RT}_{\tilde{\mathcal{F}}_3(\mathfrak{e}_1,\mathfrak{e}_2)}(\mathrm{x}), \mathrm{C}_{\tilde{\mathcal{F}}_3(\mathfrak{e}_1,\mathfrak{e}_2)}(\mathrm{x}), \mathrm{RF}_{\tilde{\mathcal{F}}_3(\mathfrak{e}_1,\mathfrak{e}_2)}(\mathrm{x}), \mathrm{F}_{\tilde{\mathcal{F}}_3(\mathfrak{e}_1,\mathfrak{e}_2)}(\mathrm{x})\rangle : \mathrm{x} \in \mathbb{X}\right) : (\mathfrak{e}_1, \mathfrak{e}_2) \in \acute{\mathcal{E}} \times \acute{\mathcal{E}}\right\},$$

where

$$\begin{aligned} \mathrm{T}_{\tilde{\mathcal{F}}_3(\mathfrak{e}_1,\mathfrak{e}_2)}(\mathrm{x}) &= \min\left\{\mathrm{T}_{\tilde{\mathcal{F}}_1(\mathfrak{e}_1,\mathfrak{e}_2)}(\mathrm{x}), \mathrm{T}_{\tilde{\mathcal{F}}_2(\mathfrak{e}_1,\mathfrak{e}_2)}(\mathrm{x})\right\}, \\ \mathrm{RT}_{\tilde{\mathcal{F}}_3(\mathfrak{e}_1,\mathfrak{e}_2)}(\mathrm{x}) &= \min\left\{\mathrm{RT}_{\tilde{\mathcal{F}}_1(\mathfrak{e}_1,\mathfrak{e}_2)}(\mathrm{x}), \mathrm{RT}_{\tilde{\mathcal{F}}_2(\mathfrak{e}_1,\mathfrak{e}_2)}(\mathrm{x})\right\}, \\ \mathrm{C}_{\tilde{\mathcal{F}}_3(\mathfrak{e}_1,\mathfrak{e}_2)}(\mathrm{x}) &= \min\left\{\mathrm{C}_{\tilde{\mathcal{F}}_1(\mathfrak{e}_1,\mathfrak{e}_2)}(\mathrm{x}), \mathrm{C}_{\tilde{\mathcal{F}}_2(\mathfrak{e}_1,\mathfrak{e}_2)}(\mathrm{x})\right\}, \\ \mathrm{RF}_{\tilde{\mathcal{F}}_3(\mathfrak{e}_1,\mathfrak{e}_2)}(\mathrm{x}) &= \max\left\{\mathrm{RF}_{\tilde{\mathcal{F}}_1(\mathfrak{e}_1,\mathfrak{e}_2)}(\mathrm{x}), \mathrm{RF}_{\tilde{\mathcal{F}}_2(\mathfrak{e}_1,\mathfrak{e}_2)}(\mathrm{x})\right\}, \\ \mathrm{F}_{\tilde{\mathcal{F}}_3(\mathfrak{e}_1,\mathfrak{e}_2)}(\mathrm{x}) &= \max\left\{\mathrm{F}_{\tilde{\mathcal{F}}_1(\mathfrak{e}_1,\mathfrak{e}_2)}(\mathrm{x}), \mathrm{F}_{\tilde{\mathcal{F}}_2(\mathfrak{e}_1,\mathfrak{e}_2)}(\mathrm{x})\right\}. \end{aligned}$$

Definition 3.8. *Let $(\tilde{\mathcal{F}}_1, \acute{\mathcal{E}})$ and $(\tilde{\mathcal{F}}_2, \acute{\mathcal{E}})$ be two CTVNS sets over the universe set $\mathbb{X}$. Then, the OR operation on them is denoted by $(\tilde{\mathcal{F}}_1, \acute{\mathcal{E}}) \vee (\tilde{\mathcal{F}}_2, \acute{\mathcal{E}}) = (\tilde{\mathcal{F}}_3, \acute{\mathcal{E}} \times \acute{\mathcal{E}})$ and is defined by:*

$$(\tilde{\mathcal{F}}_3, \acute{\mathcal{E}} \times \acute{\mathcal{E}}) = \left\{\left((\mathfrak{e}_1, \mathfrak{e}_2), \langle \mathrm{x}, \mathrm{T}_{\tilde{\mathcal{F}}_3(\mathfrak{e}_1,\mathfrak{e}_2)}(\mathrm{x}), \mathrm{RT}_{\tilde{\mathcal{F}}_3(\mathfrak{e}_1,\mathfrak{e}_2)}(\mathrm{x}), \mathrm{C}_{\tilde{\mathcal{F}}_3(\mathfrak{e}_1,\mathfrak{e}_2)}(\mathrm{x}), \mathrm{RF}_{\tilde{\mathcal{F}}_3(\mathfrak{e}_1,\mathfrak{e}_2)}(\mathrm{x}), \mathrm{F}_{\tilde{\mathcal{F}}_3(\mathfrak{e}_1,\mathfrak{e}_2)}(\mathrm{x})\rangle : \mathrm{x} \in \mathbb{X}\right) : (\mathfrak{e}_1, \mathfrak{e}_2) \in \acute{\mathcal{E}} \times \acute{\mathcal{E}}\right\},$$

where

$$\begin{aligned} \mathrm{T}_{\tilde{\mathcal{F}}_3(\mathfrak{e}_1,\mathfrak{e}_2)}(\mathrm{x}) &= \max\left\{\mathrm{T}_{\tilde{\mathcal{F}}_1(\mathfrak{e}_1,\mathfrak{e}_2)}(\mathrm{x}), \mathrm{T}_{\tilde{\mathcal{F}}_2(\mathfrak{e}_1,\mathfrak{e}_2)}(\mathrm{x})\right\}, \\ \mathrm{RT}_{\tilde{\mathcal{F}}_3(\mathfrak{e}_1,\mathfrak{e}_2)}(\mathrm{x}) &= \max\left\{\mathrm{RT}_{\tilde{\mathcal{F}}_1(\mathfrak{e}_1,\mathfrak{e}_2)}(\mathrm{x}), \mathrm{RT}_{\tilde{\mathcal{F}}_2(\mathfrak{e}_1,\mathfrak{e}_2)}(\mathrm{x})\right\}, \\ \mathrm{C}_{\tilde{\mathcal{F}}_3(\mathfrak{e}_1,\mathfrak{e}_2)}(\mathrm{x}) &= \max\left\{\mathrm{C}_{\tilde{\mathcal{F}}_1(\mathfrak{e}_1,\mathfrak{e}_2)}(\mathrm{x}), \mathrm{C}_{\tilde{\mathcal{F}}_2(\mathfrak{e}_1,\mathfrak{e}_2)}(\mathrm{x})\right\}, \\ \mathrm{RF}_{\tilde{\mathcal{F}}_3(\mathfrak{e}_1,\mathfrak{e}_2)}(\mathrm{x}) &= \min\left\{\mathrm{RF}_{\tilde{\mathcal{F}}_1(\mathfrak{e}_1,\mathfrak{e}_2)}(\mathrm{x}), \mathrm{RF}_{\tilde{\mathcal{F}}_2(\mathfrak{e}_1,\mathfrak{e}_2)}(\mathrm{x})\right\}, \\ \mathrm{F}_{\tilde{\mathcal{F}}_3(\mathfrak{e}_1,\mathfrak{e}_2)}(\mathrm{x}) &= \min\left\{\mathrm{F}_{\tilde{\mathcal{F}}_1(\mathfrak{e}_1,\mathfrak{e}_2)}(\mathrm{x}), \mathrm{F}_{\tilde{\mathcal{F}}_2(\mathfrak{e}_1,\mathfrak{e}_2)}(\mathrm{x})\right\}. \end{aligned}$$

Definition 3.9. *A CTVNS set $(\tilde{\mathcal{F}}, \acute{\mathcal{E}})$ over the universe set $\mathbb{X}$ is said to be a null CTVNS set if*

$$\mathrm{T}_{\tilde{\mathcal{F}}(\mathfrak{e})}(\mathrm{x}) = 0, \quad \mathrm{RT}_{\tilde{\mathcal{F}}(\mathfrak{e})}(\mathrm{x}) = 0, \quad \mathrm{C}_{\tilde{\mathcal{F}}(\mathfrak{e})}(\mathrm{x}) = 0, \quad \forall \mathfrak{e} \in \acute{\mathcal{E}}, \forall \mathrm{x} \in \mathbb{X},$$

$$\mathrm{RF}_{\tilde{\mathcal{F}}(\mathfrak{e})}(\mathrm{x}) = 1, \quad \mathrm{F}_{\tilde{\mathcal{F}}(\mathfrak{e})}(\mathrm{x}) = 1, \quad \forall \mathfrak{e} \in \acute{\mathcal{E}}, \forall \mathrm{x} \in \mathbb{X}.$$

It is denoted by $0_{(\mathbb{X},\acute{\mathcal{E}})}$.

Definition 3.10. *A CTVNS set $(\tilde{\mathcal{F}}, \acute{\mathcal{E}})$ over the universe set $\mathbb{X}$ is said to be an absolute CTVNS set if*

$$\mathrm{T}_{\tilde{\mathcal{F}}(\mathfrak{e})}(\mathrm{x}) = 1, \quad \mathrm{RT}_{\tilde{\mathcal{F}}(\mathfrak{e})}(\mathrm{x}) = 1, \quad \mathrm{C}_{\tilde{\mathcal{F}}(\mathfrak{e})}(\mathrm{x}) = 1, \quad \forall \mathfrak{e} \in \acute{\mathcal{E}}, \forall \mathrm{x} \in \mathbb{X},$$

$$RF_{\tilde{\mathcal{F}}(\mathfrak{e})}(x) = 0, \quad F_{\tilde{\mathcal{F}}(\mathfrak{e})}(x) = 0, \quad \forall \mathfrak{e} \in \acute{\mathcal{E}}, \forall x \in \mathbb{X}.$$

Clearly,

$$0^c_{(\mathbb{X},\acute{\mathcal{E}})} = 1_{(\mathbb{X},\acute{\mathcal{E}})}, \quad 1^c_{(\mathbb{X},\acute{\mathcal{E}})} = 0_{(\mathbb{X},\acute{\mathcal{E}})}.$$

Proposition 1. *Let $(\tilde{\mathcal{F}}_1,\acute{\mathcal{E}})$, $(\tilde{\mathcal{F}}_2,\acute{\mathcal{E}})$ and $(\tilde{\mathcal{F}}_3,\acute{\mathcal{E}})$ be three CTVNS sets over the universe set $\mathbb{X}$. Then,*

(i). $(\tilde{\mathcal{F}}_1,\acute{\mathcal{E}})\Cup[(\tilde{\mathcal{F}}_2,\acute{\mathcal{E}})\Cup(\tilde{\mathcal{F}}_3,\acute{\mathcal{E}})] = [(\tilde{\mathcal{F}}_1,\acute{\mathcal{E}})\Cup(\tilde{\mathcal{F}}_2,\acute{\mathcal{E}})]\Cup(\tilde{\mathcal{F}}_3,\acute{\mathcal{E}})$ *and* $(\tilde{\mathcal{F}}_1,\acute{\mathcal{E}})\Cap[(\tilde{\mathcal{F}}_2,\acute{\mathcal{E}})\Cap(\tilde{\mathcal{F}}_3,\acute{\mathcal{E}})] = [(\tilde{\mathcal{F}}_1,\acute{\mathcal{E}})\Cap(\tilde{\mathcal{F}}_2,\acute{\mathcal{E}})]\Cap(\tilde{\mathcal{F}}_3,\acute{\mathcal{E}})$;

(ii). $(\tilde{\mathcal{F}}_1,\acute{\mathcal{E}})\Cup[(\tilde{\mathcal{F}}_2,\acute{\mathcal{E}})\Cap(\tilde{\mathcal{F}}_3,\acute{\mathcal{E}})] = [(\tilde{\mathcal{F}}_1,\acute{\mathcal{E}})\Cup(\tilde{\mathcal{F}}_2,\acute{\mathcal{E}})]\Cap[(\tilde{\mathcal{F}}_1,\acute{\mathcal{E}})\Cup(\tilde{\mathcal{F}}_3,\acute{\mathcal{E}})]$ *and* $(\tilde{\mathcal{F}}_1,\acute{\mathcal{E}}) \Cap [(\tilde{\mathcal{F}}_2,\acute{\mathcal{E}}) \Cup (\tilde{\mathcal{F}}_3,\acute{\mathcal{E}})] = [(\tilde{\mathcal{F}}_1,\acute{\mathcal{E}}) \Cap (\tilde{\mathcal{F}}_2,\acute{\mathcal{E}})] \Cup [(\tilde{\mathcal{F}}_1,\acute{\mathcal{E}}) \Cap (\tilde{\mathcal{F}}_3,\acute{\mathcal{E}})]$;

(iii). $(\tilde{\mathcal{F}}_1,\acute{\mathcal{E}}) \Cup 0_{(\mathbb{X},\acute{\mathcal{E}})} = (\tilde{\mathcal{F}}_1,\acute{\mathcal{E}})$ *and* $(\tilde{\mathcal{F}}_1,\acute{\mathcal{E}}) \Cap 0_{(\mathbb{X},\acute{\mathcal{E}})} = 0_{(\mathbb{X},\acute{\mathcal{E}})}$;

(iv). $(\tilde{\mathcal{F}}_1,\acute{\mathcal{E}}) \Cup 1_{(\mathbb{X},\acute{\mathcal{E}})} = 1_{(\mathbb{X},\acute{\mathcal{E}})}$ *and* $(\tilde{\mathcal{F}}_1,\acute{\mathcal{E}}) \Cap 1_{(\mathbb{X},\acute{\mathcal{E}})} = (\tilde{\mathcal{F}}_1,\acute{\mathcal{E}})$.

Proof. Obvious. □

Proposition 2. *Let $(\tilde{\mathcal{F}}_1,\acute{\mathcal{E}})$ and $(\tilde{\mathcal{F}}_2,\acute{\mathcal{E}})$ be two CTVNS sets over the universe set $\mathbb{X}$. Then,*

(i). $[(\tilde{\mathcal{F}}_1,\acute{\mathcal{E}}) \Cup (\tilde{\mathcal{F}}_2,\acute{\mathcal{E}})]^c = (\tilde{\mathcal{F}}_1,\acute{\mathcal{E}})^c \Cap (\tilde{\mathcal{F}}_2,\acute{\mathcal{E}})^c$.

(ii). $[(\tilde{\mathcal{F}}_1,\acute{\mathcal{E}}) \Cap (\tilde{\mathcal{F}}_2,\acute{\mathcal{E}})]^c = (\tilde{\mathcal{F}}_1,\acute{\mathcal{E}})^c \Cup (\tilde{\mathcal{F}}_2,\acute{\mathcal{E}})^c$.

Proof. (i). For all $\mathfrak{e} \in \acute{\mathcal{E}}$ and $x \in \mathbb{X}$,

$$\begin{aligned}(\tilde{\mathcal{F}}_1,\acute{\mathcal{E}}) \Cup (\tilde{\mathcal{F}}_2,\acute{\mathcal{E}}) = \{\langle x, &\max\{T_{\tilde{\mathcal{F}}_1(\mathfrak{e})}(x), T_{\tilde{\mathcal{F}}_2(\mathfrak{e})}(x)\},\\ &\max\{RT_{\tilde{\mathcal{F}}_1(\mathfrak{e})}(x), RT_{\tilde{\mathcal{F}}_2(\mathfrak{e})}(x)\}, \max\{C_{\tilde{\mathcal{F}}_1(\mathfrak{e})}(x), C_{\tilde{\mathcal{F}}_2(\mathfrak{e})}(x)\},\\ &\min\{RF_{\tilde{\mathcal{F}}_1(\mathfrak{e})}(x), RF_{\tilde{\mathcal{F}}_2(\mathfrak{e})}(x)\}, \min\{F_{\tilde{\mathcal{F}}_1(\mathfrak{e})}(x), F_{\tilde{\mathcal{F}}_2(\mathfrak{e})}(x)\}\rangle\},\end{aligned}$$

$$\begin{aligned}[(\tilde{\mathcal{F}}_1,\acute{\mathcal{E}}) \Cup (\tilde{\mathcal{F}}_2,\acute{\mathcal{E}})]^c = \{\langle x, &\min\{F_{\tilde{\mathcal{F}}_1(\mathfrak{e})}(x), F_{\tilde{\mathcal{F}}_2(\mathfrak{e})}(x)\},\\ &\min\{RF_{\tilde{\mathcal{F}}_1(\mathfrak{e})}(x), RF_{\tilde{\mathcal{F}}_2(\mathfrak{e})}(x)\},\\ &1 - \max\{C_{\tilde{\mathcal{F}}_1(\mathfrak{e})}(x), C_{\tilde{\mathcal{F}}_2(\mathfrak{e})}(x)\},\\ &\max\{RT_{\tilde{\mathcal{F}}_1(\mathfrak{e})}(x), RT_{\tilde{\mathcal{F}}_2(\mathfrak{e})}(x)\},\\ &\max\{T_{\tilde{\mathcal{F}}_1(\mathfrak{e})}(x), T_{\tilde{\mathcal{F}}_2(\mathfrak{e})}(x)\}\rangle\}.\end{aligned}$$

Now,

$$(\tilde{\mathcal{F}}_1,\acute{\mathcal{E}})^c = \{\langle \begin{matrix} x, F_{\tilde{\mathcal{F}}_1(\mathfrak{e})}(x), RF_{\tilde{\mathcal{F}}_1(\mathfrak{e})}(x), 1 - C_{\tilde{\mathcal{F}}_1(\mathfrak{e})}(x), \\ RT_{\tilde{\mathcal{F}}_1(\mathfrak{e})}(x), T_{\tilde{\mathcal{F}}_1(\mathfrak{e})}(x) \end{matrix} \rangle\},$$

$$(\tilde{\mathcal{F}}_2,\acute{\mathcal{E}})^c = \{\langle \begin{matrix} x, F_{\tilde{\mathcal{F}}_2(\mathfrak{e})}(x), RF_{\tilde{\mathcal{F}}_2(\mathfrak{e})}(x), 1 - C_{\tilde{\mathcal{F}}_2(\mathfrak{e})}(x), \\ RT_{\tilde{\mathcal{F}}_2(\mathfrak{e})}(x), T_{\tilde{\mathcal{F}}_2(\mathfrak{e})}(x) \end{matrix} \rangle\}.$$

Then,

$$\begin{aligned}(\tilde{\mathcal{F}}_1,\acute{\mathcal{E}})^c \Cap (\tilde{\mathcal{F}}_2,\acute{\mathcal{E}})^c = \{\langle x, &\min\{F_{\tilde{\mathcal{F}}_1(\mathfrak{e})}(x), F_{\tilde{\mathcal{F}}_2(\mathfrak{e})}(x)\},\\ &\min\{RF_{\tilde{\mathcal{F}}_1(\mathfrak{e})}(x), RF_{\tilde{\mathcal{F}}_2(\mathfrak{e})}(x)\},\\ &\min\{1 - C_{\tilde{\mathcal{F}}_1(\mathfrak{e})}(x), 1 - C_{\tilde{\mathcal{F}}_2(\mathfrak{e})}(x)\},\\ &\max\{RT_{\tilde{\mathcal{F}}_1(\mathfrak{e})}(x), RT_{\tilde{\mathcal{F}}_2(\mathfrak{e})}(x)\},\\ &\max\{T_{\tilde{\mathcal{F}}_1(\mathfrak{e})}(x), T_{\tilde{\mathcal{F}}_2(\mathfrak{e})}(x)\}\rangle\}\end{aligned}$$

$$\begin{aligned}(\tilde{\mathcal{F}}_1,\acute{\mathcal{E}})^c \Cap (\tilde{\mathcal{F}}_2,\acute{\mathcal{E}})^c = \{\langle x, &\min\{F_{\tilde{\mathcal{F}}_1(\mathfrak{e})}(x), F_{\tilde{\mathcal{F}}_2(\mathfrak{e})}(x)\},\\ &\min\{RF_{\tilde{\mathcal{F}}_1(\mathfrak{e})}(x), RF_{\tilde{\mathcal{F}}_2(\mathfrak{e})}(x)\},\\ &1 - \max\{C_{\tilde{\mathcal{F}}_1(\mathfrak{e})}(x), C_{\tilde{\mathcal{F}}_2(\mathfrak{e})}(x)\},\\ &\max\{RT_{\tilde{\mathcal{F}}_1(\mathfrak{e})}(x), RT_{\tilde{\mathcal{F}}_2(\mathfrak{e})}(x)\},\\ &\max\{T_{\tilde{\mathcal{F}}_1(\mathfrak{e})}(x), T_{\tilde{\mathcal{F}}_2(\mathfrak{e})}(x)\}\rangle\}.\end{aligned}$$

Therefore, $[(\tilde{\mathcal{F}}_1,\acute{\mathcal{E}}) \Cup (\tilde{\mathcal{F}}_2,\acute{\mathcal{E}})]^c = (\tilde{\mathcal{F}}_1,\acute{\mathcal{E}})^c \Cap (\tilde{\mathcal{F}}_2,\acute{\mathcal{E}})^c$.
(ii). It is obtained in a similar way. □

Proposition 3. *Let $(\tilde{\mathcal{F}}_1,\acute{\mathcal{E}})$ and $(\tilde{\mathcal{F}}_2,\acute{\mathcal{E}})$ be two CTVNS sets over the universe set $\mathbb{X}$. Then,*

(i). $[(\tilde{\mathcal{F}}_1,\acute{\mathcal{E}}) \vee (\tilde{\mathcal{F}}_2,\acute{\mathcal{E}})]^c = (\tilde{\mathcal{F}}_1,\acute{\mathcal{E}})^c \wedge (\tilde{\mathcal{F}}_2,\acute{\mathcal{E}})^c$.

(ii). $[(\tilde{\mathcal{F}}_1,\acute{\mathcal{E}}) \wedge (\tilde{\mathcal{F}}_2,\acute{\mathcal{E}})]^c = (\tilde{\mathcal{F}}_1,\acute{\mathcal{E}})^c \vee (\tilde{\mathcal{F}}_2,\acute{\mathcal{E}})^c$.

Proof. (i). For all $\mathfrak{e} \in \acute{\mathcal{E}}$ and $x \in \mathbb{X}$,

$$\begin{aligned}(\tilde{\mathcal{F}}_1,\acute{\mathcal{E}}) \vee (\tilde{\mathcal{F}}_2,\acute{\mathcal{E}}) = \{\langle x, &\max\{T_{\tilde{\mathcal{F}}_1(\mathfrak{e})}(x), T_{\tilde{\mathcal{F}}_2(\mathfrak{e})}(x)\},\\ &\max\{RT_{\tilde{\mathcal{F}}_1(\mathfrak{e})}(x), RT_{\tilde{\mathcal{F}}_2(\mathfrak{e})}(x)\},\\ &\max\{C_{\tilde{\mathcal{F}}_1(\mathfrak{e})}(x), C_{\tilde{\mathcal{F}}_2(\mathfrak{e})}(x)\},\\ &\min\{RF_{\tilde{\mathcal{F}}_1(\mathfrak{e})}(x), RF_{\tilde{\mathcal{F}}_2(\mathfrak{e})}(x)\},\\ &\min\{F_{\tilde{\mathcal{F}}_1(\mathfrak{e})}(x), F_{\tilde{\mathcal{F}}_2(\mathfrak{e})}(x)\}\rangle\},\end{aligned}$$

$$\begin{aligned}[(\tilde{\mathcal{F}}_1,\acute{\mathcal{E}}) \vee (\tilde{\mathcal{F}}_2,\acute{\mathcal{E}})]^c = \{\langle x, &\min\{F_{\tilde{\mathcal{F}}_1(\mathfrak{e})}(x), F_{\tilde{\mathcal{F}}_2(\mathfrak{e})}(x)\},\\ &\min\{RF_{\tilde{\mathcal{F}}_1(\mathfrak{e})}(x), RF_{\tilde{\mathcal{F}}_2(\mathfrak{e})}(x)\},\\ &1 - \max\{C_{\tilde{\mathcal{F}}_1(\mathfrak{e})}(x), C_{\tilde{\mathcal{F}}_2(\mathfrak{e})}(x)\},\\ &\max\{RT_{\tilde{\mathcal{F}}_1(\mathfrak{e})}(x), RT_{\tilde{\mathcal{F}}_2(\mathfrak{e})}(x)\},\\ &\max\{T_{\tilde{\mathcal{F}}_1(\mathfrak{e})}(x), T_{\tilde{\mathcal{F}}_2(\mathfrak{e})}(x)\}\rangle\}.\end{aligned}$$

Now,

$$(\tilde{\mathcal{F}}_1,\acute{\mathcal{E}})^c = \{\langle \begin{matrix} x, F_{\tilde{\mathcal{F}}_1(\mathfrak{e})}(x), RF_{\tilde{\mathcal{F}}_1(\mathfrak{e})}(x), 1 - C_{\tilde{\mathcal{F}}_1(\mathfrak{e})}(x), \\ RT_{\tilde{\mathcal{F}}_1(\mathfrak{e})}(x), T_{\tilde{\mathcal{F}}_1(\mathfrak{e})}(x) \end{matrix} \rangle\},$$

$$(\tilde{\mathcal{F}}_2,\acute{\mathcal{E}})^c = \{\langle \begin{matrix} x, F_{\tilde{\mathcal{F}}_2(\mathfrak{e})}(x), RF_{\tilde{\mathcal{F}}_2(\mathfrak{e})}(x), 1 - C_{\tilde{\mathcal{F}}_2(\mathfrak{e})}(x), \\ RT_{\tilde{\mathcal{F}}_2(\mathfrak{e})}(x), T_{\tilde{\mathcal{F}}_2(\mathfrak{e})}(x) \end{matrix} \rangle\}.$$

Then,

$$\begin{aligned}(\tilde{\mathcal{F}}_1,\acute{\mathcal{E}})^c \wedge (\tilde{\mathcal{F}}_2,\acute{\mathcal{E}})^c = \{\langle x, &\min\{F_{\tilde{\mathcal{F}}_1(\mathfrak{e})}(x), F_{\tilde{\mathcal{F}}_2(\mathfrak{e})}(x)\},\\ &\min\{RF_{\tilde{\mathcal{F}}_1(\mathfrak{e})}(x), RF_{\tilde{\mathcal{F}}_2(\mathfrak{e})}(x)\},\\ &\min\{1 - C_{\tilde{\mathcal{F}}_1(\mathfrak{e})}(x), 1 - C_{\tilde{\mathcal{F}}_2(\mathfrak{e})}(x)\},\\ &\max\{RT_{\tilde{\mathcal{F}}_1(\mathfrak{e})}(x), RT_{\tilde{\mathcal{F}}_2(\mathfrak{e})}(x)\},\\ &\max\{T_{\tilde{\mathcal{F}}_1(\mathfrak{e})}(x), T_{\tilde{\mathcal{F}}_2(\mathfrak{e})}(x)\}\rangle\}\end{aligned}$$

$$\begin{aligned}(\tilde{\mathcal{F}}_1,\acute{\mathcal{E}})^c \wedge (\tilde{\mathcal{F}}_2,\acute{\mathcal{E}})^c = \{\langle x, &\min\{F_{\tilde{\mathcal{F}}_1(\mathfrak{e})}(x), F_{\tilde{\mathcal{F}}_2(\mathfrak{e})}(x)\},\\ &\min\{RF_{\tilde{\mathcal{F}}_1(\mathfrak{e})}(x), RF_{\tilde{\mathcal{F}}_2(\mathfrak{e})}(x)\},\\ &1 - \max\{C_{\tilde{\mathcal{F}}_1(\mathfrak{e})}(x), C_{\tilde{\mathcal{F}}_2(\mathfrak{e})}(x)\},\end{aligned}$$

$$\max\{\mathrm{RT}_{\tilde{\mathcal{F}}_1(\mathrm{e})}(\mathrm{x}), \mathrm{RT}_{\tilde{\mathcal{F}}_2(\mathrm{e})}(\mathrm{x})\},$$
$$\max\{\mathrm{T}_{\tilde{\mathcal{F}}_1(\mathrm{e})}(\mathrm{x}), \mathrm{T}_{\tilde{\mathcal{F}}_2(\mathrm{e})}(\mathrm{x})\}\rangle\}.$$

Therefore, $[(\tilde{\mathcal{F}}_1, \acute{\mathcal{E}}) \vee (\tilde{\mathcal{F}}_2, \acute{\mathcal{E}})]^c = (\tilde{\mathcal{F}}_1, \acute{\mathcal{E}})^c \wedge (\tilde{\mathcal{F}}_2, \acute{\mathcal{E}})^c$.
(ii). It is obtained in a similar way. □

Example 3.1. *Suppose that, the universe set* $\mathbb{X}$ *given by* $\mathbb{X} = \{\mathrm{x}_1, \mathrm{x}_2, \mathrm{x}_3, \mathrm{x}_4\}$ *and the set of parameters* $\mathcal{E} = (\mathrm{e}_1, \mathrm{e}_2)$. *Let us consider CTVNS sets* $(\tilde{\mathcal{F}}_1, \acute{\mathcal{E}})$*and*$(\tilde{\mathcal{F}}_2, \acute{\mathcal{E}})$ *over the universe set* $\mathbb{X}$ *as follows*

$$(\tilde{\mathcal{F}}_1, \acute{\mathcal{E}}) = \begin{bmatrix} \mathrm{e}_1 = \langle \mathrm{x}_1, 0.3e^{\iota\pi(0.2)}, 0.4e^{\iota\pi(0.3)}, 0.5e^{\iota\pi(0.3)}, 0.3e^{\iota\pi(0.2)}, 0.6e^{\iota\pi(0.5)}\rangle, \\ \langle \mathrm{x}_2, 0.4e^{\iota\pi(0.3)}, 0.2e^{\iota\pi(0.1)}, 0.4e^{\iota\pi(0.4)}, 0.1e^{\iota\pi(0.1)}, 0.8e^{\iota\pi(0.7)}\rangle, \\ \langle \mathrm{x}_3, 0.6e^{\iota\pi(0.5)}, 0.2e^{\iota\pi(0.1)}, 0.3e^{\iota\pi(0.3)}, 0.2e^{\iota\pi(0.1)}, 0.5e^{\iota\pi(0.4)}\rangle, \\ \langle \mathrm{x}_4, 0.2e^{\iota\pi(0.1)}, 0.3e^{\iota\pi(0.2)}, 0.6e^{\iota\pi(0.5)}, 0.2e^{\iota\pi(0.1)}, 0.4e^{\iota\pi(0.3)}\rangle \\ \mathrm{e}_2 = \langle \mathrm{x}_1, 0.4e^{\iota\pi(0.3)}, 0.3e^{\iota\pi(0.2)}, 0.4e^{\iota\pi(0.2)}, 0.3e^{\iota\pi(0.2)}, 0.8e^{\iota\pi(0.7)}\rangle, \\ \langle \mathrm{x}_2, 0.3e^{\iota\pi(0.2)}, 0.4e^{\iota\pi(0.3)}, 0.5e^{\iota\pi(0.3)}, 0.3e^{\iota\pi(0.2)}, 0.2e^{\iota\pi(0.1)}\rangle, \\ \langle \mathrm{x}_3, 0.3e^{\iota\pi(0.2)}, 0.2e^{\iota\pi(0.1)}, 0.6e^{\iota\pi(0.7)}, 0.1e^{\iota\pi(0.1)}, 0.7e^{\iota\pi(0.6)}\rangle, \\ \langle \mathrm{x}_4, 0.1e^{\iota\pi(0.1)}, 0.2e^{\iota\pi(0.1)}, 0.4e^{\iota\pi(0.3)}, 0.2e^{\iota\pi(0.1)}, 0.9e^{\iota\pi(0.8)}\rangle \end{bmatrix},$$

$$(\tilde{\mathcal{F}}_2, \acute{\mathcal{E}}) = \begin{bmatrix} \mathrm{e}_1 = \langle \mathrm{x}_1, 0.6e^{\iota\pi(0.5)}, 0.3e^{\iota\pi(0.2)}, 0.7e^{\iota\pi(0.6)}, 0.3e^{\iota\pi(0.2)}, 0.8e^{\iota\pi(0.7)}\rangle, \\ \langle \mathrm{x}_2, 0.2e^{\iota\pi(0.1)}, 0.5e^{\iota\pi(0.4)}, 0.6e^{\iota\pi(0.3)}, 0.4e^{\iota\pi(0.3)}, 0.8e^{\iota\pi(0.7)}\rangle, \\ \langle \mathrm{x}_3, 0.1e^{\iota\pi(0.1)}, 0.1e^{\iota\pi(0.1)}, 0.2e^{\iota\pi(0.3)}, 0.1e^{\iota\pi(0.1)}, 0.4e^{\iota\pi(0.3)}\rangle, \\ \langle \mathrm{x}_4, 0.5e^{\iota\pi(0.4)}, 0.2e^{\iota\pi(0.1)}, 0.4e^{\iota\pi(0.4)}, 0.2e^{\iota\pi(0.1)}, 0.3e^{\iota\pi(0.2)}\rangle \\ \mathrm{e}_2 = \langle \mathrm{x}_1, 0.7e^{\iota\pi(0.6)}, 0.5e^{\iota\pi(0.4)}, 0.8e^{\iota\pi(0.3)}, 0.4e^{\iota\pi(0.3)}, 0.6e^{\iota\pi(0.5)}\rangle, \\ \langle \mathrm{x}_2, 0.4e^{\iota\pi(0.3)}, 0.2e^{\iota\pi(0.1)}, 0.6e^{\iota\pi(0.6)}, 0.2e^{\iota\pi(0.1)}, 0.3e^{\iota\pi(0.2)}\rangle, \\ \langle \mathrm{x}_3, 0.5e^{\iota\pi(0.4)}, 0.3e^{\iota\pi(0.2)}, 0.3e^{\iota\pi(0.3)}, 0.2e^{\iota\pi(0.1)}, 0.4e^{\iota\pi(0.3)}\rangle, \\ \langle \mathrm{x}_4, 0.4e^{\iota\pi(0.3)}, 0.2e^{\iota\pi(0.1)}, 0.4e^{\iota\pi(0.5)}, 0.1e^{\iota\pi(0.1)}, 0.6e^{\iota\pi(0.5)}\rangle \end{bmatrix}.$$

Then, their union, intersection, AND, and OR operations are given as follows:

$$(\tilde{\mathcal{F}}_1, \acute{\mathcal{E}}) \uplus (\tilde{\mathcal{F}}_2, \acute{\mathcal{E}}) = \begin{bmatrix} \mathrm{e}_1 = \langle \mathrm{x}_1, \frac{0.6e^{\iota\pi(0.5)}, 0.4e^{\iota\pi(0.3)}, 0.7e^{\iota\pi(0.6)}, 0.3e^{\iota\pi(0.2)}}{0.6e^{\iota\pi(0.5)}}\rangle, \\ \langle \mathrm{x}_2, \frac{0.4e^{\iota\pi(0.3)}, 0.5e^{\iota\pi(0.4)}, 0.6e^{\iota\pi(0.3)}, 0.1e^{\iota\pi(0.1)}}{0.8e^{\iota\pi(0.7)}}\rangle, \\ \langle \mathrm{x}_3, \frac{0.6e^{\iota\pi(0.5)}, 0.2e^{\iota\pi(0.1)}, 0.3e^{\iota\pi(0.3)}, 0.1e^{\iota\pi(0.1)}}{0.4e^{\iota\pi(0.3)}}\rangle, \\ \langle \mathrm{x}_4, \frac{0.5e^{\iota\pi(0.4)}, 0.3e^{\iota\pi(0.2)}, 0.6e^{\iota\pi(0.5)}, 0.2e^{\iota\pi(0.1)}}{0.3e^{\iota\pi(0.2)}}\rangle \\ \mathrm{e}_2 = \langle \mathrm{x}_1, \frac{0.7e^{\iota\pi(0.6)}, 0.5e^{\iota\pi(0.4)}, 0.8e^{\iota\pi(0.3)}, 0.3e^{\iota\pi(0.2)}}{0.6e^{\iota\pi(0.5)}}\rangle, \\ \langle \mathrm{x}_2, \frac{0.4e^{\iota\pi(0.3)}, 0.4e^{\iota\pi(0.3)}, 0.6e^{\iota\pi(0.6)}, 0.2e^{\iota\pi(0.1)}}{0.2e^{\iota\pi(0.1)}}\rangle, \\ \langle \mathrm{x}_3, \frac{0.5e^{\iota\pi(0.4)}, 0.3e^{\iota\pi(0.2)}, 0.6e^{\iota\pi(0.7)}, 0.1e^{\iota\pi(0.1)}}{0.4e^{\iota\pi(0.3)}}\rangle, \\ \langle \mathrm{x}_4, \frac{0.4e^{\iota\pi(0.3)}, 0.2e^{\iota\pi(0.1)}, 0.4e^{\iota\pi(0.5)}, 0.1e^{\iota\pi(0.1)}}{0.6e^{\iota\pi(0.5)}}\rangle \end{bmatrix},$$

$$(\tilde{\mathcal{F}}_1, \acute{\mathcal{E}}) \Cap (\tilde{\mathcal{F}}_2, \acute{\mathcal{E}}) = \begin{bmatrix} \mathrm{e}_1 = \langle \mathrm{x}_1, \frac{0.3e^{\iota\pi(0.2)}, 0.3e^{\iota\pi(0.3)}, 0.5e^{\iota\pi(0.3)}, 0.3e^{\iota\pi(0.2)}}{0.8e^{\iota\pi(0.7)}}\rangle, \\ \langle \mathrm{x}_2, 0.2e^{\iota\pi(0.1)}, 0.2e^{\iota\pi(0.1)}, 0.4e^{\iota\pi(0.4)}, 0.4e^{\iota\pi(0.3)}, \quad 0.8e^{\iota\pi(0.7)}\rangle, \\ \langle \mathrm{x}_3, \frac{0.1e^{\iota\pi(0.1)}, 0.1e^{\iota\pi(0.1)}, 0.2e^{\iota\pi(0.3)}, 0.2e^{\iota\pi(0.1)}}{0.5e^{\iota\pi(0.4)}}\rangle, \\ \langle \mathrm{x}_4, \frac{0.2e^{\iota\pi(0.1)}, 0.2e^{\iota\pi(0.2)}, 0.4e^{\iota\pi(0.4)}, 0.2e^{\iota\pi(0.1)}}{0.4e^{\iota\pi(0.4)}}\rangle \\ \mathrm{e}_2 = \langle \mathrm{x}_1, \frac{0.3e^{\iota\pi(0.2)}, 0.3e^{\iota\pi(0.3)}, 0.4e^{\iota\pi(0.2)}, 0.3e^{\iota\pi(0.2)}}{0.8e^{\iota\pi(0.7)}}\rangle, \\ \langle \mathrm{x}_2, \frac{0.2e^{\iota\pi(0.1)}, 0.2e^{\iota\pi(0.1)}, 0.5e^{\iota\pi(0.3)}, 0.3e^{\iota\pi(0.2)}}{0.4e^{\iota\pi(0.3)}}\rangle, \\ \langle \mathrm{x}_3, \frac{0.1e^{\iota\pi(0.1)}, 0.1e^{\iota\pi(0.1)}, 0.3e^{\iota\pi(0.3)}, 0.2e^{\iota\pi(0.1)}}{0.5e^{\iota\pi(0.4)}}\rangle, \\ \langle \mathrm{x}_4, \frac{0.2e^{\iota\pi(0.1)}, 0.2e^{\iota\pi(0.2)}, 0.4e^{\iota\pi(0.3)}, 0.2e^{\iota\pi(0.1)}}{0.4e^{\iota\pi(0.3)}}\rangle \end{bmatrix},$$

$$(\tilde{\mathcal{F}}_1, \acute{\mathcal{E}}) \setminus (\tilde{\mathcal{F}}_2, \acute{\mathcal{E}}) = \begin{bmatrix} \mathrm{e}_1 = \langle \mathrm{x}_1, \frac{0.3e^{\iota\pi(0.2)}, 0.3e^{\iota\pi(0.2)}, 0.5e^{\iota\pi(0.3)}, 0.3e^{\iota\pi(0.2)}}{0.6e^{\iota\pi(0.5)}}\rangle, \\ \langle \mathrm{x}_2, \frac{0.4e^{\iota\pi(0.3)}, 0.2e^{\iota\pi(0.1)}, 0.4e^{\iota\pi(0.4)}, 0.5e^{\iota\pi(0.4)}}{0.8e^{\iota\pi(0.7)}}\rangle, \\ \langle \mathrm{x}_3, \frac{0.4e^{\iota\pi(0.3)}, 0.1e^{\iota\pi(0.1)}, 0.2e^{\iota\pi(0.3)}, 0.2e^{\iota\pi(0.1)}}{0.5e^{\iota\pi(0.4)}}\rangle, \\ \langle \mathrm{x}_4, \frac{0.2e^{\iota\pi(0.1)}, 0.2e^{\iota\pi(0.1)}, 0.4e^{\iota\pi(0.4)}, 0.2e^{\iota\pi(0.1)}}{0.5e^{\iota\pi(0.4)}}\rangle \\ \mathrm{e}_2 = \langle \mathrm{x}_1, \frac{0.4e^{\iota\pi(0.3)}, 0.3e^{\iota\pi(0.2)}, 0.4e^{\iota\pi(0.2)}, 0.5e^{\iota\pi(0.4)}}{0.8e^{\iota\pi(0.7)}}\rangle, \\ \langle \mathrm{x}_2, \frac{0.3e^{\iota\pi(0.2)}, 0.2e^{\iota\pi(0.1)}, 0.5e^{\iota\pi(0.3)}, 0.3e^{\iota\pi(0.2)}}{0.4e^{\iota\pi(0.3)}}\rangle, \\ \langle \mathrm{x}_3, \frac{0.3e^{\iota\pi(0.2)}, 0.2e^{\iota\pi(0.1)}, 0.3e^{\iota\pi(0.3)}, 0.3e^{\iota\pi(0.2)}}{0.7e^{\iota\pi(0.6)}}\rangle, \\ \langle \mathrm{x}_4, \frac{0.1e^{\iota\pi(0.1)}, 0.1e^{\iota\pi(0.1)}, 0.4e^{\iota\pi(0.3)}, 0.2e^{\iota\pi(0.1)}}{0.9e^{\iota\pi(0.8)}}\rangle \end{bmatrix},$$

$$(\tilde{\mathcal{F}}_1, \acute{\mathcal{E}}) \wedge (\tilde{\mathcal{F}}_2, \acute{\mathcal{E}}) = \begin{bmatrix} (\mathrm{e}_1, \mathrm{e}_1) = \langle \mathrm{x}_1, \frac{0.3e^{\iota\pi(0.2)}, 0.3e^{\iota\pi(0.3)}, 0.5e^{\iota\pi(0.3)}, 0.3e^{\iota\pi(0.2)}}{0.8e^{\iota\pi(0.7)}}\rangle, \\ \langle \mathrm{x}_2, \frac{0.2e^{\iota\pi(0.1)}, 0.2e^{\iota\pi(0.1)}, 0.4e^{\iota\pi(0.4)}, 0.4e^{\iota\pi(0.3)}}{0.8e^{\iota\pi(0.7)}}\rangle, \\ \langle \mathrm{x}_3, \frac{0.1e^{\iota\pi(0.1)}, 0.1e^{\iota\pi(0.1)}, 0.2e^{\iota\pi(0.3)}, 0.2e^{\iota\pi(0.1)}}{0.5e^{\iota\pi(0.4)}}\rangle, \\ \langle \mathrm{x}_4, \frac{0.2e^{\iota\pi(0.1)}, 0.2e^{\iota\pi(0.2)}, 0.4e^{\iota\pi(0.4)}, 0.2e^{\iota\pi(0.1)}}{0.4e^{\iota\pi(0.4)}}\rangle \\ \mathrm{e}_2 = \langle \mathrm{x}_1, \frac{0.3e^{\iota\pi(0.2)}, 0.3e^{\iota\pi(0.3)}, 0.4e^{\iota\pi(0.2)}, 0.3e^{\iota\pi(0.2)}}{0.8e^{\iota\pi(0.7)}}\rangle, \\ (\mathrm{e}_1, \mathrm{e}_2) = \langle \mathrm{x}_1, \frac{0.3e^{\iota\pi(0.2)}, 0.4e^{\iota\pi(0.3)}, 0.5e^{\iota\pi(0.3)}, 0.4e^{\iota\pi(0.3)}}{0.6e^{\iota\pi(0.5)}}\rangle, \\ \langle \mathrm{x}_2, \frac{0.4e^{\iota\pi(0.3)}, 0.2e^{\iota\pi(0.1)}, 0.4e^{\iota\pi(0.4)}, 0.2e^{\iota\pi(0.1)}}{0.8e^{\iota\pi(0.7)}}\rangle, \\ \langle \mathrm{x}_3, \frac{0.5e^{\iota\pi(0.4)}, 0.2e^{\iota\pi(0.1)}, 0.3e^{\iota\pi(0.3)}, 0.2e^{\iota\pi(0.1)}}{0.5e^{\iota\pi(0.4)}}\rangle, \\ \langle \mathrm{x}_4, \frac{0.2e^{\iota\pi(0.1)}, 0.2e^{\iota\pi(0.1)}, 0.4e^{\iota\pi(0.5)}, 0.2e^{\iota\pi(0.1)}}{0.6e^{\iota\pi(0.5)}}\rangle \\ (\mathrm{e}_2, \mathrm{e}_1) = \langle \mathrm{x}_1, \frac{0.4e^{\iota\pi(0.3)}, 0.3e^{\iota\pi(0.2)}, 0.4e^{\iota\pi(0.2)}, 0.3e^{\iota\pi(0.2)}}{0.8e^{\iota\pi(0.7)}}\rangle, \\ \langle \mathrm{x}_2, \frac{0.2e^{\iota\pi(0.1)}, 0.4e^{\iota\pi(0.3)}, 0.5e^{\iota\pi(0.3)}, 0.4e^{\iota\pi(0.3)}}{0.8e^{\iota\pi(0.7)}}\rangle, \\ \langle \mathrm{x}_3, \frac{0.1e^{\iota\pi(0.1)}, 0.1e^{\iota\pi(0.1)}, 0.2e^{\iota\pi(0.3)}, 0.1e^{\iota\pi(0.1)}}{0.7e^{\iota\pi(0.6)}}\rangle, \\ \langle \mathrm{x}_4, \frac{0.1e^{\iota\pi(0.1)}, 0.2e^{\iota\pi(0.1)}, 0.4e^{\iota\pi(0.3)}, 0.2e^{\iota\pi(0.1)}}{0.9e^{\iota\pi(0.8)}}\rangle \\ (\mathrm{e}_2, \mathrm{e}_2) = \langle \mathrm{x}_1, \frac{0.3e^{\iota\pi(0.2)}, 0.3e^{\iota\pi(0.3)}, 0.4e^{\iota\pi(0.2)}, 0.3e^{\iota\pi(0.2)}}{0.8e^{\iota\pi(0.7)}}\rangle, \\ \langle \mathrm{x}_2, \frac{0.2e^{\iota\pi(0.1)}, 0.2e^{\iota\pi(0.1)}, 0.5e^{\iota\pi(0.3)}, 0.4e^{\iota\pi(0.3)}}{0.8e^{\iota\pi(0.7)}}\rangle, \\ \langle \mathrm{x}_3, \frac{0.1e^{\iota\pi(0.1)}, 0.1e^{\iota\pi(0.1)}, 0.3e^{\iota\pi(0.3)}, 0.2e^{\iota\pi(0.1)}}{0.5e^{\iota\pi(0.4)}}\rangle, \\ \langle \mathrm{x}_4, \frac{0.2e^{\iota\pi(0.1)}, 0.2e^{\iota\pi(0.2)}, 0.4e^{\iota\pi(0.3)}, 0.2e^{\iota\pi(0.1)}}{0.4e^{\iota\pi(0.3)}}\rangle \end{bmatrix},$$

$$(\tilde{\mathcal{F}_1},\acute{\mathcal{E}}) \vee (\tilde{\mathcal{F}_2},\acute{\mathcal{E}}) = \begin{bmatrix} (e_1,e_1) = \langle x_1, \frac{0.6e^{\iota\pi(0.5)}, 0.4e^{\iota\pi(0.3)}, 0.7e^{\iota\pi(0.6)}}{0.3e^{\iota\pi(0.2)}, 0.6e^{\iota\pi(0.5)}}\rangle, \\ \langle x_2, \frac{0.4e^{\iota\pi(0.3)}, 0.5e^{\iota\pi(0.4)}, 0.6e^{\iota\pi(0.3)}}{0.1e^{\iota\pi(0.1)}, 0.8e^{\iota\pi(0.7)}}\rangle, \\ \langle x_3, \frac{0.6e^{\iota\pi(0.5)}, 0.2e^{\iota\pi(0.1)}, 0.3e^{\iota\pi(0.3)}}{0.1e^{\iota\pi(0.1)}, 0.4e^{\iota\pi(0.3)}}\rangle, \\ \langle x_4, \frac{0.5e^{\iota\pi(0.4)}, 0.3e^{\iota\pi(0.2)}, 0.6e^{\iota\pi(0.5)}}{0.2e^{\iota\pi(0.1)}, 0.3e^{\iota\pi(0.2)}}\rangle \\ (e_1,e_2) = \langle x_1, 0.7e^{\iota\pi(0.6)}, \frac{0.5e^{\iota\pi(0.4)}, 0.8e^{\iota\pi(0.3)}}{0.3e^{\iota\pi(0.2)}, 0.8e^{\iota\pi(0.7)}}\rangle, \\ \langle x_2, \frac{0.4e^{\iota\pi(0.3)}, 0.2e^{\iota\pi(0.1)}, 0.6e^{\iota\pi(0.6)}}{0.1e^{\iota\pi(0.1)}, 0.3e^{\iota\pi(0.2)}}\rangle, \\ \langle x_3, \frac{0.6e^{\iota\pi(0.5)}, 0.3e^{\iota\pi(0.2)}, 0.3e^{\iota\pi(0.3)}}{0.2e^{\iota\pi(0.1)}, 0.4e^{\iota\pi(0.3)}}\rangle, \\ \langle x_4, \frac{0.4e^{\iota\pi(0.3)}, 0.3e^{\iota\pi(0.2)}, 0.6e^{\iota\pi(0.5)}}{0.1e^{\iota\pi(0.1)}, 0.4e^{\iota\pi(0.3)}}\rangle \\ (e_2,e_1) = \langle x_1, \frac{0.6e^{\iota\pi(0.5)}, 0.3e^{\iota\pi(0.2)}, 0.7e^{\iota\pi(0.6)}}{0.3e^{\iota\pi(0.2)}, 0.8e^{\iota\pi(0.7)}}\rangle, \\ \langle x_2, \frac{0.3e^{\iota\pi(0.2)}, 0.5e^{\iota\pi(0.4)}, 0.6e^{\iota\pi(0.3)}}{0.3e^{\iota\pi(0.2)}, 0.2e^{\iota\pi(0.1)}}\rangle, \\ \langle x_3, \frac{0.3e^{\iota\pi(0.2)}, 0.2e^{\iota\pi(0.1)}, 0.6e^{\iota\pi(0.7)}}{0.1e^{\iota\pi(0.1)}, 0.4e^{\iota\pi(0.3)}}\rangle, \\ \langle x_4, \frac{0.5e^{\iota\pi(0.4)}, 0.2e^{\iota\pi(0.1)}, 0.4e^{\iota\pi(0.4)}}{0.2e^{\iota\pi(0.1)}, 0.3e^{\iota\pi(0.2)}}\rangle \\ (e_2,e_2) = \langle x_1, \frac{0.7e^{\iota\pi(0.6)}, 0.5e^{\iota\pi(0.4)}, 0.8e^{\iota\pi(0.3)}}{0.3e^{\iota\pi(0.2)}, 0.6e^{\iota\pi(0.5)}}\rangle, \\ \langle x_2, \frac{0.4e^{\iota\pi(0.3)}, 0.4e^{\iota\pi(0.3)}, 0.6e^{\iota\pi(0.6)}}{0.2e^{\iota\pi(0.1)}, 0.2e^{\iota\pi(0.1)}}\rangle, \\ \langle x_3, \frac{0.5e^{\iota\pi(0.4)}, 0.3e^{\iota\pi(0.2)}, 0.6e^{\iota\pi(0.7)}}{0.1e^{\iota\pi(0.1)}, 0.4e^{\iota\pi(0.3)}}\rangle, \\ \langle x_4, \frac{0.4e^{\iota\pi(0.3)}, 0.2e^{\iota\pi(0.1)}, 0.4e^{\iota\pi(0.5)}}{0.1e^{\iota\pi(0.1)}, 0.6e^{\iota\pi(0.5)}}\rangle \end{bmatrix}.$$

4. Complex triple-valued neutrosophic soft topological spaces

This section exhibits a newly defined structure, which is known as CTVN soft topological space. In addition to this, its basic operations are given. Interior and closures of CTVNS sets are defined. In continuation, the linkages between these operations are studied. Some examples are also installed for better understanding.

Definition 4.1. *Let $CTVNSS(\mathbb{X},\acute{\mathcal{E}})$ be the family of all CTVNS sets over the universe set $\mathbb{X}$ and $\tau \subset CTVNSS(\mathbb{X},\acute{\mathcal{E}})$. Then τ is said to be a CTVNS topology on $\mathbb{X}$ if*

(i). $0_{(\mathbb{X},\acute{\mathcal{E}})}$ *and* $1_{(\mathbb{X},\acute{\mathcal{E}})} \in \tau$,

(ii). *The union of any number of CTVNS sets in τ belongs to τ,*

(iii). *The intersection of a finite number of CTVNS sets in τ belongs to τ.*

Then, $(\mathbb{X},\tau,\acute{\mathcal{E}})$ is said to be a CTVNS topological space (CTVNSTS) over $\mathbb{X}$. The members of τ are called CTVNS open sets.

Definition 4.2. *Let $(\mathbb{X},\tau,\acute{\mathcal{E}})$ be a CTVNS topological space over $\mathbb{X}$ and $(\tilde{\mathcal{F}},\acute{\mathcal{E}})$ be a CTVNS set over $\mathbb{X}$. Then $(\tilde{\mathcal{F}},\acute{\mathcal{E}})$ is said to be a CTVNS closed set iff its complement is a CTVNS open set.*

Proposition 4. *Let $(\mathbb{X},\tau,\acute{\mathcal{E}})$ be a CTVNS topological space over the universe set $\mathbb{X}$. Then,*

(i). $0_{(\mathbb{X},\acute{\mathcal{E}})}$ *and* $1_{(\mathbb{X},\acute{\mathcal{E}})}$ *are CTVNS closed sets over $\mathbb{X}$,*

(ii). *The union of a finite number of CTVNS sets is a CTVNS closed set over $\mathbb{X}$,*

(iii). *The intersection of an arbitrary number of CTVNS sets is a CTVNS closed set over $\mathbb{X}$.*

Definition 4.3. *Let $CTVNSS(\mathbb{X},\acute{\mathcal{E}})$ be the family of all CTVNS sets over the universe set $\mathbb{X}$.*

(i). *If $\tau = \{0_{(\mathbb{X},\acute{\mathcal{E}})}, 1_{(\mathbb{X},\acute{\mathcal{E}})}\}$, then τ is said to be CTVNS indiscrete topology and $(\mathbb{X},\tau,\acute{\mathcal{E}})$ is said to be a CTVNS indiscrete topological space over $\mathbb{X}$.*

(ii). *If $\tau = CTVNSS(\mathbb{X},\acute{\mathcal{E}})$, then τ is said to be CTVNS discrete topology and $(\mathbb{X},\tau,\acute{\mathcal{E}})$ is said to be a CTVNS discrete topological space over $\mathbb{X}$.*

Proposition 5. *Let $(\mathbb{X},\tau_1,\acute{\mathcal{E}})$ and $(\mathbb{X},\tau_2,\acute{\mathcal{E}})$ be two CTVNS topological spaces over the same universe set $\mathbb{X}$. Then $(\mathbb{X},\tau_1 \Cap \tau_2,\acute{\mathcal{E}})$ is a CTVNS topological space over $\mathbb{X}$.*

Proof. (i). Since $0_{(\mathbb{X},\acute{\mathcal{E}})}, 1_{(\mathbb{X},\acute{\mathcal{E}})} \in \tau_1$ and $0_{(\mathbb{X},\acute{\mathcal{E}})}, 1_{(\mathbb{X},\acute{\mathcal{E}})} \in \tau_2$, then $0_{(\mathbb{X},\acute{\mathcal{E}})}, 1_{(\mathbb{X},\acute{\mathcal{E}})} \in \tau_1 \Cap \tau_2$.
(ii). Suppose that $\{(\tilde{\mathcal{F}_i},\acute{\mathcal{E}})|i \in I\}$ be a family of CTVNS sets in $\tau_1 \Cap \tau_2$.
Then $(\tilde{\mathcal{F}_i},\acute{\mathcal{E}}) \in \tau_1$ and $(\tilde{\mathcal{F}_i},\acute{\mathcal{E}}) \in \tau_2$ for all $i \in I$, so $\Cup_{i\in I}(\tilde{\mathcal{F}_i},\acute{\mathcal{E}}) \in \tau_1$ and $\Cup_{i\in I}(\tilde{\mathcal{F}_i},\acute{\mathcal{E}}) \in \tau_2$. Thus $\Cup_{i\in I}(\tilde{\mathcal{F}_i},\acute{\mathcal{E}}) \in \tau_1 \Cap \tau_2$. (iii). Let $\{(\tilde{\mathcal{F}_i},\acute{\mathcal{E}})|i = \overline{1,n}\}$ be a family of finite number of CTVNS sets in $\tau_1 \Cap \tau_2$.
Then $(\tilde{\mathcal{F}_i},\acute{\mathcal{E}}) \in \tau_1$ and $(\tilde{\mathcal{F}_i},\acute{\mathcal{E}}) \in \tau_2$ for all $i = \overline{1,n}$, so $\bigcap_{i=1}^{n}(\tilde{\mathcal{F}_i},\acute{\mathcal{E}}) \in \tau_1$ and $\bigcap_{i=1}^{n}(\tilde{\mathcal{F}_i},\acute{\mathcal{E}}) \in \tau_2$. Thus $\bigcap_{i=1}^{n}(\tilde{\mathcal{F}_i},\acute{\mathcal{E}}) \in \tau_1 \Cap \tau_2$. □

Remark 4.1. *The union of two CTVNS topologies over $\mathbb{X}$ may not be a CTVNS topology on $\mathbb{X}$.*

Example 4.1. *Let $\mathbb{X} = \{x_1,x_2,x_3\}$ be an initial universe set, $\mathcal{E} = \{e_1,e_2\}$ be a set of parameters and:*

$$\tau_1 = \{0_{(\mathbb{X},\acute{\mathcal{E}})}, 1_{(\mathbb{X},\acute{\mathcal{E}})}, (\tilde{\mathcal{F}_1},\acute{\mathcal{E}}), (\tilde{\mathcal{F}_2},\acute{\mathcal{E}}), (\tilde{\mathcal{F}_3},\acute{\mathcal{E}})\},$$
$$\tau_2 = \{0_{(\mathbb{X},\acute{\mathcal{E}})}, 1_{(\mathbb{X},\acute{\mathcal{E}})}, (\tilde{\mathcal{F}_2},\acute{\mathcal{E}}), (\tilde{\mathcal{F}_4},\acute{\mathcal{E}})\},$$

be two CTVNS topologies over $\mathbb{X}$. Here, the CTVNS sets $(\tilde{\mathcal{F}_1},\acute{\mathcal{E}})$, $(\tilde{\mathcal{F}_2},\acute{\mathcal{E}})$, $(\tilde{\mathcal{F}_3},\acute{\mathcal{E}})$ and $(\tilde{\mathcal{F}_4},\acute{\mathcal{E}})$ are defined as follows:

$$(\tilde{\mathcal{F}_1},\acute{\mathcal{E}}) = \begin{bmatrix} e_1 = \langle x_1, 0.9e^{\iota\pi(0.9)}, 0.6e^{\iota\pi(0.8)}, 0.9e^{\iota\pi(0.8)}, 0.2e^{\iota\pi(0.4)}, 0.3e^{\iota\pi(0.5)}\rangle, \\ \langle x_2, 0.7e^{\iota\pi(0.7)}, 0.6e^{\iota\pi(0.5)}, 0.8e^{\iota\pi(0.7)}, 0.3e^{\iota\pi(0.3)}, 0.5e^{\iota\pi(0.4)}\rangle \\ \langle x_3, 0.4e^{\iota\pi(0.3)}, 0.5e^{\iota\pi(0.2)}, 0.8e^{\iota\pi(0.8)}, 0.3e^{\iota\pi(0.4)}, 0.4e^{\iota\pi(0.2)}\rangle; \\ e_2 = \langle x_1, 0.7e^{\iota\pi(0.9)}, 0.3e^{\iota\pi(0.8)}, 0.7e^{\iota\pi(0.9)}, 0.3e^{\iota\pi(0.1)}, 0.4e^{\iota\pi(0.7)}\rangle, \\ \langle x_2, 0.6e^{\iota\pi(0.5)}, 0.5e^{\iota\pi(0.7)}, 0.6e^{\iota\pi(0.8)}, 0.3e^{\iota\pi(0.3)}, 0.4e^{\iota\pi(0.2)}\rangle, \\ \langle x_3, 0.7e^{\iota\pi(0.8)}, 0.4e^{\iota\pi(0.4)}, 0.9e^{\iota\pi(0.8)}, 0.2e^{\iota\pi(0.3)}, 0.3e^{\iota\pi(0.4)}\rangle. \end{bmatrix},$$

$$(\tilde{\mathcal{F}_2},\acute{\mathcal{E}}) = \begin{bmatrix} e_1 = \langle x_1, 0.7e^{\iota\pi(0.8)}, 0.5e^{\iota\pi(0.4)}, 0.8e^{\iota\pi(0.7)}, 0.4e^{\iota\pi(0.4)}, 0.5e^{\iota\pi(0.5)}\rangle, \\ \langle x_2, 0.6e^{\iota\pi(0.4)}, 0.5e^{\iota\pi(0.5)}, 0.7e^{\iota\pi(0.7)}, 0.4e^{\iota\pi(0.4)}, 0.7e^{\iota\pi(0.6)}\rangle \\ \langle x_3, 0.3e^{\iota\pi(0.2)}, 0.4e^{\iota\pi(0.2)}, 0.6e^{\iota\pi(0.7)}, 0.5e^{\iota\pi(0.7)}, 0.6e^{\iota\pi(0.8)}\rangle; \\ e_2 = \langle x_1, 0.6e^{\iota\pi(0.6)}, 0.2e^{\iota\pi(0.6)}, 0.6e^{\iota\pi(0.9)}, 0.4e^{\iota\pi(0.3)}, 0.5e^{\iota\pi(0.7)}\rangle, \\ \langle x_2, 0.5e^{\iota\pi(0.4)}, 0.4e^{\iota\pi(0.1)}, 0.5e^{\iota\pi(0.7)}, 0.4e^{\iota\pi(0.5)}, 0.6e^{\iota\pi(0.7)}\rangle, \\ \langle x_3, 0.4e^{\iota\pi(0.3)}, 0.3e^{\iota\pi(0.3)}, 0.8e^{\iota\pi(0.8)}, 0.6e^{\iota\pi(0.7)}, 0.5e^{\iota\pi(0.4)}\rangle. \end{bmatrix},$$

$$(\tilde{\mathcal{F}}_3,\acute{\mathcal{E}}) = \begin{bmatrix} \mathfrak{e}_1 = \langle \mathrm{x}_1, 0.5e^{\iota\pi(0.6)}, 0.4e^{\iota\pi(0.2)}, 0.7e^{\iota\pi(0.7)}, 0.5e^{\iota\pi(0.4)}, 0.6e^{\iota\pi(0.5)}\rangle, \\ \langle \mathrm{x}_2, 0.4e^{\iota\pi(0.2)}, 0.3e^{\iota\pi(0.1)}, 0.6e^{\iota\pi(0.6)}, 0.5e^{\iota\pi(0.6)}, 0.7e^{\iota\pi(0.7)}\rangle \\ \langle \mathrm{x}_3, 0.2e^{\iota\pi(0.1)}, 0.3e^{\iota\pi(0.2)}, 0.5e^{\iota\pi(0.6)}, 0.6e^{\iota\pi(0.8)}, 0.8e^{\iota\pi(0.9)}\rangle; \\ \mathfrak{e}_2 = \langle \mathrm{x}_1, 0.4e^{\iota\pi(0.3)}, 0.2e^{\iota\pi(0.1)}, 0.5e^{\iota\pi(0.7)}, 0.5e^{\iota\pi(0.4)}, 0.6e^{\iota\pi(0.8)}\rangle, \\ \langle \mathrm{x}_2, 0.4e^{\iota\pi(0.3)}, 0.2e^{\iota\pi(0.1)}, 0.4e^{\iota\pi(0.6)}, 0.5e^{\iota\pi(0.6)}, 0.8e^{\iota\pi(0.9)}\rangle, \\ \langle \mathrm{x}_3, 0.3e^{\iota\pi(0.2)}, 0.3e^{\iota\pi(0.1)}, 0.6e^{\iota\pi(0.8)}, 0.7e^{\iota\pi(0.9)}, 0.6e^{\iota\pi(0.5)}\rangle. \end{bmatrix},$$

$$(\tilde{\mathcal{F}}_4,\acute{\mathcal{E}}) = \begin{bmatrix} \mathfrak{e}_1 = \langle \mathrm{x}_1, 0.6e^{\iota\pi(0.7)}, 0.3e^{\iota\pi(0.2)}, 0.5e^{\iota\pi(0.6)}, 0.1e^{\iota\pi(0.1)}, 0.2e^{\iota\pi(0.1)}\rangle, \\ \langle \mathrm{x}_2, 0.5e^{\iota\pi(0.4)}, 0.3e^{\iota\pi(0.3)}, 0.5e^{\iota\pi(0.5)}, 0.6e^{\iota\pi(0.6)}, 0.8e^{\iota\pi(0.9)}\rangle \\ \langle \mathrm{x}_3, 0.2e^{\iota\pi(0.2)}, 0.3e^{\iota\pi(0.1)}, 0.4e^{\iota\pi(0.5)}, 0.7e^{\iota\pi(0.8)}, 0.9e^{\iota\pi(0.9)}\rangle; \\ \mathfrak{e}_2 = \langle \mathrm{x}_1, 0.3e^{\iota\pi(0.3)}, 0.2e^{\iota\pi(0.1)}, 0.4e^{\iota\pi(0.7)}, 0.6e^{\iota\pi(0.5)}, 0.7e^{\iota\pi(0.8)}\rangle, \\ \langle \mathrm{x}_2, 0.4e^{\iota\pi(0.2)}, 0.1e^{\iota\pi(0.1)}, 0.3e^{\iota\pi(0.5)}, 0.7e^{\iota\pi(0.8)}, 0.9e^{\iota\pi(0.9)}\rangle, \\ \langle \mathrm{x}_3, 0.2e^{\iota\pi(0.2)}, 0.2e^{\iota\pi(0.1)}, 0.6e^{\iota\pi(0.7)}, 0.8e^{\iota\pi(0.9)}, 0.7e^{\iota\pi(0.8)}\rangle. \end{bmatrix}.$$

Since $(\tilde{\mathcal{F}}_1,\acute{\mathcal{E}}) \Cup (\tilde{\mathcal{F}}_4,\acute{\mathcal{E}}) \notin \tau_1 \Cup \tau_2$*, then* $\tau_1 \Cup \tau_2$ *is not a CTVNS topology over* $\mathbb{X}$.

Proposition 6. *Let* $(\mathbb{X},\tau,\acute{\mathcal{E}})$ *be a CTVNS topological space over* $\mathbb{X}$ *and*

$$\tau = \{(\tilde{\mathcal{F}}_i,\acute{\mathcal{E}}) : (\tilde{\mathcal{F}}_i,\acute{\mathcal{E}}) \in CTVNSS(\mathbb{X},\acute{\mathcal{E}})\},$$

$$= \{[e,\tilde{\mathcal{F}}_i(\mathfrak{e})]_{\mathfrak{e}\in\acute{\mathcal{E}}} : (\tilde{\mathcal{F}}_i,\acute{\mathcal{E}}) \in CTVNSS(\mathbb{X},\acute{\mathcal{E}})\},$$

where

$$\tilde{\mathcal{F}}_i(\mathfrak{e}) = \{\langle \mathrm{x}, \mathrm{T}_{\tilde{\mathcal{F}}_i(\mathfrak{e})}(\mathrm{x}), \mathrm{RT}_{\tilde{\mathcal{F}}_i(\mathfrak{e})}(\mathrm{x}), \mathrm{C}_{\tilde{\mathcal{F}}_i(\mathfrak{e})}(\mathrm{x}), \mathrm{RF}_{\tilde{\mathcal{F}}_i(\mathfrak{e})}(\mathrm{x}), \mathrm{F}_{\tilde{\mathcal{F}}_i(\mathfrak{e})}(\mathrm{x})\rangle : \mathrm{x} \in \mathbb{X}\}.$$

Then

$$\tau_1 = \{[\mathrm{T}_{\tilde{\mathcal{F}}_i(\mathfrak{e})}(\mathbb{X})]_{\mathfrak{e}\in\acute{\mathcal{E}}}\}$$
$$\tau_2 = \{[\mathrm{RT}_{\tilde{\mathcal{F}}_i(\mathfrak{e})}(\mathbb{X})]_{\mathfrak{e}\in\acute{\mathcal{E}}}\}$$
$$\tau_3 = \{[\mathrm{C}_{\tilde{\mathcal{F}}_i(\mathfrak{e})}(\mathbb{X})]_{\mathfrak{e}\in\acute{\mathcal{E}}}\}$$
$$\tau_4 = \{[\mathrm{RF}_{\tilde{\mathcal{F}}_i(\mathfrak{e})}(\mathbb{X})]_{\mathfrak{e}\in\acute{\mathcal{E}}}\}$$
$$\tau_5 = \{[\mathrm{F}_{\tilde{\mathcal{F}}_i(\mathfrak{e})}(\mathbb{X})]_{\mathfrak{e}\in\acute{\mathcal{E}}}\},$$

define complex fuzzy soft topologies on $\mathbb{X}$.

Proof. (i). $0_{(\mathbb{X},\acute{\mathcal{E}})}, 1_{(\mathbb{X},\acute{\mathcal{E}})} \in \tau \Rightarrow 0,1 \in \tau_1, 0,1 \in \tau_2, 0,1 \in \tau_3, 0,1 \in \tau_4 and 0,1 \in \tau_5$. (ii). Suppose that $(\tilde{\mathcal{F}}_i,\acute{\mathcal{E}})|i \in I$ be a family of CTVNS sets in τ. Then $\{[\mathrm{T}_{\tilde{\mathcal{F}}_i(\mathfrak{e})}(\mathbb{X})]_{\mathfrak{e}\in\acute{\mathcal{E}}}\}_{i\in I}$ is a family of complex fuzzy soft sets in τ_1, $\{[\mathrm{RT}_{\tilde{\mathcal{F}}_i(\mathfrak{e})}(\mathbb{X})]_{\mathfrak{e}\in\acute{\mathcal{E}}}\}_{i\in I}$ is a family of complex fuzzy soft sets in τ_2, $\{[\mathrm{C}_{\tilde{\mathcal{F}}_i(\mathfrak{e})}(\mathbb{X})]_{\mathfrak{e}\in\acute{\mathcal{E}}}\}_{i\in I}$ is a family of complex fuzzy soft sets in τ_3, $\{[\mathrm{RF}_{\tilde{\mathcal{F}}_i(\mathfrak{e})}(\mathbb{X})]_{\mathfrak{e}\in\acute{\mathcal{E}}}\}_{i\in I}$ is a family of complex fuzzy soft sets in τ_4, $\{[\mathrm{F}_{\tilde{\mathcal{F}}_i(\mathfrak{e})}(\mathbb{X})]_{\mathfrak{e}\in\acute{\mathcal{E}}}\}_{i\in I}$ is a family of complex fuzzy soft sets in τ_5. Since τ is a CTVNS topology, then $\Cup_{i\in I}(\tilde{\mathcal{F}}_i,\acute{\mathcal{E}}) \in \tau_1$. That is,

$$\Cup_{i\in I}(\tilde{\mathcal{F}}_i,\acute{\mathcal{E}}) = \{\langle \sup[\mathrm{T}_{\tilde{\mathcal{F}}_i(\mathfrak{e})}(\mathbb{X})]_{\mathfrak{e}\in\acute{\mathcal{E}}}, \sup[\mathrm{RT}_{\tilde{\mathcal{F}}_i(\mathfrak{e})}(\mathbb{X})]_{\mathfrak{e}\in\acute{\mathcal{E}}}, \sup[\mathrm{C}_{\tilde{\mathcal{F}}_i(\mathfrak{e})}(\mathbb{X})]_{\mathfrak{e}\in\acute{\mathcal{E}}}, \inf[\mathrm{RF}_{\tilde{\mathcal{F}}_i(\mathfrak{e})}(\mathbb{X})]_{\mathfrak{e}\in\acute{\mathcal{E}}}, \inf[\mathrm{F}_{\tilde{\mathcal{F}}_i(\mathfrak{e})}(\mathbb{X})]_{\mathfrak{e}\in\acute{\mathcal{E}}}\rangle\}_{i\in I} \in \tau.$$

Therefore,

$$\{\sup[\mathrm{T}_{\tilde{\mathcal{F}}_i(\mathfrak{e})}(\mathbb{X})]_{\mathfrak{e}\in\acute{\mathcal{E}}}\}_{i\in I} \in \tau_1$$
$$\{\sup[\mathrm{RT}_{\tilde{\mathcal{F}}_i(\mathfrak{e})}(\mathbb{X})]_{\mathfrak{e}\in\acute{\mathcal{E}}}\}_{i\in I} \in \tau_2$$
$$\{\sup[\mathrm{C}_{\tilde{\mathcal{F}}_i(\mathfrak{e})}(\mathbb{X})]_{\mathfrak{e}\in\acute{\mathcal{E}}}\}_{i\in I} \in \tau_3$$
$$\{\inf[\mathrm{RF}_{\tilde{\mathcal{F}}_i(\mathfrak{e})}(\mathbb{X})]_{\mathfrak{e}\in\acute{\mathcal{E}}}\}_{i\in I} \in \tau_4$$
$$\{\inf[\mathrm{F}_{\tilde{\mathcal{F}}_i(\mathfrak{e})}(\mathbb{X})]_{\mathfrak{e}\in\acute{\mathcal{E}}}\}_{i\in I} \in \tau_5.$$

(iii). Suppose $\{(\tilde{\mathcal{F}}_i,\acute{\mathcal{E}})|i = \overline{1,n}\}$ be a family of finite number of CTVNS sets in τ.
Then $\{[\mathrm{T}_{\tilde{\mathcal{F}}_i(\mathfrak{e})}(\mathbb{X})]_{\mathfrak{e}\in\acute{\mathcal{E}}}\}_{i=\overline{1,n}}$ is a family of complex fuzzy soft sets in τ_1, $\{[\mathrm{RT}_{\tilde{\mathcal{F}}_i(\mathfrak{e})}(\mathbb{X})]_{\mathfrak{e}\in\acute{\mathcal{E}}}\}_{i=\overline{1,n}}$ is a family of complex fuzzy soft sets in τ_2, $\{[\mathrm{C}_{\tilde{\mathcal{F}}_i(\mathfrak{e})}(\mathbb{X})]_{\mathfrak{e}\in\acute{\mathcal{E}}}\}_{i=\overline{1,n}}$ is a family of complex fuzzy soft sets in τ_3, $\{[\mathrm{RF}_{\tilde{\mathcal{F}}_i(\mathfrak{e})}(\mathbb{X})]_{\mathfrak{e}\in\acute{\mathcal{E}}}\}_{i=\overline{1,n}}$ is a family of complex fuzzy soft sets in τ_4, $\{[\mathrm{F}_{\tilde{\mathcal{F}}_i(\mathfrak{e})}(\mathbb{X})]_{\mathfrak{e}\in\acute{\mathcal{E}}}\}_{i=\overline{1,n}}$ is a family of complex fuzzy soft sets in τ_5. Since τ is a CTVNS topology, then $\Cap_{i=1}^{n}(\tilde{\mathcal{F}}_i,\acute{\mathcal{E}}) \in \tau_1$. That is,

$$\Cap_{i=1}^{n}(\tilde{\mathcal{F}}_i,\acute{\mathcal{E}}) = \{\langle \min[\mathrm{T}_{\tilde{\mathcal{F}}_i(\mathfrak{e})}(\mathbb{X})]_{\mathfrak{e}\in\acute{\mathcal{E}}}, \min[\mathrm{RT}_{\tilde{\mathcal{F}}_i(\mathfrak{e})}(\mathbb{X})]_{\mathfrak{e}\in\acute{\mathcal{E}}}, \min[\mathrm{C}_{\tilde{\mathcal{F}}_i(\mathfrak{e})}(\mathbb{X})]_{\mathfrak{e}\in\acute{\mathcal{E}}}, \max[\mathrm{RF}_{\tilde{\mathcal{F}}_i(\mathfrak{e})}(\mathbb{X})]_{\mathfrak{e}\in\acute{\mathcal{E}}}, \max[\mathrm{F}_{\tilde{\mathcal{F}}_i(\mathfrak{e})}(\mathbb{X})]_{\mathfrak{e}\in\acute{\mathcal{E}}}\rangle\}_{i=\overline{1,n}} \in \tau.$$

Therefore,

$$\{\min[\mathrm{T}_{\tilde{\mathcal{F}}_i(\mathfrak{e})}(\mathbb{X})]_{\mathfrak{e}\in\acute{\mathcal{E}}}\}_{i\in I} \in \tau_1$$
$$\{\min[\mathrm{RT}_{\tilde{\mathcal{F}}_i(\mathfrak{e})}(\mathbb{X})]_{\mathfrak{e}\in\acute{\mathcal{E}}}\}_{i\in I} \in \tau_2$$
$$\{\min[\mathrm{C}_{\tilde{\mathcal{F}}_i(\mathfrak{e})}(\mathbb{X})]_{\mathfrak{e}\in\acute{\mathcal{E}}}\}_{i\in I} \in \tau_3$$
$$\{\min[\mathrm{RF}_{\tilde{\mathcal{F}}_i(\mathfrak{e})}(\mathbb{X})]^{c}_{\mathfrak{e}\in\acute{\mathcal{E}}}\}_{i\in I} \in \tau_4$$
$$\{\min[\mathrm{F}_{\tilde{\mathcal{F}}_i(\mathfrak{e})}(\mathbb{X})]^{c}_{\mathfrak{e}\in\acute{\mathcal{E}}}\}_{i\in I} \in \tau_5.$$

This completes the proof. □

Remark 4.2. *Generally, converse of the above proposition is not true.*

Example 4.2. *Let* $\mathbb{X} = \{\mathrm{x}_1, \mathrm{x}_2, \mathrm{x}_3\}$ *be an initial universe set,* $\mathcal{E} = \{\mathfrak{e}_1, \mathfrak{e}_2\}$ *be a set of parameters and:*

$$\tau_1 = \{0_{(\mathbb{X},\acute{\mathcal{E}})}, 1_{(\mathbb{X},\acute{\mathcal{E}})}, (\tilde{\mathcal{F}}_1,\acute{\mathcal{E}}), (\tilde{\mathcal{F}}_2,\acute{\mathcal{E}}), (\tilde{\mathcal{F}}_3,\acute{\mathcal{E}})\},$$

be a family of CTVNS sets over $\mathbb{X}$. *Here, the CTVNS sets* $(\tilde{\mathcal{F}}_1,\acute{\mathcal{E}})$, $(\tilde{\mathcal{F}}_2,\acute{\mathcal{E}})$ *and* $(\tilde{\mathcal{F}}_3,\acute{\mathcal{E}})$ *are defined as follows:*

$$(\tilde{\mathcal{F}}_1,\acute{\mathcal{E}}) = \begin{bmatrix} \mathfrak{e}_1 = \langle \mathrm{x}_1, 0.9e^{\iota\pi(0.9)}, 0.6e^{\iota\pi(0.8)}, 0.9e^{\iota\pi(0.8)}, 0.2e^{\iota\pi(0.4)}, 0.3e^{\iota\pi(0.5)}\rangle, \\ \langle \mathrm{x}_2, 0.7e^{\iota\pi(0.7)}, 0.6e^{\iota\pi(0.5)}, 0.8e^{\iota\pi(0.7)}, 0.3e^{\iota\pi(0.3)}, 0.5e^{\iota\pi(0.4)}\rangle \\ \langle \mathrm{x}_3, 0.4e^{\iota\pi(0.3)}, 0.5e^{\iota\pi(0.2)}, 0.8e^{\iota\pi(0.8)}, 0.3e^{\iota\pi(0.4)}, 0.4e^{\iota\pi(0.2)}\rangle; \\ \mathfrak{e}_2 = \langle \mathrm{x}_1, 0.7e^{\iota\pi(0.9)}, 0.3e^{\iota\pi(0.8)}, 0.7e^{\iota\pi(0.9)}, 0.3e^{\iota\pi(0.1)}, 0.4e^{\iota\pi(0.7)}\rangle, \\ \langle \mathrm{x}_2, 0.6e^{\iota\pi(0.5)}, 0.5e^{\iota\pi(0.7)}, 0.6e^{\iota\pi(0.8)}, 0.3e^{\iota\pi(0.3)}, 0.4e^{\iota\pi(0.2)}\rangle, \\ \langle \mathrm{x}_3, 0.7e^{\iota\pi(0.8)}, 0.4e^{\iota\pi(0.4)}, 0.9e^{\iota\pi(0.8)}, 0.2e^{\iota\pi(0.3)}, 0.3e^{\iota\pi(0.4)}\rangle. \end{bmatrix},$$

$$(\tilde{\mathcal{F}}_2,\acute{\mathcal{E}}) = \begin{bmatrix} \mathfrak{e}_1 = \langle \mathrm{x}_1, 0.7e^{\iota\pi(0.8)}, 0.5e^{\iota\pi(0.4)}, 0.8e^{\iota\pi(0.7)}, 0.4e^{\iota\pi(0.4)}, 0.5e^{\iota\pi(0.5)}\rangle, \\ \langle \mathrm{x}_2, 0.6e^{\iota\pi(0.4)}, 0.5e^{\iota\pi(0.5)}, 0.7e^{\iota\pi(0.7)}, 0.4e^{\iota\pi(0.4)}, 0.7e^{\iota\pi(0.6)}\rangle \\ \langle \mathrm{x}_3, 0.3e^{\iota\pi(0.2)}, 0.4e^{\iota\pi(0.2)}, 0.6e^{\iota\pi(0.7)}, 0.5e^{\iota\pi(0.7)}, 0.6e^{\iota\pi(0.8)}\rangle; \\ \mathfrak{e}_2 = \langle \mathrm{x}_1, 0.6e^{\iota\pi(0.6)}, 0.2e^{\iota\pi(0.6)}, 0.6e^{\iota\pi(0.9)}, 0.4e^{\iota\pi(0.3)}, 0.5e^{\iota\pi(0.7)}\rangle, \\ \langle \mathrm{x}_2, 0.5e^{\iota\pi(0.4)}, 0.4e^{\iota\pi(0.1)}, 0.5e^{\iota\pi(0.7)}, 0.4e^{\iota\pi(0.5)}, 0.6e^{\iota\pi(0.7)}\rangle, \\ \langle \mathrm{x}_3, 0.4e^{\iota\pi(0.3)}, 0.3e^{\iota\pi(0.3)}, 0.8e^{\iota\pi(0.8)}, 0.6e^{\iota\pi(0.7)}, 0.5e^{\iota\pi(0.4)}\rangle. \end{bmatrix},$$

$$(\tilde{\mathcal{F}}_3,\acute{\mathcal{E}}) = \begin{bmatrix} \mathfrak{e}_1 = \langle \mathrm{x}_1, 0.5e^{\iota\pi(0.6)}, 0.4e^{\iota\pi(0.2)}, 0.7e^{\iota\pi(0.7)}, 0.5e^{\iota\pi(0.4)}, 0.6e^{\iota\pi(0.5)}\rangle, \\ \langle \mathrm{x}_2, 0.4e^{\iota\pi(0.2)}, 0.3e^{\iota\pi(0.1)}, 0.6e^{\iota\pi(0.6)}, 0.5e^{\iota\pi(0.6)}, 0.7e^{\iota\pi(0.7)}\rangle \\ \langle \mathrm{x}_3, 0.2e^{\iota\pi(0.1)}, 0.3e^{\iota\pi(0.2)}, 0.5e^{\iota\pi(0.6)}, 0.6e^{\iota\pi(0.8)}, 0.8e^{\iota\pi(0.9)}\rangle; \\ \mathfrak{e}_2 = \langle \mathrm{x}_1, 0.4e^{\iota\pi(0.3)}, 0.2e^{\iota\pi(0.1)}, 0.5e^{\iota\pi(0.7)}, 0.5e^{\iota\pi(0.4)}, 0.6e^{\iota\pi(0.8)}\rangle, \\ \langle \mathrm{x}_2, 0.4e^{\iota\pi(0.3)}, 0.2e^{\iota\pi(0.1)}, 0.4e^{\iota\pi(0.6)}, 0.5e^{\iota\pi(0.6)}, 0.8e^{\iota\pi(0.9)}\rangle, \\ \langle \mathrm{x}_3, 0.3e^{\iota\pi(0.2)}, 0.3e^{\iota\pi(0.1)}, 0.6e^{\iota\pi(0.8)}, 0.7e^{\iota\pi(0.9)}, 0.6e^{\iota\pi(0.5)}\rangle. \end{bmatrix}.$$

Then,

$$\tau_1 = \{\langle \mathrm{T}_{\tilde{\mathcal{F}}_{0_{(\mathbb{X},\acute{\mathcal{E}})^{(\mathfrak{e})}}}}(\mathbb{X}), \mathrm{T}_{\tilde{\mathcal{F}}_{1_{(\mathbb{X},\acute{\mathcal{E}})^{(\mathfrak{e})}}}}(\mathbb{X}), \mathrm{T}_{\tilde{\mathcal{F}}_{1}(\mathfrak{e})}(\mathbb{X}), \mathrm{T}_{\tilde{\mathcal{F}}_{2}(\mathfrak{e})}(\mathbb{X}), \mathrm{T}_{\tilde{\mathcal{F}}_{3}(\mathfrak{e})}(\mathbb{X})\rangle_{\mathfrak{e}\in\acute{\mathcal{E}}}\},$$

$$\tau_2 = \{\langle \mathrm{RT}_{\tilde{\mathcal{F}}_{0_{(\mathbb{X},\acute{\mathcal{E}})^{(\mathfrak{e})}}}}(\mathbb{X}), \mathrm{RT}_{\tilde{\mathcal{F}}_{1_{(\mathbb{X},\acute{\mathcal{E}})^{(\mathfrak{e})}}}}(\mathbb{X}), \mathrm{RT}_{\tilde{\mathcal{F}}_{1}(\mathfrak{e})}(\mathbb{X}), \mathrm{RT}_{\tilde{\mathcal{F}}_{2}(\mathfrak{e})}(\mathbb{X}), \mathrm{RT}_{\tilde{\mathcal{F}}_{3}(\mathfrak{e})}(\mathbb{X})\rangle_{\mathfrak{e}\in\acute{\mathcal{E}}}\},$$

$$\tau_3 = \{\langle \mathrm{C}_{\tilde{\mathcal{F}}_{0_{(\mathbb{X},\acute{\mathcal{E}})^{(\mathfrak{e})}}}}(\mathbb{X}), \mathrm{C}_{\tilde{\mathcal{F}}_{1_{(\mathbb{X},\acute{\mathcal{E}})^{(\mathfrak{e})}}}}(\mathbb{X}), \mathrm{C}_{\tilde{\mathcal{F}}_{1}(\mathfrak{e})}(\mathbb{X}), \mathrm{C}_{\tilde{\mathcal{F}}_{2}(\mathfrak{e})}(\mathbb{X}), \mathrm{C}_{\tilde{\mathcal{F}}_{3}(\mathfrak{e})}(\mathbb{X})\rangle_{\mathfrak{e}\in\acute{\mathcal{E}}}\},$$

$$\tau_4 = \{\langle \mathrm{RF}_{\tilde{\mathcal{F}}_{0_{(\mathbb{X},\acute{\mathcal{E}})^{(\mathfrak{e})}}}}(\mathbb{X}), \mathrm{RF}_{\tilde{\mathcal{F}}_{1_{(\mathbb{X},\acute{\mathcal{E}})^{(\mathfrak{e})}}}}(\mathbb{X}), \mathrm{RF}_{\tilde{\mathcal{F}}_{1}(\mathfrak{e})}(\mathbb{X}), \mathrm{RF}_{\tilde{\mathcal{F}}_{2}(\mathfrak{e})}(\mathbb{X}), \mathrm{RF}_{\tilde{\mathcal{F}}_{3}(\mathfrak{e})}(\mathbb{X})\rangle_{\mathfrak{e}\in\acute{\mathcal{E}}}\},$$

$$\tau_5 = \{\langle \mathrm{F}_{\tilde{\mathcal{F}}_{0_{(\mathbb{X},\acute{\mathcal{E}})^{(\mathfrak{e})}}}}(\mathbb{X}), \mathrm{F}_{\tilde{\mathcal{F}}_{1_{(\mathbb{X},\acute{\mathcal{E}})^{(\mathfrak{e})}}}}(\mathbb{X}), \mathrm{F}_{\tilde{\mathcal{F}}_{1}(\mathfrak{e})}(\mathbb{X}), \mathrm{F}_{\tilde{\mathcal{F}}_{2}(\mathfrak{e})}(\mathbb{X}), \mathrm{F}_{\tilde{\mathcal{F}}_{3}(\mathfrak{e})}(\mathbb{X})\rangle_{\mathfrak{e}\in\acute{\mathcal{E}}}\},$$

are complex fuzzy soft topologies on $\mathbb{X}$*. For example,*

$$\begin{aligned}\tau_1 = \{&\langle(0,0,0),(1,1,1),(0.9e^{\iota\pi(0.9)},0.7e^{\iota\pi(0.7)},0.4e^{\iota\pi(0.3)}),\\ &(0.7e^{\iota\pi(0.8)},0.6e^{\iota\pi(0.4)},0.3e^{\iota\pi(0.2)}),(0.8e^{\iota\pi(0.8)},0.4e^{\iota\pi(0.2)},0.2e^{\iota\pi(0.1)})\rangle_{\mathfrak{e}_1},\\ &\langle(0,0,0),(1,1,1),(0.7e^{\iota\pi(0.9)},0.6e^{\iota\pi(0.5)},0.7e^{\iota\pi(0.8)}),\\ &(0.6e^{\iota\pi(0.6)},0.5e^{\iota\pi(0.4)},0.4e^{\iota\pi(0.3)}),(0.4e^{\iota\pi(0.3)},0.4e^{\iota\pi(0.3)},0.3e^{\iota\pi(0.2)})\rangle_{\mathfrak{e}_2}\},\end{aligned}$$

$$\begin{aligned}\tau_2 = \{&\langle(0,0,0),(1,1,1),(0.6e^{\iota\pi(0.8)},0.6e^{\iota\pi(0.5)},0.5e^{\iota\pi(0.2)}),\\ &(0.5e^{\iota\pi(0.4)},0.5e^{\iota\pi(0.5)},0.4e^{\iota\pi(0.2)}),(0.4e^{\iota\pi(0.2)},0.3e^{\iota\pi(0.1)},0.3e^{\iota\pi(0.2)})\rangle_{\mathfrak{e}_1},\\ &\langle(0,0,0),(1,1,1),(0.3e^{\iota\pi(0.8)},0.5e^{\iota\pi(0.7)},0.4e^{\iota\pi(0.4)}),\\ &(0.2e^{\iota\pi(0.6)},0.4e^{\iota\pi(0.1)},0.3e^{\iota\pi(0.3)}),(0.2e^{\iota\pi(0.1)},0.2e^{\iota\pi(0.1)},0.3e^{\iota\pi(0.1)})\rangle_{\mathfrak{e}_2}\},\end{aligned}$$

$$\begin{aligned}\tau_3 = \{&\langle(0,0,0),(1,1,1),(0.9e^{\iota\pi(0.8)},0.8e^{\iota\pi(0.7)},0.8e^{\iota\pi(0.8)}),\\ &(0.8e^{\iota\pi(0.7)},0.6e^{\iota\pi(0.7)},0.7e^{\iota\pi(0.7)}),(0.7e^{\iota\pi(0.7)},0.6e^{\iota\pi(0.6)},0.5e^{\iota\pi(0.6)})\rangle_{\mathfrak{e}_1},\\ &\langle(0,0,0),(1,1,1),(0.7e^{\iota\pi(0.9)},0.6e^{\iota\pi(0.8)},0.9e^{\iota\pi(0.8)}),\\ &(0.6e^{\iota\pi(0.9)},0.5e^{\iota\pi(0.7)},0.8e^{\iota\pi(0.8)}),(0.5e^{\iota\pi(0.7)},0.4e^{\iota\pi(0.6)},0.6e^{\iota\pi(0.8)})\rangle_{\mathfrak{e}_2}\},\end{aligned}$$

$$\begin{aligned}\tau_4 = \{&\langle(1,1,1),(0,0,0),(0.2e^{\iota\pi(0.4)},0.3e^{\iota\pi(0.3)},0.3e^{\iota\pi(0.4)}),\\ &(0.4e^{\iota\pi(0.4)},0.4e^{\iota\pi(0.4)},0.5e^{\iota\pi(0.7)}),(0.5e^{\iota\pi(0.3)},0.5e^{\iota\pi(0.6)},0.6e^{\iota\pi(0.8)})\rangle_{\mathfrak{e}_1},\\ &\langle(1,1,1),(0,0,0),(0.3e^{\iota\pi(0.1)},0.3e^{\iota\pi(0.3)},0.2e^{\iota\pi(0.3)}),\\ &(0.4e^{\iota\pi(0.3)},0.4e^{\iota\pi(0.5)},0.6e^{\iota\pi(0.7)}),(0.5e^{\iota\pi(0.4)},0.5e^{\iota\pi(0.6)},0.7e^{\iota\pi(0.9)})\rangle_{\mathfrak{e}_2}\},\end{aligned}$$

$$\begin{aligned}\tau_5 = \{&\langle(1,1,1),(0,0,0),(0.3e^{\iota\pi(0.7)},0.5e^{\iota\pi(0.4)},0.4e^{\iota\pi(0.2)}),\\ &(0.5e^{\iota\pi(0.8)},0.7e^{\iota\pi(0.6)},0.6e^{\iota\pi(0.8)}),(0.6e^{\iota\pi(0.8)},0.7e^{\iota\pi(0.7)},0.8e^{\iota\pi(0.9)})\rangle_{\mathfrak{e}_1},\\ &\langle(1,1,1),(0,0,0),(0.4e^{\iota\pi(0.7)},0.4e^{\iota\pi(0.2)},0.3e^{\iota\pi(0.4)}),\\ &(0.5e^{\iota\pi(0.8)},0.6e^{\iota\pi(0.7)},0.5e^{\iota\pi(0.4)}),(0.6e^{\iota\pi(0.8)},0.8e^{\iota\pi(0.9)},0.6e^{\iota\pi(0.5)})\rangle_{\mathfrak{e}_2}\}.\end{aligned}$$

Since $(\tilde{\mathcal{F}}_2,\acute{\mathcal{E}}) \Cap (\tilde{\mathcal{F}}_3,\acute{\mathcal{E}}) \notin \tau$*,* τ *is not a CTVNS topology on* $\mathbb{X}$*.*

Proposition 7. *Let* $(\mathbb{X},\tau,\acute{\mathcal{E}})$ *be a CTVNS topological space over* $\mathbb{X}$*. Then*

$$\begin{aligned}\tau_{1_e} &= \{[\mathrm{T}_{\tilde{\mathcal{F}}(\mathfrak{e})}(\mathbb{X})] : \tilde{\mathcal{F}}, E \in \tau\}\\ \tau_{2_e} &= \{[\mathrm{RT}_{\tilde{\mathcal{F}}(\mathfrak{e})}(\mathbb{X})] : \tilde{\mathcal{F}}, E \in \tau\}\\ \tau_{3_e} &= \{[\mathrm{C}_{\tilde{\mathcal{F}}(\mathfrak{e})}(\mathbb{X})] : \tilde{\mathcal{F}}, E \in \tau\}\\ \tau_{4_e} &= \{[\mathrm{RF}_{\tilde{\mathcal{F}}(\mathfrak{e})}(\mathbb{X})] : \tilde{\mathcal{F}}, E \in \tau\}\\ \tau_{5_e} &= \{[\mathrm{F}_{\tilde{\mathcal{F}}(\mathfrak{e})}(\mathbb{X})] : \tilde{\mathcal{F}}, E \in \tau\},\end{aligned}$$

for each $\mathfrak{e} \in \acute{\mathcal{E}}$ *define complex fuzzy topologies on* $\mathbb{X}$*.*

Remark 4.3. *Generally converse of the above proposition is not true.*

Example 4.3. *Let us consider the Example* 3*. Then,*

$$\begin{aligned}\tau_{1_{\mathfrak{e}_1}} &= \{\langle \begin{matrix}\mathrm{T}_{\tilde{\mathcal{F}}_{0_{(\mathbb{X},\acute{\mathcal{E}})^{(\mathfrak{e}_1)}}}}(\mathbb{X}), \mathrm{T}_{\tilde{\mathcal{F}}_{1_{(\mathbb{X},\acute{\mathcal{E}})^{(\mathfrak{e}_1)}}}}(\mathbb{X}), \mathrm{T}_{\tilde{\mathcal{F}}_{1}(\mathfrak{e}_1)}(\mathbb{X}),\\ \mathrm{T}_{\tilde{\mathcal{F}}_{2}(\mathfrak{e}_1)}(\mathbb{X}), \mathrm{T}_{\tilde{\mathcal{F}}_{3}(\mathfrak{e}_1)}(\mathbb{X})\end{matrix}\rangle\},\\ \tau_{2_{\mathfrak{e}_1}} &= \{\langle \begin{matrix}\mathrm{RT}_{\tilde{\mathcal{F}}_{0_{(\mathbb{X},\acute{\mathcal{E}})^{(\mathfrak{e}_1)}}}}(\mathbb{X}), \mathrm{RT}_{\tilde{\mathcal{F}}_{1_{(\mathbb{X},\acute{\mathcal{E}})^{(\mathfrak{e}_1)}}}}(\mathbb{X}), \mathrm{RT}_{\tilde{\mathcal{F}}_{1}(\mathfrak{e}_1)}(\mathbb{X}),\\ \mathrm{RT}_{\tilde{\mathcal{F}}_{2}(\mathfrak{e}_1)}(\mathbb{X}), \mathrm{RT}_{\tilde{\mathcal{F}}_{3}(\mathfrak{e}_1)}(\mathbb{X})\end{matrix}\rangle\},\\ \tau_{3_{\mathfrak{e}_1}} &= \{\langle \begin{matrix}\mathrm{C}_{\tilde{\mathcal{F}}_{0_{(\mathbb{X},\acute{\mathcal{E}})^{(\mathfrak{e}_1)}}}}(\mathbb{X}), \mathrm{C}_{\tilde{\mathcal{F}}_{1_{(\mathbb{X},\acute{\mathcal{E}})^{(\mathfrak{e}_1)}}}}(\mathbb{X}), \mathrm{C}_{\tilde{\mathcal{F}}_{1}(\mathfrak{e}_1)}(\mathbb{X}),\\ \mathrm{C}_{\tilde{\mathcal{F}}_{2}(\mathfrak{e}_1)}(\mathbb{X}), \mathrm{C}_{\tilde{\mathcal{F}}_{3}(\mathfrak{e}_1)}(\mathbb{X})\end{matrix}\rangle\},\\ \tau_{4_{\mathfrak{e}_1}} &= \{\langle \begin{matrix}\mathrm{RF}_{\tilde{\mathcal{F}}_{0_{(\mathbb{X},\acute{\mathcal{E}})^{(\mathfrak{e}_1)}}}}(\mathbb{X}), \mathrm{RF}_{\tilde{\mathcal{F}}_{1_{(\mathbb{X},\acute{\mathcal{E}})^{(\mathfrak{e}_1)}}}}(\mathbb{X}), \mathrm{RF}_{\tilde{\mathcal{F}}_{1}(\mathfrak{e}_1)}(\mathbb{X}),\\ \mathrm{RF}_{\tilde{\mathcal{F}}_{2}(\mathfrak{e}_1)}(\mathbb{X}), \mathrm{RF}_{\tilde{\mathcal{F}}_{3}(\mathfrak{e}_1)}(\mathbb{X})\end{matrix}\rangle\},\\ \tau_{5_{\mathfrak{e}_1}} &= \{\langle \begin{matrix}\mathrm{F}_{\tilde{\mathcal{F}}_{0_{(\mathbb{X},\acute{\mathcal{E}})^{(\mathfrak{e}_1)}}}}(\mathbb{X}), \mathrm{F}_{\tilde{\mathcal{F}}_{1_{(\mathbb{X},\acute{\mathcal{E}})^{(\mathfrak{e}_1)}}}}(\mathbb{X}), \mathrm{F}_{\tilde{\mathcal{F}}_{1}(\mathfrak{e}_1)}(\mathbb{X}),\\ \mathrm{F}_{\tilde{\mathcal{F}}_{2}(\mathfrak{e}_1)}(\mathbb{X}), \mathrm{F}_{\tilde{\mathcal{F}}_{3}(\mathfrak{e}_1)}(\mathbb{X})\end{matrix}\rangle\},\end{aligned}$$

are complex fuzzy soft topologies on $\mathbb{X}$*. For example,*

$$\begin{aligned}\tau_{1_{\mathfrak{e}_1}} &= \{\langle(0,0,0),(1,1,1),(0.9e^{\iota\pi(0.9)},0.7e^{\iota\pi(0.7)},0.4e^{\iota\pi(0.3)}),\\ &\quad(0.7e^{\iota\pi(0.8)},0.6e^{\iota\pi(0.4)},0.3e^{\iota\pi(0.2)}),(0.8e^{\iota\pi(0.8)},0.4e^{\iota\pi(0.2)},0.2e^{\iota\pi(0.1)})\rangle\},\\ \tau_{2_{\mathfrak{e}_1}} &= \{\langle(0,0,0),(1,1,1),(0.6e^{\iota\pi(0.8)},0.6e^{\iota\pi(0.5)},0.5e^{\iota\pi(0.2)}),\\ &\quad(0.5e^{\iota\pi(0.4)},0.5e^{\iota\pi(0.5)},0.4e^{\iota\pi(0.2)}),(0.4e^{\iota\pi(0.2)},0.3e^{\iota\pi(0.1)},0.3e^{\iota\pi(0.2)})\rangle\},\\ \tau_{3_{\mathfrak{e}_1}} &= \{\langle(0,0,0),(1,1,1),(0.9e^{\iota\pi(0.8)},0.8e^{\iota\pi(0.7)},0.8e^{\iota\pi(0.8)}),\\ &\quad(0.8e^{\iota\pi(0.7)},0.6e^{\iota\pi(0.7)},0.7e^{\iota\pi(0.7)}),(0.7e^{\iota\pi(0.7)},0.6e^{\iota\pi(0.6)},0.5e^{\iota\pi(0.6)})\rangle\},\\ \tau_{4_{\mathfrak{e}_1}} &= \{\langle(1,1,1),(0,0,0),(0.2e^{\iota\pi(0.4)},0.3e^{\iota\pi(0.3)},0.3e^{\iota\pi(0.4)}),\\ &\quad(0.4e^{\iota\pi(0.4)},0.4e^{\iota\pi(0.4)},0.5e^{\iota\pi(0.7)}),(0.5e^{\iota\pi(0.3)},0.5e^{\iota\pi(0.6)},0.6e^{\iota\pi(0.8)})\rangle\},\\ \tau_{5_{\mathfrak{e}_1}} &= \{\langle(1,1,1),(0,0,0),(0.3e^{\iota\pi(0.7)},0.5e^{\iota\pi(0.4)},0.4e^{\iota\pi(0.2)}),\\ &\quad(0.5e^{\iota\pi(0.8)},0.7e^{\iota\pi(0.6)},0.6e^{\iota\pi(0.8)}),(0.6e^{\iota\pi(0.8)},0.7e^{\iota\pi(0.7)},0.8e^{\iota\pi(0.9)})\rangle\}.\end{aligned}$$

Here, $\{\tau_{1_{\mathfrak{e}_1}},\tau_{2_{\mathfrak{e}_1}},\tau_{3_{\mathfrak{e}_1}},\tau_{4_{\mathfrak{e}_1}},\tau_{5_{\mathfrak{e}_1}}\}$ *and* $\{\tau_{1_{\mathfrak{e}_2}},\tau_{2_{\mathfrak{e}_2}},\tau_{3_{\mathfrak{e}_2}},\tau_{4_{\mathfrak{e}_2}},\tau_{5_{\mathfrak{e}_2}}\}$ *are complex fuzzy quadri-topology on* $\mathbb{X}$*. But* τ *is not a CTVNS topology on* $\mathbb{X}$*.*

Definition 4.4. *Let* $(\mathbb{X},\tau,\acute{\mathcal{E}})$ *be a CTVNS topological space over* $\mathbb{X}$ *and* $(\tilde{\mathcal{F}},\acute{\mathcal{E}}) \in CTVNSS(\mathbb{X},\acute{\mathcal{E}})$ *be a CTVNS set. Then, the CTVNS interior of* $(\tilde{\mathcal{F}},\acute{\mathcal{E}})$*, denoted by* $(\tilde{\mathcal{F}},\acute{\mathcal{E}})^\circ$ *is defined as the CTVNS union of all the CTVNS open subsets of* $(\tilde{\mathcal{F}},\acute{\mathcal{E}})$*. Clearly* $(\tilde{\mathcal{F}},\acute{\mathcal{E}})^\circ$ *is biggest CTVNS open set that is contained by* $(\tilde{\mathcal{F}},\acute{\mathcal{E}})$*.*

Example 4.4. *Let* τ_1 *be the CTVNS topology given in Example 4.2, and let*

$$(\tilde{\mathcal{F}},\acute{\mathcal{E}}) \in CTVNSS(\mathbb{X},\acute{\mathcal{E}}),$$

be a CTVNS set. Then

$$(\tilde{\mathcal{F}},\acute{\mathcal{E}}) = \begin{bmatrix}\mathfrak{e}_1 = \langle \mathrm{x}_1, 0.9e^{\iota\pi(0.9)}, 0.7e^{\iota\pi(0.8)}, 0.9e^{\iota\pi(0.9)}, 0.1e^{\iota\pi(0.2)}, 0.2e^{\iota\pi(0.1)}\rangle,\\ \langle \mathrm{x}_2, 0.8e^{\iota\pi(0.7)}, 0.6e^{\iota\pi(0.6)}, 0.9e^{\iota\pi(0.8)}, 0.2e^{\iota\pi(0.2)}, 0.4e^{\iota\pi(0.3)}\rangle\\ \langle \mathrm{x}_3, 0.5e^{\iota\pi(0.6)}, 0.6e^{\iota\pi(0.4)}, 0.8e^{\iota\pi(0.9)}, 0.2e^{\iota\pi(0.3)}, 0.3e^{\iota\pi(0.1)}\rangle;\\ \mathfrak{e}_2 = \langle \mathrm{x}_1, 0.8e^{\iota\pi(0.9)}, 0.5e^{\iota\pi(0.8)}, 0.8e^{\iota\pi(0.9)}, 0.3e^{\iota\pi(0.1)}, 0.3e^{\iota\pi(0.6)}\rangle,\\ \langle \mathrm{x}_2, 0.7e^{\iota\pi(0.6)}, 0.6e^{\iota\pi(0.8)}, 0.7e^{\iota\pi(0.8)}, 0.2e^{\iota\pi(0.3)}, 0.4e^{\iota\pi(0.1)}\rangle,\\ \langle \mathrm{x}_3, 0.7e^{\iota\pi(0.9)}, 0.5e^{\iota\pi(0.5)}, 0.9e^{\iota\pi(0.9)}, 0.1e^{\iota\pi(0.1)}, 0.3e^{\iota\pi(0.3)}\rangle.\end{bmatrix}.$$

Then $0_{(\mathbb{X},\acute{\mathcal{E}})}, (\tilde{\mathcal{F}}_2,\acute{\mathcal{E}}), (\tilde{\mathcal{F}}_3,\acute{\mathcal{E}}) \subseteq (\tilde{\mathcal{F}},\acute{\mathcal{E}})$. *Therefore,* $(\tilde{\mathcal{F}},\acute{\mathcal{E}})^\circ = 0_{(\mathbb{X},\acute{\mathcal{E}})} \Cup (\tilde{\mathcal{F}}_2,\acute{\mathcal{E}}) \Cup (\tilde{\mathcal{F}}_3,\acute{\mathcal{E}}) = (\tilde{\mathcal{F}}_2,\acute{\mathcal{E}})$.

Theorem 4.1. *Let* $(\mathbb{X},\tau,\acute{\mathcal{E}})$ *be a CTVNS topological space over* $\mathbb{X}$ *and* $(\tilde{\mathcal{F}},\acute{\mathcal{E}}) \in CTVNSS(\mathbb{X},\acute{\mathcal{E}})$. $(\tilde{\mathcal{F}},\acute{\mathcal{E}})$ *is a CTVNS open set if and only if* $(\tilde{\mathcal{F}},\acute{\mathcal{E}}) = (\tilde{\mathcal{F}},\acute{\mathcal{E}})^\circ$.

Proof. Let $(\tilde{\mathcal{F}},\acute{\mathcal{E}})$ be a CTVNS open set. Then the largest CTVNS open set contained in $(\tilde{\mathcal{F}},\acute{\mathcal{E}})$ is equal to $(\tilde{\mathcal{F}},\acute{\mathcal{E}})$. Hence, $(\tilde{\mathcal{F}},\acute{\mathcal{E}}) = (\tilde{\mathcal{F}},\acute{\mathcal{E}})^\circ$
Conversely, it is known that $(\tilde{\mathcal{F}},\acute{\mathcal{E}})^\circ$ is a CTVNS open set and if $(\tilde{\mathcal{F}},\acute{\mathcal{E}}) = (\tilde{\mathcal{F}},\acute{\mathcal{E}})^\circ$, then $(\tilde{\mathcal{F}},\acute{\mathcal{E}})$ is a CTVNS open set. □

Theorem 4.2. *Let* $(\mathbb{X},\tau,\acute{\mathcal{E}})$ *be a CTVNS topological space over* $\mathbb{X}$ *and* $(\tilde{\mathcal{F}}_1,\acute{\mathcal{E}}), (\tilde{\mathcal{F}}_2,\acute{\mathcal{E}}) \in CTVNSS(\mathbb{X},\acute{\mathcal{E}})$. *Then,*

(i). $[(\tilde{\mathcal{F}},\acute{\mathcal{E}})^\circ]^\circ = (\tilde{\mathcal{F}},\acute{\mathcal{E}})^\circ$,

(ii). $(0_{(\mathbb{X},\acute{\mathcal{E}})})^\circ = 0_{(\mathbb{X},\acute{\mathcal{E}})}$ *and* $(1_{(\mathbb{X},\acute{\mathcal{E}})})^\circ = 1_{(\mathbb{X},\acute{\mathcal{E}})}$,

(iii). $(\tilde{\mathcal{F}}_1,\acute{\mathcal{E}}) \subseteq (\tilde{\mathcal{F}}_2,\acute{\mathcal{E}}) \Rightarrow (\tilde{F}_1,\acute{\mathcal{E}})^\circ \subseteq (\tilde{\mathcal{F}}_2,\acute{\mathcal{E}})^\circ$,

(iv). $[(\tilde{\mathcal{F}}_1,\acute{\mathcal{E}}) \Cap (\tilde{\mathcal{F}}_2,\acute{\mathcal{E}})]^\circ = (\tilde{\mathcal{F}}_1,\acute{\mathcal{E}})^\circ \Cap (\tilde{\mathcal{F}}_2,\acute{\mathcal{E}})^\circ$,

(v). $(\tilde{\mathcal{F}}_1,\acute{\mathcal{E}})^\circ \Cup (\tilde{\mathcal{F}}_2,\acute{\mathcal{E}})^\circ \subseteq [(\tilde{\mathcal{F}}_1,\acute{\mathcal{E}}) \Cup (\tilde{\mathcal{F}}_2,\acute{\mathcal{E}})]^\circ$.

Proof. **(i).** Let $(\tilde{\mathcal{F}}_1,\acute{\mathcal{E}})^\circ = (\tilde{\mathcal{F}}_2,\acute{\mathcal{E}})$ Then $(\tilde{\mathcal{F}}_2,\acute{\mathcal{E}}) \in \tau iff (\tilde{\mathcal{F}}_2,\acute{\mathcal{E}}) = (\tilde{\mathcal{F}}_2,\acute{\mathcal{E}})^\circ$. So $[(\tilde{\mathcal{F}}_1,\acute{\mathcal{E}})^\circ]^\circ = (\tilde{\mathcal{F}}_1,\acute{\mathcal{E}})^\circ$.

(ii). Since $0_{(\mathbb{X},\acute{\mathcal{E}})}$ and $1_{(\mathbb{X},\acute{\mathcal{E}})}$ are always CTVNS open sets, we have:

$$(0_{(\mathbb{X},\acute{\mathcal{E}})})^\circ = 0_{(\mathbb{X},\acute{\mathcal{E}})}, \quad \text{and} \quad (1_{(\mathbb{X},\acute{\mathcal{E}})})^\circ = 1_{(\mathbb{X},\acute{\mathcal{E}})}.$$

(iii). It is known that $(\tilde{\mathcal{F}}_1,\acute{\mathcal{E}})^\circ \subseteq (\tilde{\mathcal{F}}_1,\acute{\mathcal{E}}) \subseteq (\tilde{\mathcal{F}}_2,\acute{\mathcal{E}})$ and $(\tilde{\mathcal{F}}_2,\acute{\mathcal{E}})^\circ \subseteq (\tilde{\mathcal{F}}_2,\acute{\mathcal{E}})$. Since $(\tilde{\mathcal{F}}_2,\acute{\mathcal{E}})^\circ$ is the biggest CTVNS open set contained in $(\tilde{\mathcal{F}}_2,\acute{\mathcal{E}})$ and so $(\tilde{\mathcal{F}}_1,\acute{\mathcal{E}})^\circ \subseteq (\tilde{\mathcal{F}}_2,\acute{\mathcal{E}})^\circ$.

(iv). Since $(\tilde{\mathcal{F}}_1,\acute{\mathcal{E}}) \Cap (\tilde{\mathcal{F}}_2,\acute{\mathcal{E}}) \subseteq (\tilde{\mathcal{F}}_1,\acute{\mathcal{E}})$ and $(\tilde{\mathcal{F}}_1,\acute{\mathcal{E}}) \Cap (\tilde{\mathcal{F}}_2,\acute{\mathcal{E}}) \subseteq (\tilde{\mathcal{F}}_2,\acute{\mathcal{E}})$, then $[(\tilde{\mathcal{F}}_1,\acute{\mathcal{E}}) \Cap (\tilde{\mathcal{F}}_2,\acute{\mathcal{E}})]^\circ \subseteq (\tilde{\mathcal{F}}_1,\acute{\mathcal{E}})^\circ$ and $[(\tilde{\mathcal{F}}_1,\acute{\mathcal{E}}) \Cap (\tilde{\mathcal{F}}_2,\acute{\mathcal{E}})]^\circ \subseteq (\tilde{\mathcal{F}}_2,\acute{\mathcal{E}})^\circ$ and so,

$$[(\tilde{\mathcal{F}}_1,\acute{\mathcal{E}}) \Cap (\tilde{\mathcal{F}}_2,\acute{\mathcal{E}})]^\circ \subseteq (\tilde{\mathcal{F}}_1,\acute{\mathcal{E}})^\circ \Cap (\tilde{\mathcal{F}}_2,\acute{\mathcal{E}})^\circ.$$

On the other hand, since $(\tilde{\mathcal{F}}_1,\acute{\mathcal{E}})^\circ \subseteq (\tilde{\mathcal{F}}_1,\acute{\mathcal{E}})$ and $(\tilde{\mathcal{F}}_2,\acute{\mathcal{E}})^\circ \subseteq (\tilde{\mathcal{F}}_2,\acute{\mathcal{E}})$, then:

$$(\tilde{\mathcal{F}}_1,\acute{\mathcal{E}})^\circ \Cap (\tilde{\mathcal{F}}_2,\acute{\mathcal{E}})^\circ \subseteq (\tilde{\mathcal{F}}_1,\acute{\mathcal{E}}) \Cap (\tilde{\mathcal{F}}_2,\acute{\mathcal{E}}).$$

Besides,$[(\tilde{\mathcal{F}}_1,\acute{\mathcal{E}}) \Cap (\tilde{\mathcal{F}}_2,\acute{\mathcal{E}})]^\circ \subseteq (\tilde{\mathcal{F}}_1,\acute{\mathcal{E}}) \Cap (\tilde{\mathcal{F}}_2,\acute{\mathcal{E}})$ and is the biggest CTVNS open set. Therefore, $(\tilde{\mathcal{F}}_1,\acute{\mathcal{E}})^\circ \Cap (\tilde{\mathcal{F}}_2,\acute{\mathcal{E}})^\circ \subseteq [(\tilde{\mathcal{F}}_1,\acute{\mathcal{E}}) \Cap (\tilde{\mathcal{F}}_2,\acute{\mathcal{E}})]^\circ$. Thus, $[(\tilde{\mathcal{F}}_1,\acute{\mathcal{E}}) \Cap (\tilde{\mathcal{F}}_2,\acute{\mathcal{E}})]^\circ = (\tilde{\mathcal{F}}_1,\acute{\mathcal{E}})^\circ \Cap (\tilde{\mathcal{F}}_2,\acute{\mathcal{E}})^\circ$.

(v). Since $(\tilde{\mathcal{F}}_1,\acute{\mathcal{E}}) \subseteq (\tilde{\mathcal{F}}_1,\acute{\mathcal{E}}) \Cup (\tilde{\mathcal{F}}_2,\acute{\mathcal{E}})$ and $(\tilde{\mathcal{F}}_2,\acute{\mathcal{E}}) \subseteq (\tilde{\mathcal{F}}_1,\acute{\mathcal{E}}) \Cup (\tilde{\mathcal{F}}_2,\acute{\mathcal{E}})$, then:

$$(\tilde{\mathcal{F}}_1,\acute{\mathcal{E}})^\circ \subseteq [(\tilde{\mathcal{F}}_1,\acute{\mathcal{E}}) \Cup (\tilde{\mathcal{F}}_2,\acute{\mathcal{E}})]^\circ, \text{ and } (\tilde{\mathcal{F}}_2,\acute{\mathcal{E}})^\circ \subseteq [(\tilde{\mathcal{F}}_1,\acute{\mathcal{E}}) \Cup (\tilde{\mathcal{F}}_2,\acute{\mathcal{E}})]^\circ.$$

Therefore,

$$(\tilde{\mathcal{F}}_1,\acute{\mathcal{E}})^\circ \Cup (\tilde{\mathcal{F}}_2,\acute{\mathcal{E}})^\circ \subseteq [(\tilde{\mathcal{F}}_1,\acute{\mathcal{E}}) \Cup (\tilde{\mathcal{F}}_2,\acute{\mathcal{E}})]^\circ.$$

□

Definition 4.5. *Let* $(\mathbb{X},\tau,\acute{\mathcal{E}})$ *be a CTVNS topological space over* $\mathbb{X}$ *and* $(\tilde{\mathcal{F}},\acute{\mathcal{E}}) \in CTVNSS(\mathbb{X},\acute{\mathcal{E}})$ *be a CTVNS set. Then, the CTVNS closure of* $(\tilde{\mathcal{F}},\acute{\mathcal{E}})$*, denoted by* $\overline{(\tilde{\mathcal{F}},\acute{\mathcal{E}})}$ *is defined as the CTVNS intersection of all the CTVNS closed supersets of* $(\tilde{\mathcal{F}},\acute{\mathcal{E}})$.
Clearly $\overline{(\tilde{\mathcal{F}},\acute{\mathcal{E}})}$ *is the smallest CTVNS closed set containing* $(\tilde{\mathcal{F}},\acute{\mathcal{E}})$.

Example 4.5. *Consider the CTVNS topology* τ_1 *given in Example 4.2. Let*

$$(\tilde{\mathcal{F}},\acute{\mathcal{E}}) \in CTVNSS(\mathbb{X},\acute{\mathcal{E}}),$$

be a CTVNS set defined as follows:

$$(\tilde{\mathcal{F}},\acute{\mathcal{E}}) = \begin{bmatrix} e_1 = \langle x_1, \dfrac{0.5e^{\iota\pi(0.4)}, 0.2e^{\iota\pi(0.2)}, 0.4e^{\iota\pi(0.5)}, 0.6e^{\iota\pi(0.7)}}{0.7e^{\iota\pi(0.6)}} \rangle, \\ \langle x_2, \dfrac{0.4e^{\iota\pi(0.3)}, 0.3e^{\iota\pi(0.3)}, 0.5e^{\iota\pi(0.4)}, 0.7e^{\iota\pi(0.7)}}{0.8e^{\iota\pi(0.9)}} \rangle \\ \langle x_3, \dfrac{0.1e^{\iota\pi(0.1)}, 0.2e^{\iota\pi(0.1)}, 0.3e^{\iota\pi(0.4)}, 0.8e^{\iota\pi(0.8)}}{0.9e^{\iota\pi(0.9)}} \rangle; \\ e_2 = \langle x_1, \dfrac{0.2e^{\iota\pi(0.2)}, 0.2e^{\iota\pi(0.1)}, 0.4e^{\iota\pi(0.6)}, 0.6e^{\iota\pi(0.6)}}{0.7e^{\iota\pi(0.8)}} \rangle, \\ \langle x_2, \dfrac{0.3e^{\iota\pi(0.1)}, 0.1e^{\iota\pi(0.1)}, 0.2e^{\iota\pi(0.4)}, 0.8e^{\iota\pi(0.9)}}{0.9e^{\iota\pi(0.9)}} \rangle, \\ \langle x_3, \dfrac{0.1e^{\iota\pi(0.2)}, 0.2e^{\iota\pi(0.1)}, 0.5e^{\iota\pi(0.6)}, 0.9e^{\iota\pi(0.9)}}{0.7e^{\iota\pi(0.9)}} \rangle. \end{bmatrix}.$$

Obviously, $(0_{(\mathbb{X},\acute{\mathcal{E}})})^c, (1_{(\mathbb{X},\acute{\mathcal{E}})})^c, (\tilde{\mathcal{F}}_1,\acute{\mathcal{E}})^c, (\tilde{\mathcal{F}}_2,\acute{\mathcal{E}})^c$, *and*$(\tilde{\mathcal{F}}_3,\acute{\mathcal{E}})^c$ *are all CTVNS closed sets over* $(\mathbb{X},\tau_1,\acute{\mathcal{E}})$.

$$(0_{(\mathbb{X},\acute{\mathcal{E}})})^c = 1_{(\mathbb{X},\acute{\mathcal{E}})}, \quad (1_{(\mathbb{X},\acute{\mathcal{E}})})^c = 0_{(\mathbb{X},\acute{\mathcal{E}})},$$

$$(\tilde{\mathcal{F}}_1,\acute{\mathcal{E}})^c = \begin{bmatrix} e_1 = \langle x_1, \dfrac{0.3e^{\iota\pi(0.5)}, 0.2e^{\iota\pi(0.4)}, 0.1e^{\iota\pi(0.2)}, 0.6e^{\iota\pi(0.8)}}{0.9e^{\iota\pi(0.9)}} \rangle, \\ \langle x_2, \dfrac{0.5e^{\iota\pi(0.4)}, 0.3e^{\iota\pi(0.3)}, 0.2e^{\iota\pi(0.3)}, 0.6e^{\iota\pi(0.5)}}{0.7e^{\iota\pi(0.7)}} \rangle \\ \langle x_3, \dfrac{0.4e^{\iota\pi(0.2)}, 0.3e^{\iota\pi(0.4)}, 0.2e^{\iota\pi(0.2)}, 0.5e^{\iota\pi(0.2)}}{0.4e^{\iota\pi(0.3)}} \rangle; \\ e_2 = \langle x_1, \dfrac{0.4e^{\iota\pi(0.7)}, 0.3e^{\iota\pi(0.1)}, 0.3e^{\iota\pi(0.1)}, 0.3e^{\iota\pi(0.8)}}{0.7e^{\iota\pi(0.9)}} \rangle, \\ \langle x_2, \dfrac{0.4e^{\iota\pi(0.2)}, 0.3e^{\iota\pi(0.3)}, 0.4e^{\iota\pi(0.2)}, 0.5e^{\iota\pi(0.7)}}{0.6e^{\iota\pi(0.5)}} \rangle, \\ \langle x_3, \dfrac{0.3e^{\iota\pi(0.4)}, 0.2e^{\iota\pi(0.3)}, 0.1e^{\iota\pi(0.2)}, 0.4e^{\iota\pi(0.4)}}{0.7e^{\iota\pi(0.8)}} \rangle. \end{bmatrix},$$

$$(\tilde{\mathcal{F}}_2,\acute{\mathcal{E}})^c=\begin{bmatrix} e_1=\langle x_1,\dfrac{0.5e^{\iota\pi(0.5)},0.4e^{\iota\pi(0.4)},0.2e^{\iota\pi(0.3)},0.5e^{\iota\pi(0.4)}}{0.7e^{\iota\pi(0.8)}}\rangle,\\ \langle x_2,\dfrac{0.7e^{\iota\pi(0.6)},0.4e^{\iota\pi(0.4)},0.3e^{\iota\pi(0.3)},0.5e^{\iota\pi(0.5)}}{0.6e^{\iota\pi(0.4)}}\rangle\\ \langle x_3,\dfrac{0.6e^{\iota\pi(0.8)},0.5e^{\iota\pi(0.7)},0.4e^{\iota\pi(0.3)},0.4e^{\iota\pi(0.2)}}{0.3e^{\iota\pi(0.2)}}\rangle;\\ e_2=\langle x_1,\dfrac{0.5e^{\iota\pi(0.7)},0.4e^{\iota\pi(0.3)},0.4e^{\iota\pi(0.1)},0.2e^{\iota\pi(0.6)}}{0.6e^{\iota\pi(0.6)}}\rangle,\\ \langle x_2,\dfrac{0.6e^{\iota\pi(0.7)},0.4e^{\iota\pi(0.5)},0.5e^{\iota\pi(0.3)},0.4e^{\iota\pi(0.1)}}{0.5e^{\iota\pi(0.4)}}\rangle,\\ \langle x_3,\dfrac{0.5e^{\iota\pi(0.4)},0.6e^{\iota\pi(0.7)},0.2e^{\iota\pi(0.2)},0.3e^{\iota\pi(0.3)}}{0.4e^{\iota\pi(0.3)}}\rangle. \end{bmatrix},$$

$$(\tilde{\mathcal{F}}_3,\acute{\mathcal{E}})^c=\begin{bmatrix} e_1=\langle x_1,\dfrac{0.6e^{\iota\pi(0.5)},0.5e^{\iota\pi(0.4)},0.3e^{\iota\pi(0.3)},0.4e^{\iota\pi(0.2)}}{0.5e^{\iota\pi(0.6)}}\rangle,\\ \langle x_2,\dfrac{0.7e^{\iota\pi(0.7)},0.5e^{\iota\pi(0.6)},0.4e^{\iota\pi(0.4)},0.3e^{\iota\pi(0.1)}}{0.4e^{\iota\pi(0.2)}}\rangle\\ \langle x_3,\dfrac{0.8e^{\iota\pi(0.9)},0.6e^{\iota\pi(0.8)},0.5e^{\iota\pi(0.4)},0.3e^{\iota\pi(0.2)}}{0.2e^{\iota\pi(0.1)}}\rangle;\\ e_2=\langle x_1,\dfrac{0.6e^{\iota\pi(0.8)},0.5e^{\iota\pi(0.4)},0.5e^{\iota\pi(0.3)},0.2e^{\iota\pi(0.1)}}{0.4e^{\iota\pi(0.3)}}\rangle,\\ \langle x_2,\dfrac{0.8e^{\iota\pi(0.9)},0.5e^{\iota\pi(0.6)},0.6e^{\iota\pi(0.4)},0.2e^{\iota\pi(0.1)}}{0.4e^{\iota\pi(0.3)}}\rangle,\\ \langle x_3,\dfrac{0.6e^{\iota\pi(0.5)},0.7e^{\iota\pi(0.9)},0.4e^{\iota\pi(0.2)},0.3e^{\iota\pi(0.1)}}{0.3e^{\iota\pi(0.2)}}\rangle. \end{bmatrix}.$$

Then $(1_{(\mathbb{X},\acute{\mathcal{E}})})^c,(\tilde{\mathcal{F}}_1,\acute{\mathcal{E}})^c,(\tilde{\mathcal{F}}_2,\acute{\mathcal{E}})^c,(\tilde{\mathcal{F}}_3,\acute{\mathcal{E}})^c\supseteq(\tilde{\mathcal{F}},\acute{\mathcal{E}})$. *Therefore,*

$$\overline{(\tilde{\mathcal{F}},\acute{\mathcal{E}})}=(1_{(\mathbb{X},\acute{\mathcal{E}})})^c\Cap(\tilde{\mathcal{F}}_1,\acute{\mathcal{E}})^c\Cap(\tilde{\mathcal{F}}_3,\acute{\mathcal{E}})^c\Cap(\tilde{\mathcal{F}}_2,\acute{\mathcal{E}})^c=(\tilde{\mathcal{F}}_1,\acute{\mathcal{E}})^c.$$

Theorem 4.3. *Let* $(\mathbb{X},\tau,\acute{\mathcal{E}})$ *be a CTVNS topological space over* $\mathbb{X}$ *and* $(\tilde{\mathcal{F}},\acute{\mathcal{E}})\in CTVNSS(\mathbb{X},\acute{\mathcal{E}})$. $(\tilde{\mathcal{F}},\acute{\mathcal{E}})$ *is a CTVNS closed set if and only if* $(\tilde{\mathcal{F}},\acute{\mathcal{E}})=\overline{(\tilde{\mathcal{F}},\acute{\mathcal{E}})}$

Proof. Let $(\tilde{\mathcal{F}},\acute{\mathcal{E}})$ be a CTVNS closed set. Then the smallest CTVNS closed set containing $(\tilde{\mathcal{F}},\acute{\mathcal{E}})$ is equal to $(\tilde{\mathcal{F}},\acute{\mathcal{E}})$. Hence, $(\tilde{\mathcal{F}},\acute{\mathcal{E}})=\overline{(\tilde{\mathcal{F}},\acute{\mathcal{E}})}$

Conversely, it is known that $\overline{(\tilde{\mathcal{F}},\acute{\mathcal{E}})}$ is a CTVNS closed set and if $(\tilde{\mathcal{F}},\acute{\mathcal{E}})=\overline{(\tilde{\mathcal{F}},\acute{\mathcal{E}})}$, then $(\tilde{\mathcal{F}},\acute{\mathcal{E}})$ is a CTVNS closed set. □

Theorem 4.4. *Let* $(\mathbb{X},\tau,\acute{\mathcal{E}})$ *be a CTVNS topological space over* $\mathbb{X}$ *and* $(\tilde{\mathcal{F}}_1,\acute{\mathcal{E}}),(\tilde{\mathcal{F}}_2,\acute{\mathcal{E}})\in CTVNSS(\mathbb{X},\acute{\mathcal{E}})$. *Then,*

(i). $\overline{[\overline{(\tilde{\mathcal{F}},\acute{\mathcal{E}})}]}=\overline{(\tilde{\mathcal{F}},\acute{\mathcal{E}})}$,

(ii). $\overline{(0_{(\mathbb{X},\acute{\mathcal{E}})})}=0_{(\mathbb{X},\acute{\mathcal{E}})}$ *and* $\overline{(1_{(\mathbb{X},\acute{\mathcal{E}})})}=1_{(\mathbb{X},\acute{\mathcal{E}})}$,

(iii). $(\tilde{\mathcal{F}}_1,\acute{\mathcal{E}})\subseteq(\tilde{\mathcal{F}}_2,\acute{\mathcal{E}})\Rightarrow\overline{(\tilde{F}_1,\acute{\mathcal{E}})}\subseteq\overline{(\tilde{\mathcal{F}}_2,\acute{\mathcal{E}})}$,

(iv). $\overline{[(\tilde{\mathcal{F}}_1,\acute{\mathcal{E}})\Cup(\tilde{\mathcal{F}}_2,\acute{\mathcal{E}})]}=\overline{(\tilde{\mathcal{F}}_1,\acute{\mathcal{E}})}\Cup\overline{(\tilde{\mathcal{F}}_2,\acute{\mathcal{E}})}$,

(v). $\overline{(\tilde{\mathcal{F}}_1,\acute{\mathcal{E}})}\Cap\overline{(\tilde{\mathcal{F}}_2,\acute{\mathcal{E}})}\subseteq\overline{[(\tilde{\mathcal{F}}_1,\acute{\mathcal{E}})\Cap(\tilde{\mathcal{F}}_2,\acute{\mathcal{E}})]}$.

Proof. **(i).** Let $\overline{(\tilde{\mathcal{F}}_1,\acute{\mathcal{E}})}=(\tilde{\mathcal{F}}_2,\acute{\mathcal{E}})$ Then $(\tilde{\mathcal{F}}_2,\acute{\mathcal{E}})$ is a CTVNS closed set. Hence $(\tilde{\mathcal{F}}_2,\acute{\mathcal{E}})$ and $\overline{(\tilde{\mathcal{F}}_2,\acute{\mathcal{E}})}$ are equal. Therefore $\overline{[\overline{(\tilde{\mathcal{F}}_1,\acute{\mathcal{E}})}]}=\overline{(\tilde{\mathcal{F}}_1,\acute{\mathcal{E}})}$.

(ii). Since $0_{(\mathbb{X},\acute{\mathcal{E}})}$ and $1_{(\mathbb{X},\acute{\mathcal{E}})}$ are always CTVNS closed sets, we have:

$$\overline{(0_{(\mathbb{X},\acute{\mathcal{E}})})}=0_{(\mathbb{X},\acute{\mathcal{E}})},\quad\text{and}\quad\overline{(1_{(\mathbb{X},\acute{\mathcal{E}})})}=1_{(\mathbb{X},\acute{\mathcal{E}})}.$$

(iii). It is known that $(\tilde{\mathcal{F}}_1,\acute{\mathcal{E}})\subseteq\overline{(\tilde{\mathcal{F}}_1,\acute{\mathcal{E}})}$ and $(\tilde{\mathcal{F}}_2,\acute{\mathcal{E}})\subseteq\overline{(\tilde{\mathcal{F}}_2,\acute{\mathcal{E}})}$, so $(\tilde{\mathcal{F}}_1,\acute{\mathcal{E}})\subseteq(\tilde{\mathcal{F}}_2,\acute{\mathcal{E}})\subseteq\overline{(\tilde{\mathcal{F}}_2,\acute{\mathcal{E}})}$. Since $\overline{(\tilde{\mathcal{F}}_2,\acute{\mathcal{E}})}$ is the smallest CTVNS closed set containing $(\tilde{\mathcal{F}}_1,\acute{\mathcal{E}})$, then $\overline{(\tilde{\mathcal{F}}_1,\acute{\mathcal{E}})}\subseteq\overline{(\tilde{\mathcal{F}}_2,\acute{\mathcal{E}})}$.

(iv). Since $(\tilde{\mathcal{F}}_1,\acute{\mathcal{E}})\subseteq(\tilde{\mathcal{F}}_1,\acute{\mathcal{E}})\Cup(\tilde{\mathcal{F}}_2,\acute{\mathcal{E}})$ and $(\tilde{\mathcal{F}}_2,\acute{\mathcal{E}})\subseteq(\tilde{\mathcal{F}}_1,\acute{\mathcal{E}})\Cup(\tilde{\mathcal{F}}_2,\acute{\mathcal{E}})$, then $\overline{(\tilde{\mathcal{F}}_1,\acute{\mathcal{E}})}\subseteq\overline{[(\tilde{\mathcal{F}}_1,\acute{\mathcal{E}})\Cup(\tilde{\mathcal{F}}_2,\acute{\mathcal{E}})]}$ and $\overline{(\tilde{\mathcal{F}}_2,\acute{\mathcal{E}})}\subseteq\overline{[(\tilde{\mathcal{F}}_1,\acute{\mathcal{E}})\Cup(\tilde{\mathcal{F}}_2,\acute{\mathcal{E}})]}$ and so,

$$\overline{(\tilde{\mathcal{F}}_1,\acute{\mathcal{E}})}\Cup\overline{(\tilde{\mathcal{F}}_2,\acute{\mathcal{E}})}\subseteq\overline{[(\tilde{\mathcal{F}}_1,\acute{\mathcal{E}})\Cup(\tilde{\mathcal{F}}_2,\acute{\mathcal{E}})]}.$$

Conversely, since $(\tilde{\mathcal{F}}_1,\acute{\mathcal{E}})\subseteq\overline{(\tilde{\mathcal{F}}_1,\acute{\mathcal{E}})}$ and $(\tilde{\mathcal{F}}_2,\acute{\mathcal{E}})\subseteq\overline{(\tilde{\mathcal{F}}_2,\acute{\mathcal{E}})}$, then:

$$(\tilde{\mathcal{F}}_1,\acute{\mathcal{E}})\Cup(\tilde{\mathcal{F}}_2,\acute{\mathcal{E}})\subseteq\overline{(\tilde{\mathcal{F}}_1,\acute{\mathcal{E}})}\Cup\overline{(\tilde{\mathcal{F}}_2,\acute{\mathcal{E}})}.$$

Besides, $\overline{[(\tilde{\mathcal{F}}_1,\acute{\mathcal{E}})\Cup(\tilde{\mathcal{F}}_2,\acute{\mathcal{E}})]}$ is the smallest CTVNS closed set containing $(\tilde{\mathcal{F}}_1,\acute{\mathcal{E}})\Cup(\tilde{\mathcal{F}}_2,\acute{\mathcal{E}})$. Therefore, $\overline{[(\tilde{\mathcal{F}}_1,\acute{\mathcal{E}})\Cup(\tilde{\mathcal{F}}_2,\acute{\mathcal{E}})]}\subseteq\overline{(\tilde{\mathcal{F}}_1,\acute{\mathcal{E}})}\Cup\overline{(\tilde{\mathcal{F}}_2,\acute{\mathcal{E}})}$. Thus, $\overline{[(\tilde{\mathcal{F}}_1,\acute{\mathcal{E}})\Cup(\tilde{\mathcal{F}}_2,\acute{\mathcal{E}})]}=\overline{(\tilde{\mathcal{F}}_1,\acute{\mathcal{E}})}\Cup\overline{(\tilde{\mathcal{F}}_2,\acute{\mathcal{E}})}$.

(v). Since

$$(\tilde{\mathcal{F}}_1,\acute{\mathcal{E}})\Cap(\tilde{\mathcal{F}}_2,\acute{\mathcal{E}})\subseteq\overline{[(\tilde{\mathcal{F}}_1,\acute{\mathcal{E}})\Cap(\tilde{\mathcal{F}}_2,\acute{\mathcal{E}})]},\quad\text{and}\quad\overline{[(\tilde{\mathcal{F}}_1,\acute{\mathcal{E}})\Cap(\tilde{\mathcal{F}}_2,\acute{\mathcal{E}})]}$$

is the smallest CTVNS closed set containing $(\tilde{\mathcal{F}}_1,\acute{\mathcal{E}})\Cap(\tilde{\mathcal{F}}_2,\acute{\mathcal{E}})$. Then,

$$\overline{[(\tilde{\mathcal{F}}_1,\acute{\mathcal{E}})\Cap(\tilde{\mathcal{F}}_2,\acute{\mathcal{E}})]}\subseteq\overline{(\tilde{\mathcal{F}}_1,\acute{\mathcal{E}})}\Cap\overline{(\tilde{\mathcal{F}}_2,\acute{\mathcal{E}})}.$$

□

Theorem 4.5. *Let* $(\mathbb{X},\tau,\acute{\mathcal{E}})$ *be a CTVNS topological space over* $\mathbb{X}$, *and let* $(\tilde{\mathcal{F}},\acute{\mathcal{E}})\in CTVNSS(\mathbb{X},\acute{\mathcal{E}})$. *Then:*

(i). $\overline{[(\tilde{\mathcal{F}},\acute{\mathcal{E}})]^c}=[(\tilde{\mathcal{F}},\acute{\mathcal{E}})^c]^\circ$,

(ii). $[(\tilde{\mathcal{F}},\acute{\mathcal{E}})^\circ]^c=\overline{[(\tilde{\mathcal{F}},\acute{\mathcal{E}})^c]}$.

Proof. **(i).**

$$\begin{aligned}\overline{(\tilde{\mathcal{F}},\acute{\mathcal{E}})}&=\Cap\{(\tilde{\mathcal{G}},\acute{\mathcal{E}})\in\tau^c:(\tilde{\mathcal{G}},\acute{\mathcal{E}})\supseteq(\tilde{\mathcal{F}},\acute{\mathcal{E}})\}\\ &\Rightarrow[\overline{(\tilde{\mathcal{F}},\acute{\mathcal{E}})}]^c=\left[\Cap\{(\tilde{\mathcal{G}},\acute{\mathcal{E}})\in\tau^c:(\tilde{\mathcal{G}},\acute{\mathcal{E}})\supseteq(\tilde{\mathcal{F}},\acute{\mathcal{E}})\}\right]^c\\ &=\Cup\{(\tilde{\mathcal{G}},\acute{\mathcal{E}})^c\in\tau:(\tilde{\mathcal{G}},\acute{\mathcal{E}})^c\subseteq(\tilde{\mathcal{F}},\acute{\mathcal{E}})^c\}\\ &=[(\tilde{\mathcal{F}},\acute{\mathcal{E}})^c]^\circ.\end{aligned}$$

(ii).

$$
\begin{aligned}
(\tilde{\mathcal{F}},\acute{\mathcal{E}})^{\circ} &= \Cup\{(\tilde{\mathcal{G}},\acute{\mathcal{E}}) \in \tau : (\tilde{\mathcal{G}},\acute{\mathcal{E}}) \subseteq (\tilde{\mathcal{F}},\acute{\mathcal{E}})\} \\
&\Rightarrow [(\tilde{\mathcal{F}},\acute{\mathcal{E}})^{\circ}]^{c} = \left[\Cup\{(\tilde{\mathcal{G}},\acute{\mathcal{E}}) \in \tau : (\tilde{\mathcal{G}},\acute{\mathcal{E}}) \subseteq (\tilde{\mathcal{F}},\acute{\mathcal{E}})\}\right]^{c} \\
&= \Cap\{(\tilde{\mathcal{G}},\acute{\mathcal{E}})^{c} \in \tau^{c} : (\tilde{\mathcal{G}},\acute{\mathcal{E}})^{c} \supseteq (\tilde{\mathcal{F}},\acute{\mathcal{E}})^{c}\} \\
&= \overline{[(\tilde{\mathcal{F}},\acute{\mathcal{E}})^{c}]}.
\end{aligned}
$$

□

5. AI-driven cotangent similarity framework for triple-valued neutrosophic soft sets

The Cotangent Similarity Measure (CSM), a technique that discusses the geometric orientation of two data vectors to determine how similar they are, is the brains behind an AI-based system. Depending on the orientation of the data points, CSM is far more effective than simple distance measures at uncovering some hidden patterns and relationships, which makes it a valuable tool for comparative research. In a military setting, CSM is used to classify potential targets according on surveillance data. This is accomplished by comparing an unknown target's operating characteristics with a database that contains threat profiles that have already been stored. It is a method that calculates how similar the target is to known designs, so there is a good likelihood that the danger will be correctly classified and categorized. A vast array of statistical and machine learning elements are added to this pattern identification capability. Heatmaps, bar graphs, 3D surface plots, correlation analysis, spline-smoothed functional curves, and K-Means clustering (with normalizations for each) are examples of a basic set of approaches. Important elements in the working process, like data preparation, model validation, and above all the intuitive human interpretation of outcomes, are worked with using such a toolbox. The CSM engine and visualization techniques are intended to provide a comprehensive artificial intelligence system for classifying military targets. The end result provides military decision-makers with a solution that is not just computationally sound but also operationally understandable and useful.

5.1. Cotangent similarity measures

Let $T_i = (\mathrm{T}_{ik}, \mathrm{RT}_{ik}, \mathrm{C}_{ik}, \mathrm{RF}_{ik}, \mathrm{F}_{ik}), C_j = (\mathrm{T}_{jk}, \mathrm{RT}_{jk}, \mathrm{C}_{jk}, \mathrm{RF}_{jk}, \mathrm{F}_{jk})$ are two CTVNSSs. Each set is represented by three components for each feature k:
T_{ik}: Truth membership of feature $k\ for\ T_i$.
RT_{ik}: Relative truth membership of feature $k\ for\ T_i$.
C_{ik}: Contradiction of feature $k\ for\ T_i$.
RF_{ik}: Relative false membership of feature $k\ for\ T_i$.
F_{ik}: False membership degree of feature $k\ for\ T_i$.
The values typically satisfy: $\mathrm{T}_{ik}, \mathrm{RT}_{ik}, \mathrm{C}_{ik}, \mathrm{RF}_{ik}, \mathrm{F}_{ik} \in [0, 1]$
Similarly, for object C_j:
T_{jk}: Truth membership of feature $k\ for\ C_j$.
RT_{jk}: Relative truth membership of feature $k\ for\ C_j$.
C_{jk}: Contradiction of feature $k\ for\ C_j$.
RF_{jk}: Relative false membership of feature $k\ for\ C_j$.
F_{jk}: False membership degree of feature $k\ for\ C_j$.
The values typically satisfy: $\mathrm{T}_{jk}, \mathrm{RT}_{jk}, \mathrm{C}_{jk}, \mathrm{RF}_{jk}, \mathrm{F}_{jk} \in [0, 1]$
$Cotangent_{TNSS}(T_i, C_j) =$

$$
\frac{1}{n}\sum_{k=1}^{n}\{\cot[\frac{\pi}{4} + \frac{\pi}{12}(|\mathrm{T}_{ik} - \mathrm{T}_{jk}| + |\mathrm{RT}_{ik} - \mathrm{RT}_{jk}| + |\mathrm{C}_{ik} - \mathrm{C}_{jk}| + |\mathrm{RF}_{ik} - \mathrm{RF}_{jk}| + |\mathrm{F}_{ik} - \mathrm{F}_{jk}|)]\}.
$$

5.2. Multi-source target classification using cotangent similarity in a cotangent-type complex triple-valued neutrosophic framework

Effective target classification in contemporary surveillance and reconnaissance settings is a challenging task owing to the multi-source, uncertain and even contradictory characteristics of the data. This research focuses on the classification of a collection of operational targets using multiple data sources (radar, thermal, and electronic) to obtain signal observations. The uncertainty, vagueness and possible contradictions in such data require a powerful mathematical model that can simultaneously address truth, falsity, relative truth, relative falsity, and contradiction. In pursuit of this goal, we present a new classification approach based on the Cotangent Type Complex Triple-valued Neutrosophic Set. This method involves a cotangent similarity measure that assesses the association between targets and operational classes, considering five key attributes: truth membership, relative truth, contradiction, relative falsity, and falsity. These attributes are structured within a multi-dimensional operational classification matrix, which captures the complex relationships between targets, sources of signals and multiple classes in an event-driven environment. The new cotangent similarity measure can deal with nonlinear associations and uncertainty in the data. Through normalization and weighting of the multi-dimensional attributes, this approach yields comparative similarity scores for each target class combination, thus facilitating ranking and decision-making. The experimental results show that the proposed approach offers a holistic and flexible approach to modeling complex surveillance data, thus improving the performance and reliability of multi-source target classification systems.

5.3. A computational example of multi-source signal-based target classification

In today's fast-paced world of surveillance and reconnaissance, the ability to identify operational targets $T = \{T_1, T_2, T_3, T_4\}$ from multi-source signal samples $S = \{S_1, S_2, S_3, S_4\}$, and classify them into their proper operational status $C = \{C_1, C_2, C_3, C_4\}$, is a primary and challenging task. This challenge arises due to the uncertain nature of the information. Data obtained from radar, thermal, electronic and other types of sensing technologies can be uncertain, inexact and highly variable. This presents challenges for consistent classification. A complex mathematical approach is needed to deal with the uncertainty, which must be able to simultaneously account for degrees of truth, falsity, relative truth, relative falsity, and contradiction. This enables a more realistic understanding of the signal data. The multi-faceted relationships between

targets, signals and classification classes (especially when assessed with event-based measures and evaluations) are effectively captured within the operational classification matrix (Table 2).

Nevertheless, the straightforward comparison of raw signal response to targets and classes is unsuitable because of similarity values, unreliability and nonlinear correlation between attributes. To overcome this, the similarity measure between a target and a class, called Cotangent similarity measure, within the framework of the CTVNS set (Cotangent TNSS)is implemented, which permits measuring the similarity between any target-class pair. In both pairs (T_i, C_j), the approach uses the joint impact of truth membership, relative truth membership, contradiction, relative false membership and false membership functions, which are normalized by $n = 5$ attributes. This produces cotangent similarity scores which can be used to rank candidate target profiles comparatively with operational class templates. The raw surveillance parameters for each target T_i, as gathered from each data source S_i, are displayed in Table 1, while Table 2 presents the operational classification matrix. These are represented by the 5-dimensional feature vectors found in each cell, giving each target-source combination a thorough feature profile for preliminary analysis and threat modeling.

Table 2 illustrates how multi-dimensional representation can be used to organize complex, noisy and diverse data. The model does not ignore the uncertainty, but includes it, thereby producing a more accurate and realistic model for classification. The cotangent values that were calculated for every pair of targets and categorized profiles are then added to average all target-classification pairs.

The computed cotangent similarities have the following values:

$Cotangent_{TNSS}(T_1, C_1) = 0.0520$
$Cotangent_{TNSS}(T_1, C_2) = 0.0953$
$Cotangent_{TNSS}(T_1, C_3) = 0.0462$
$Cotangent_{TNSS}(T_1, C_4) = 0.1530$
$Cotangent_{TNSS}(T_2, C_1) = 0.0038$
$Cotangent_{TNSS}(T_2, C_2) = 0.0336$
$Cotangent_{TNSS}(T_2, C_3) = 0.0031$
$Cotangent_{TNSS}(T_2, C_4) = 0.1250$
$Cotangent_{TNSS}(T_3, C_1) = 0.0605$
$Cotangent_{TNSS}(T_3, C_2) = 0.0390$
$Cotangent_{TNSS}(T_3, C_3) = 0.1257$
$Cotangent_{TNSS}(T_3, C_4) = 0.0856$
$Cotangent_{TNSS}(T_4, C_1) = 0.1103$
$Cotangent_{TNSS}(T_4, C_2) = 0.2348$
$Cotangent_{TNSS}(T_4, C_3) = 0.1542$
$Cotangent_{TNSS}(T_4, C_4) = 0.0895$

The cotangent-similarity result indicates that there is a clear preference for Template T_4, which is present in every situation and, to the greatest extent possible, is comparable to Subjects $S_1 - S_3$. S_2 is a clear-cut, high-confidence match with no discernible ambiguity. Signal alignment but less support is implied by the moderate but reasonable relationship between S_1 and T_4. S_3 and S_4 are borderline decisions; they narrowly concur with T_4 and T_1, respectively. Any final assignment should be followed by a formal tie-break process.

Furthermore, Template T_2 performs poorly as well and most likely has to be expanded or changed (e.g., enrichment of features). Finally, before downstream interpretation, the persistently low S_1 scores should be preprocessed to remove noise or misregistration and scale mismatch.

6. Statistical and AI techniques

The cotangent similarity analysis and visualization, normalization, interpolation, and clustering approaches are employed in this study to evaluate the connection of the signals (S_1-S_4) and templates (T_1-T_4).

6.1. Cotangent similarity computation

Cotangent similarity, a trigonometric measure based on angular connections among vectors, was used to calculate pairwise similarity between signals and templates. Due to their effectiveness in directional similarity, cosine similarity and other angular similarity metrics are mainly used in pattern recognition and information retrieval [52].

6.2. Heatmap visualization

Segmented and gradient colormaps were used to produce two-dimensional heatmaps that displayed similarity matrices. The visualizations are commonly used in exploratory data analysis and can be used to intuitively illustrate relationships between matrices [53].

6.3. Normalization

To make it easier to compare similarity values among templates and interpret the results, similarity values were standardized using min-max to lie within the range [0,1]. Pipelines for data mining and machine learning frequently employ this preprocessing [54].

6.4. Bar plot analysis

Three-dimensional bar charts and grouped bar plots were used to compare the similarity values between signal-template pairs. When communicating the relative values of structured data, certain graphical techniques are suitable [55].

6.5. Correlation analysis

Correlation heatmaps with a value between -1 and 1 were made in order to analyze the relationship between signals. Determining the dependence, clusters, and inverses of variables is made easier by correlation analysis [56].

6.6. Curve modeling and interpolation

To produce a continuous representation of the discrete similarity data, cubic representations were used for interpolation and spline representations for smoothing. These techniques reduce noise and highlight some of the data's underlying patterns [57].

Table 1. Matrix of target intelligence features based on cotangent similarity ($T \times S$).

	S_1	S_2	...	S_n
T_1	$T_{11}, RT_{11}, C_{11}, RF_{11}, F_{11}$	$T_{12}, RT_{12}, C_{12}, RF_{12}, F_{12}$	...	$T_{1n}, RT_{1n}, C_{1n}, RF_{1n}, F_{1n}$
T_2	$T_{21}, RT_{21}, C_{21}, RF_{21}, F_{21}$	$T_{22}, RT_{22}, C_{22}, RF_{22}, F_{22}$	...	$T_{2n}, RT_{2n}, C_{2n}, RF_{2n}, F_{2n}$
...	...	...	...	...
T_m	$T_{m1}, RT_{m1}, C_{m1}, RF_{m1}, F_{m1}$	$T_{m2}, RT_{m2}, C_{m2}, RF_{m2}, F_{m2}$	...	$T_{mn}, RT_{mn}, C_{mn}, RF_{mn}, F_{mn}$

Table 2. Operational classification matrix for target surveillance data ($T \times S \rightarrow C$).

Row-I	S_1	S_2	S_3	S_4	**Row-II**	C_1	C_2	C_3	C_4
T_1	$\begin{pmatrix}0.6e^{\iota\pi(0.7)}\\0.4e^{\iota\pi(0.9)}\\0.5e^{\iota\pi(0.6)}\\0.8e^{\iota\pi(0.8)}\\0.2e^{\iota\pi(0.9)}\end{pmatrix}$	$\begin{pmatrix}0.4e^{\iota\pi(0.6)}\\0.7e^{\iota\pi(0.9)}\\0.6e^{\iota\pi(0.6)}\\0.9e^{\iota\pi(0.8)}\\0.3e^{\iota\pi(0.2)}\end{pmatrix}$	$\begin{pmatrix}0.5e^{\iota\pi(0.2)}\\0.6e^{\iota\pi(0.5)}\\0.5e^{\iota\pi(0.5)}\\0.7e^{\iota\pi(0.9)}\\0.4e^{\iota\pi(0.2)}\end{pmatrix}$	$\begin{pmatrix}0.7e^{\iota\pi(0.7)}\\0.2e^{\iota\pi(0.8)}\\0.9e^{\iota\pi(0.6)}\\0.4e^{\iota\pi(0.4)}\\0.6e^{\iota\pi(0.9)}\end{pmatrix}$	S_1	$\begin{pmatrix}0.6e^{\iota\pi(0.1)}\\0.8e^{\iota\pi(0.3)}\\0.7e^{\iota\pi(0.4)}\\0.3e^{\iota\pi(0.8)}\\0.1e^{\iota\pi(0.9)}\end{pmatrix}$	$\begin{pmatrix}0.5e^{\iota\pi(0.6)}\\0.1e^{\iota\pi(0.8)}\\0.9e^{\iota\pi(0.6)}\\0.7e^{\iota\pi(0.8)}\\0.9e^{\iota\pi(0.1)}\end{pmatrix}$	$\begin{pmatrix}0.4e^{\iota\pi(0.2)}\\0.6e^{\iota\pi(0.1)}\\0.2e^{\iota\pi(0.3)}\\0.5e^{\iota\pi(0.4)}\\0.1e^{\iota\pi(0.1)}\end{pmatrix}$	$\begin{pmatrix}0.2e^{\iota\pi(0.7)}\\0.4e^{\iota\pi(0.4)}\\0.3e^{\iota\pi(0.2)}\\0.7e^{\iota\pi(0.7)}\\0.1e^{\iota\pi(0.5)}\end{pmatrix}$
T_2	$\begin{pmatrix}0.8e^{\iota\pi(0.8)}\\0.5e^{\iota\pi(0.2)}\\0.6e^{\iota\pi(0.3)}\\0.9e^{\iota\pi(0.8)}\\0.4e^{\iota\pi(0.3)}\end{pmatrix}$	$\begin{pmatrix}0.2e^{\iota\pi(0.2)}\\0.6e^{\iota\pi(0.1)}\\0.7e^{\iota\pi(0.9)}\\0.8e^{\iota\pi(0.1)}\\0.9e^{\iota\pi(0.2)}\end{pmatrix}$	$\begin{pmatrix}0.3e^{\iota\pi(0.4)}\\0.7e^{\iota\pi(0.6)}\\0.6e^{\iota\pi(0.4)}\\0.9e^{\iota\pi(0.8)}\\0.4e^{\iota\pi(0.3)}\end{pmatrix}$	$\begin{pmatrix}0.6e^{\iota\pi(0.5)}\\0.8e^{\iota\pi(0.9)}\\0.4e^{\iota\pi(0.5)}\\0.3e^{\iota\pi(0.7)}\\0.5e^{\iota\pi(0.1)}\end{pmatrix}$	S_2	$\begin{pmatrix}0.2e^{\iota\pi(0.3)}\\0.7e^{\iota\pi(0.2)}\\0.5e^{\iota\pi(0.6)}\\0.3e^{\iota\pi(0.9)}\\0.5e^{\iota\pi(0.3)}\end{pmatrix}$	$\begin{pmatrix}0.4e^{\iota\pi(0.2)}\\0.9e^{\iota\pi(0.4)}\\0.6e^{\iota\pi(0.3)}\\0.2e^{\iota\pi(0.2)}\\0.1e^{\iota\pi(0.4)}\end{pmatrix}$	$\begin{pmatrix}0.1e^{\iota\pi(0.1)}\\0.5e^{\iota\pi(0.8)}\\0.7e^{\iota\pi(0.8)}\\0.6e^{\iota\pi(0.6)}\\0.2e^{\iota\pi(0.6)}\end{pmatrix}$	$\begin{pmatrix}0.7e^{\iota\pi(0.7)}\\0.5e^{\iota\pi(0.1)}\\0.8e^{\iota\pi(0.6)}\\0.4e^{\iota\pi(0.8)}\\0.3e^{\iota\pi(0.9)}\end{pmatrix}$
T_3	$\begin{pmatrix}0.4e^{\iota\pi(0.2)}\\0.7e^{\iota\pi(0.9)}\\0.3e^{\iota\pi(0.3)}\\0.2e^{\iota\pi(0.2)}\\0.1e^{\iota\pi(0.6)}\end{pmatrix}$	$\begin{pmatrix}0.5e^{\iota\pi(0.9)}\\0.4e^{\iota\pi(0.6)}\\0.3e^{\iota\pi(0.5)}\\0.4e^{\iota\pi(0.3)}\\0.7e^{\iota\pi(0.7)}\end{pmatrix}$	$\begin{pmatrix}0.6e^{\iota\pi(0.5)}\\0.4e^{\iota\pi(0.7)}\\0.8e^{\iota\pi(0.7)}\\0.5e^{\iota\pi(0.6)}\\0.2e^{\iota\pi(0.1)}\end{pmatrix}$	$\begin{pmatrix}0.3e^{\iota\pi(0.1)}\\0.6e^{\iota\pi(0.4)}\\0.6e^{\iota\pi(0.2)}\\0.8e^{\iota\pi(0.8)}\\0.3e^{\iota\pi(0.4)}\end{pmatrix}$	S_3	$\begin{pmatrix}0.3e^{\iota\pi(0.3)}\\0.4e^{\iota\pi(0.2)}\\0.6e^{\iota\pi(0.1)}\\0.2e^{\iota\pi(0.4)}\\0.5e^{\iota\pi(0.6)}\end{pmatrix}$	$\begin{pmatrix}0.7e^{\iota\pi(0.1)}\\0.5e^{\iota\pi(0.5)}\\0.8e^{\iota\pi(0.9)}\\0.4e^{\iota\pi(0.4)}\\0.2e^{\iota\pi(0.6)}\end{pmatrix}$	$\begin{pmatrix}0.5e^{\iota\pi(0.7)}\\0.4e^{\iota\pi(0.1)}\\0.2e^{\iota\pi(0.7)}\\0.9e^{\iota\pi(0.3)}\\0.6e^{\iota\pi(0.9)}\end{pmatrix}$	$\begin{pmatrix}0.1e^{\iota\pi(0.9)}\\0.6e^{\iota\pi(0.6)}\\0.4e^{\iota\pi(0.1)}\\0.9e^{\iota\pi(0.8)}\\0.7e^{\iota\pi(0.8)}\end{pmatrix}$
T_4	$\begin{pmatrix}0.5e^{\iota\pi(0.6)}\\0.1e^{\iota\pi(0.7)}\\0.8e^{\iota\pi(0.4)}\\0.6e^{\iota\pi(0.6)}\\0.4e^{\iota\pi(0.2)}\end{pmatrix}$	$\begin{pmatrix}0.6e^{\iota\pi(0.8)}\\0.8e^{\iota\pi(0.5)}\\0.5e^{\iota\pi(0.2)}\\0.6e^{\iota\pi(0.1)}\\0.2e^{\iota\pi(0.4)}\end{pmatrix}$	$\begin{pmatrix}0.2e^{\iota\pi(0.9)}\\0.8e^{\iota\pi(0.2)}\\0.7e^{\iota\pi(0.3)}\\0.3e^{\iota\pi(0.2)}\\0.5e^{\iota\pi(0.5)}\end{pmatrix}$	$\begin{pmatrix}0.9e^{\iota\pi(0.4)}\\0.4e^{\iota\pi(0.4)}\\0.8e^{\iota\pi(0.6)}\\0.2e^{\iota\pi(0.9)}\\0.7e^{\iota\pi(0.6)}\end{pmatrix}$	S_4	$\begin{pmatrix}0.4e^{\iota\pi(0.1)}\\0.6e^{\iota\pi(0.5)}\\0.3e^{\iota\pi(0.8)}\\0.7e^{\iota\pi(0.1)}\\0.8e^{\iota\pi(0.8)}\end{pmatrix}$	$\begin{pmatrix}0.6e^{\iota\pi(0.7)}\\0.2e^{\iota\pi(0.1)}\\0.5e^{\iota\pi(0.5)}\\0.1e^{\iota\pi(0.6)}\\0.7e^{\iota\pi(0.7)}\end{pmatrix}$	$\begin{pmatrix}0.2e^{\iota\pi(0.2)}\\0.6e^{\iota\pi(0.9)}\\0.4e^{\iota\pi(0.5)}\\0.7e^{\iota\pi(0.4)}\\0.4e^{\iota\pi(0.1)}\end{pmatrix}$	$\begin{pmatrix}0.5e^{\iota\pi(0.2)}\\0.3e^{\iota\pi(0.9)}\\0.6e^{\iota\pi(0.3)}\\0.5e^{\iota\pi(0.3)}\\0.4e^{\iota\pi(0.7)}\end{pmatrix}$

Table 3. Cotangent similarity scores between class templates/targets (T_1–T_4) and signal samples (S_1–S_4).

Cot SM	S_1	S_2	S_3	S_4
T_1	0.0520	0.0953	0.0462	0.1530
T_2	0.0038	0.0336	0.0031	0.1250
T_3	0.0605	0.0390	0.1257	0.0856
T_4	0.1103	0.2348	0.1542	0.0895

6.7. *Surface visualization*

Three-dimensional surface plots were used to display the distributions of signal and template similarity across surface plots. The peaks, valleys, and global maxima of the multivariate data can be identified using such maps [58].

6.8. *Clustering and dimensionality reduction*

Unsupervised learning techniques were used to employ structural patterns:

- Signals were grouped together in a similar way using K-Means Clustering [59].
- The dimensionality was reduced and visualized using Principal Component Analysis (PCA) [56].

6.9. *Benchmark dataset validation*

The Iris Dataset, a common benchmark dataset in a clustering and classification study, was used to validate the approach [60].

7. Results and discussion

A segmented color map (red, yellow, green, cyan, and blue) is used in Figure 1 to create 2D cotangent similarity-matrix heatmap that shows how well signals ($S_1 - S_4$) correspond with templates ($T_1 - T_4$). Very low similarity is (0.052) indicated by deep red shades, and the gradient color's strength is directly correlated with the alignment's strength. The most plausible mapping is shown by the white highlights on the $T_4 - S_2$ match (0.235), which is the strongest and most decisive in the matrix. Additionally, there is close resemblance between $T_1 - S_4$ (0.153) and $T_4 - S_3$ (0.154), both of which are shown by the color cyan, which denotes a confident connection between the template and the signal. Green colors (less than 0.12–0.13), which are seen in $T_2 - S_4$ (0.125) and $T_3 - S_3$ (0.126), indicate moderate resemblance. All of these suggest the potential, but they are not all definitive matches, thus more research may be required before they can be regarded as strong alignments. Yellow dots ($\sim 0.06 - 0.11$), such as $T_2 - S_2$ (0.095), $T_3 - S_1$

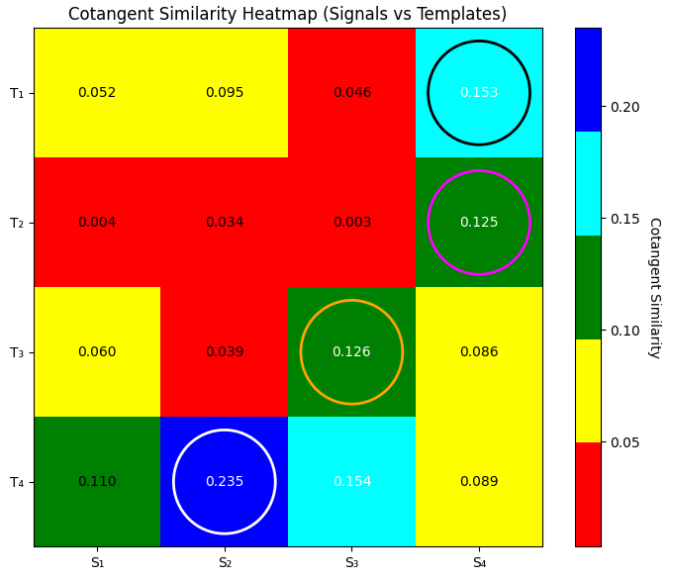

Figure 1. 2D cotangent similarity matrix heatmap.

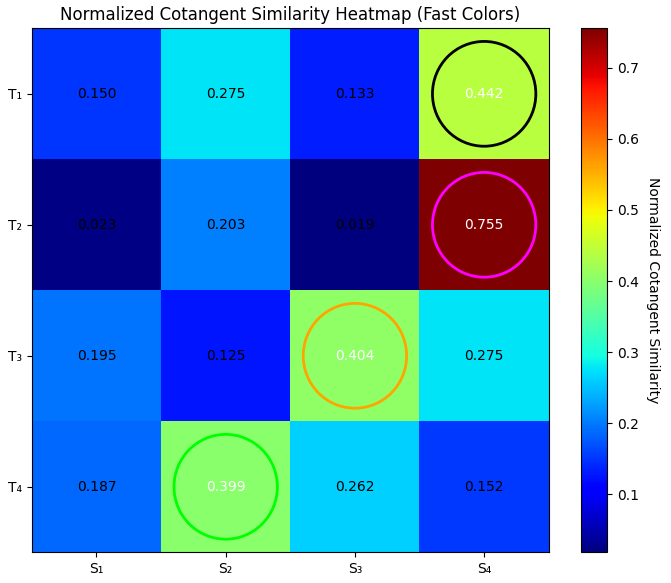

Figure 2. Normalized cotangent similarity heatmap.

(0.060), and $T_4 - S_1$ (0.110), indicate less similarity. A borderline or transitional similarity, with little certainty, is implied by these values. Last but not least, dark red spots, such as those for T_2S_1 (0.004) and T_2S_3 (0.003), indicate very weak matches and suggest a lack of alignment and most likely a failure to categorize. All things considered, the heatmap provides a gradable and intuitive depiction of the classification's dependability based on color intensity. It allows for more thorough analysis of the distribution of signals across weaker and stronger templates, revealing which templates are strong (T_4) and which contribute little to the signal (T_2), as well as instant visual assessment, where the majority of T_4 is immediately apparent.

To display the similarity between signals ($S_1 - S_4$) and templates ($T_1 - T_4$), a normalized cotangent similarity heatmap is created using the fast colormap (blue to cyan to green to yellow to red) of Figure 2. The warmer shades of green, yellow, and red show increasing signs of linkage, whereas deep blue and near-black are thought to have very low similarities (0.01–0.15). The color's intensity is directly correlated with the similarity value. T_2S_4 (0.755), the most conclusive match in the matrix, is highlighted by being ringed in magenta and tinted a saturated red, highlighting the fact that it is the most frequent and legitimate signal template coupling. Additionally, T_1S_4 shows a close relationship (0.442, circled in black, green-yellow in color, confirming a steady and reliable fit). T_4S_2 (0.399, in brilliant green) and T_3S_3 (0.404, in orange) show a moderate resemblance with greenish color (=0.39041). These numbers are useful for classification reliability even though they are less accurate coincidences. Blue hues (cyan and lighter blue) (0.20–0.28), such as T_1S_2 (0.275), T_2S_2 (0.203), and T_3S_1 (0.195), indicate reduced similarity. These suggest borderline or transitional matches that might contribute little to the categorization confidence. Last but not least, deep blue (= 0.02–0.15), T_2S_1 (= 0.023), T_2S_3 (= 0.019), and T_1S_3 (=0.133) represent the least strong alignments. These scores are extremely low, exhibit negligible similarity, and are unlikely to produce any reliable and significant matches. All things considered, this Heatmap makes it possible to quickly and visually identify the most prevalent matches, with T_2S_4 serving as the most evident classification anchor. Secondary but important matches (T_1S_4, T_3S_3, and T_4S_2) add to this structure, whereas the remaining low values show that there isn't much alignment in other pairs. At first glance, strong and weak similarities can be distinguished because to the rapid colormap, which highlights contrast between extremes. Cotangent similarity scores are shown in Figure 3 as grouped bar plots that illustrate how well four signals ($S_1 - S_4$) and four templates ($T_1 - T_4$) match. The template is represented by each color in the color codes (red = T_1, orange = T_2, green = T_3, blue = T_4), and the cotangent similarity score is shown by the height of the bar. The dataset's most notable matches are indicated by magenta ellipses. The highest blue bar, encircled by emphasis, is in $S_2 - T_4$ (0.235), which has the strongest and most conclusive fit. This number is the most reliable and shows that template T_4 best represents signal S_2. Magenta ellipses are used to suggest other potential stable pairs, and secondary strong correspondences between $S_3 - T_4$ (0.154) and $S_4 - T_1$ (0.153) are also observed. Moderate resemblance is seen by the range of bar heights between 0.126 and 0.13 (as in S_3T_2 and S_4T_2). Despite their importance, these matches are not yet definitive and may require verification before being deemed strong. Lower similarity is shown by smaller bar heights (= 0.06–0.11), which include S_1–T_3 (0.060) and S_1–T_4 (0.110). These are ambiguous fits that can be indicative of less stable or transitory fits. The lowest alignments (0.0034) are found for S_2T_2(0.034), T_3 (0.039), and S_3T_2 (0.003). The bar heights are extremely low, nearly matching the baseline. These values display negligible parallels and most likely unworkable categories. Overall, the signal template alignment strength is

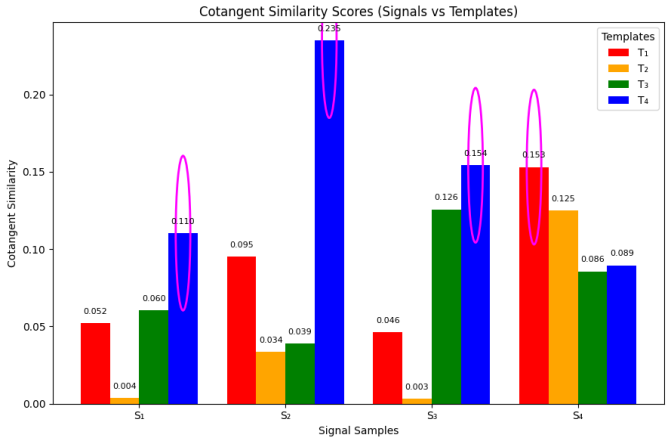

Figure 3. Cotangent similarity scores.

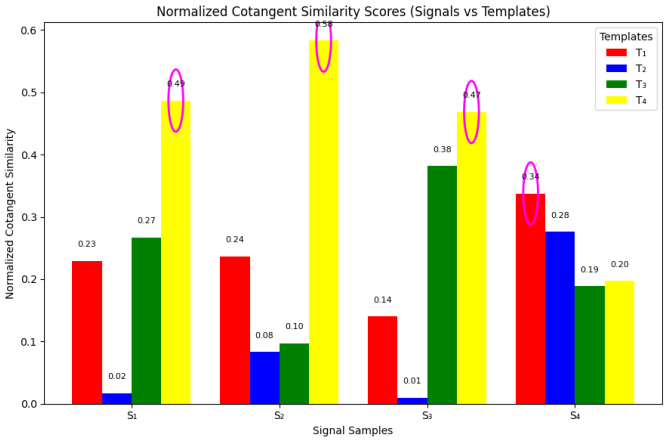

Figure 4. Normalized scores of cotangent similarities.

effectively compared in this bar chart. T_4 is clearly superior, especially when S_2 and S_3 are present, while T_2 consistently performs worse with extremely low scores. In addition to making it possible to quickly identify the top matches, this format can also be used to convey the distribution of weak and average matches in the dataset. The normalized scores of cotangent similarities are shown as grouped bar plots in Figure 4, which shows the alignment between the signals ($S_1 - S_4$) and the templates ($T_1 - T_4$). The height of the bars is proportional to the normalized similarity value, and the colour of the bar corresponds to the corresponding template (red: T_1, blue: T_2, green: T_3, yellow: T_4). The dataset's most significant matches are indicated with magenta ellipses, with the strongest and most decisive match between $S_2 - T_4$ (0.58) as the tallest yellow bar in the graph. The score is clearly dominant in the matrix, indicating that the template T_4 and S_2 have the strongest correlation. Consistent signal-template couplings are indicated by the circles surrounding S_1T_4 (0.49), S_3T_4 (0.47), and S_4T_1 (0.34), which also show some good alignments. Moderate similarity is defined as a value of around 0.27 to 0.38, such as $S_1 - T_3$ (0.27), $S_3 - T_3$ (0.38), and $S_4 - T_2$ (0.28). These are helpful classifications that need to be demonstrated; they are likely but less certain matches. At values of 0.14–0.24, such as $S_2 - T_1$ (0.24) and $S_3 - T_1$ (0.14), there is less resemblance. Poor correspondence, which may contribute only somewhat to the classification's reliability, is shown by the borderline values. S_1T_2 (= 0.02), S_2T_2 (= 0.08), and S_3T_2 (= 0.01) are the signals that have the weakest alignments (= −0.10–0.01) with template T_2. The near-baseline values demonstrate that T_2 has a minor impact on successful categorization and are signs of negligible alignment. With the highest similarity scores across the three signals (S_1, S_2, and S_3), T_4 is the most prevalent template overall, according to this normalized comparison. While templates T_1 and T_3 are moderate matches and occasionally exhibit stronger performance (e.g., S_4T_1, S_3T_3), template T_2 consistently performs below expectations. Normalization highlights T_4's relative primacy and clarifies the other templates' less important responsibilities. The findings of cotangent similarities are displayed in a three-dimensional bar chart (Figure 5) as a template ($T_1 - T_4$) versus signal ($S_1 - S_4$). Each bar's height represents its similarity score, and each template and signal pair's contributions are distinguished using color coding. The top of each bar displays numerical values that aid in precise interpretation. The highest bar on the entire chart represents ($T_4 - S_2$)(0.2348), the most significant and potent match. As was previously demonstrated in the 2D Heatmaps, this is a definite sign that S_2 fits T_4 nicely. significant secondary matches are indicated by a significant peak formed by additional high matches between $T_4 - S_3$ (0.1542) and $T_1 - S_4$ (0.1530). Moderate and comparable scores fall into the range of 0.1103 to 0.1257 (T_4S_1) and 0.1250 to 0.13 (T_2S_4). Although they require confirmation, these intermediate bars show believable but weaker pairings with which classification reliability is added. T_3S_1 (0.0605) and T_3S_4 (0.0856) are examples of the lower similarity that falls within the range of 0.06–0.09. Only in cases when there are no strong alignments can these borderline matches be employed. The worst matches, such as T_2S_1 (0.0038), T_2S_3 (0.0031), and T_3S_2 (0.0390), are at the bottom of the chart with extremely low scores (= 0.00–0.04). These template signal pairs are essentially misclassifications since the near-baseline bars show negligible resemblance. All things considered, this 3D visualization shows that T_4 and S_2 in particular are the most validated templates in the collection. Additionally, it shows that T_4 consistently provides stronger matches across a range of signals in contrast to T_2, which has the worst matching. The 3D format makes the strongest peaks (like $T_4 - S_2$) immediately visible in the topography of signal-template interactions by spatially differentiating relative magnitudes. Normalized cotangent similarity scores are displayed in a bar graph (3D) in Figure 6, where the templates ($T_1 - T_4$) and signals ($S_1 - S_4$) are represented by symbols. Normalized similarity values are shown by bar heights, and distinct templates are indicated by each color-coded group (green, light blue, yellow, and red). To ensure precise reading, some values are printed on the top of the charts. The tallest bar in red, T_1S_2 (1.00), indicates the highest normalized association of the whole collection of data and is the most conclusive match. T_1 is a very representative template of S_2 because this couplet dominates the chart. T_3S_3 (0.65), T_2S_3 (0.54), and

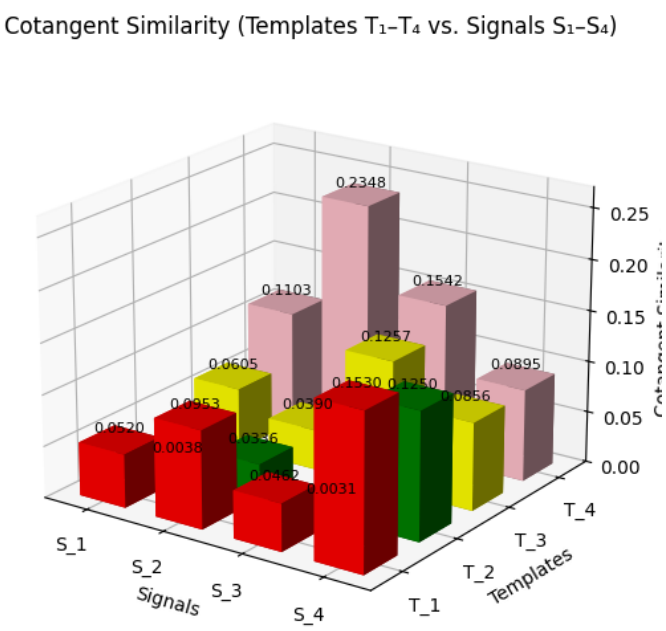

Figure 5. Cotangent similarity.

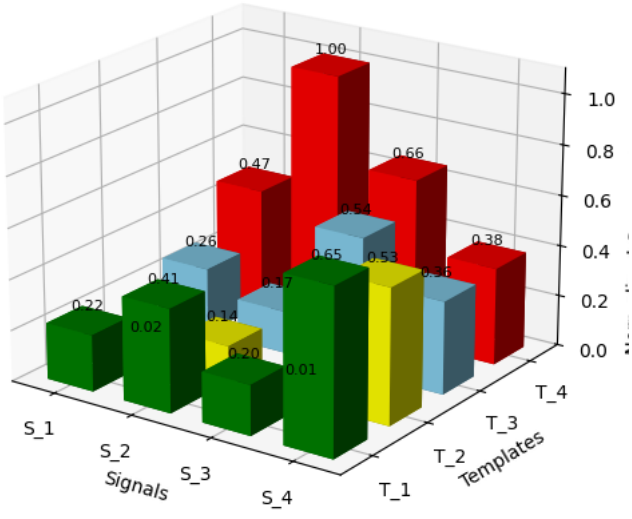

Figure 6. Normalized cotangent similarity scores (3D bar graph).

T_1S_3 (0.47) are secondary strong alignments with high peaks that improve correlations between stable template signals. Values between 0.35 and 0.53, such as T_4S_3 (0.53), T_1S_4 (0.66), and T_4S_4 (0.38), show middle similarity. These can nonetheless offer useful classification information because they show constant but less noticeable correspondences than the most noticeable peaks. T_2S_1 (0.26), T_3S_2 (0.17), and T_3S_1 (0.14) had the least amount of similarities. These numbers represent transitional matches, which provide the template-based classification with less support. Finally, T_2S_2 (0.02), T_3S_4 (0.01), and almost baseline bars have the lowest alignments ($\approx 0.01 - 0.02$). Implicitly non-contributory coincidences, which are unlikely to be helpful in any meaningful classification, are indicated by these negligible values. All things considered, this normalized 3D visualization highlights that T_1S_2 is the most prominent alignment and has a larger dominance in relation to S_2. T_2, T_3, and T_4 have prominent secondary peaks that demonstrate their selective involvement in the remaining signals. The strongest match (like T_1S_2) stands out clearly and explains the small contribution of weakly aligned pairs, while the normalization technique accentuates the relative difference. A correlation heatmap of signals ($S_1 - S_4$) based on cotangent similarity values ranging from -1.0 to 1.0 is shown in Figure 7. Red indicates a strong negative association, yellow indicates a mild link, and green indicates a high positive correlation. The circled cells highlight the most important relationships. The strongest and most definitive self-correlations are the diagonal ones (S_1–S_1, S_2-S_2, S_3-S_3, S_4-S_4), which are all equal to 1.00. As expected, these are encircled and show a perfect match in every signal. There is a strong positive association between S_1S_3 (0.92), S_1S_2 (0.86), and S_2S_3 (0.64). The fact that these values are green-shaded indicates that the signals are highly comparable and that S_1, S_2, and S_3 are all a member of the cohesive cluster of patterns that support one another. Their close correlation is increased by the strength of the S_1S_3 pair (0.92). Yellow indicates weak or moderate correlations (S_2S_4, -0.28). These values suggest a slight or close resemblance and may indicate transitional links between signals that belong to separate groups otherwise. The red-stained cells, like S_3S_4 (-0.79) and S_1S_4 (-0.52), have a very significant negative correlation. Because S_4 has significantly diverse properties and does not belong to the cluster of signals $S_1 - S_3$, these numbers show how opposed S_4 is to the other signals. In conclusion, the heatmap shows a clear structural cluster: S_4 is anti-connected and generally anti-correlated with respect to other signals, while S_1, S_2, and S_3 form a highly correlated positive cluster. In contrast to the strong dependency of the other three signals, this duality suggests that S_4 can be understood as a unique type of signal. Normalized correlation heatmaps of signals ($S_1 - S_4$) based on cotangent similarity are shown in Figure 8. The color scale's darkest and lightest points are orange/yellow (moderate correlation, (0.7–0.8) and cyan/purple (weak or no correlation, (0.0–0.3), respectively (deep red is strongly correlated, around 1.0). Circles highlight significant relationships. As expected, the diagonal elements ($S_1 - S_1$, $S_2 - S_2$, $S_3 - S_3$, $S_4 - S_4$) are surrounded by the colors green, orange, blue, and magenta, respectively, and exhibit a perfect self-correlation of 1.00. These values serve as normalization references. Bright red cells show close connections with S_1T_3 (0.95) and S_1T_2 (0.92). This suggests that there is a narrowing band of signals that support one another since S_1, S_2, and S_3 are highly connected. Similarly, a substantial correlation exists between S_2T_3 (0.80), which is marginally lower than the others and demonstrates the grouping's unity. The S_1S_4 (0.15) and S_2S_4 (0.29) pairs have moderate correlations. The faint but noticeable connections between

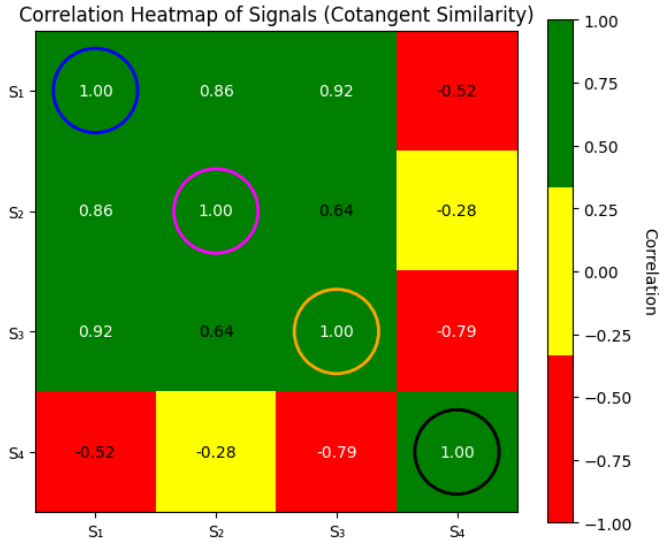

Figure 7. Correlation heatmap.

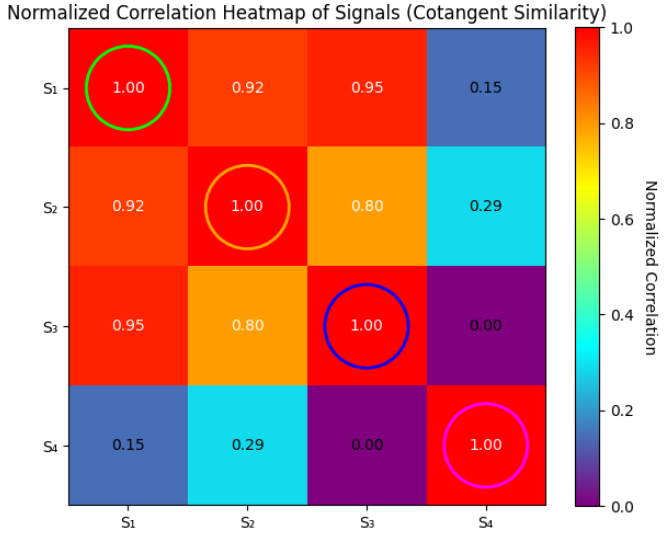

Figure 8. Normalized correlation heatmap.

S_4 and the other cues that these cyan values show may suggest incomplete and inconsistent conformance. $S_3 - S_4$ (0.00), which is deep purple, shows little to no association. According to this result, S_4 is essentially independent of the S_1–S_3 cluster with respect to cotangent similarity. S_4 is nearly alone, with little to no association to the other three, while S_1, S_2, and S_3 are all highly associated (0.80–0.95), as the heatmap illustrates. The normalization, which suggests that S_4 is an independent signal pattern while S_1–S_3 form a coherent group, highlights these contrasts. When comparing templates ($T_1 - T_4$) with signals ($S_1 - S_4$), Figure 9 displays the initial values of cotangent similarity, spline-smoothing functional curves, and cubic interpolants. The original discrete states (open markers), smooth spline curves (solid lines), and cubic interpolant approximations (dashed lines) are the three states in which each template is shown. Direct comparison of the raw similarity values and

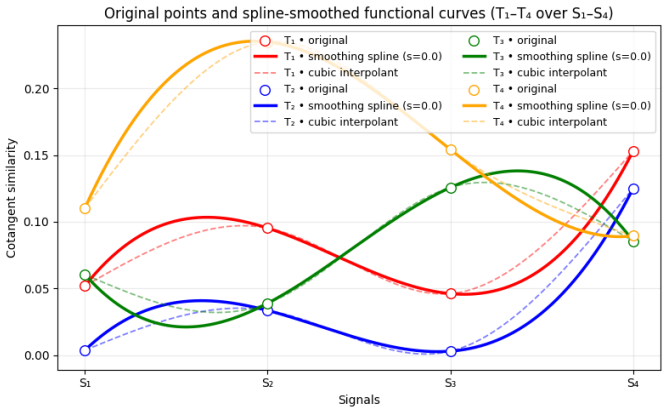

Figure 9. Spline-smoothed functional curves.

observation of functional bottom trends are made possible by this layer-based format. T_4 (orange) exhibits the steepest curve, beginning with a high value at S_1 (= about 0.11), rising abruptly to peak at S_2 (= roughly 0.23), and then falling steadily at S_3 (= roughly 0.15), and S_4 (= roughly 0.09). With consistently high similarity among the signals, this overriding curve indicates that T_4 is the most active template overall. Less grandiose in style, Template T_1 (red) starts with S_1 (0.05), peaks at S_2S_3 (0.10%), dips somewhat at S_3 (0.05), and then returns to S_4 (0.15%). More wave-form indicates different but significant T_1 contributions to the signals. At S_1–S_2 (=0.06–0.04), Template T_3 (green) shows a rising trend with low similarity. At S_3 (=0.13), it rises to a mid-range level, and then falls again at S_4 (=0.09). A selected yet potent portion of T_3 in recognizing similarity surrounding that signal is indicated by this positive slope to S_3. The worst curve is always produced by template T_2 (blue), which starts at S_1 at 0.01 and has little peaks between S_2–S_4 (0.03–0.12). Its weak classification position is demonstrated by the fact that its low amplitude is consistently determined to be low in comparison to the other templates. Generally speaking, the smoothed functional curves exhibit three distinct behaviors:

1. Of all the signals, T_4 is the most dominant and stable.
2. With peaks near S_2 and S_3, respectively, T_1 and T_3 make a selective but secondary contribution.
3. There is little indication of strong signal alignment, and T_2 is continuously weak.

Interpretability is enhanced by smoothing out local changes and emphasizing structural responses through the use of cubic interpolants and smoothing splines, making the strengths of T_4 and the deficiencies of T_2 both statistically and visually evident. The values of the normalized cotangent similarity curves between templates (T_1–T_4) and signals ($S_1 - S_4$) are scaled per template using minmax normalization, as shown in Figure 10. Discrete normalized points (open markers), spline smoothing curves (solid lines), and curves of cubic interpolants (dashed lines) are used to model each template. Better form and trajectory comparisons are made possible by this approach, which displays the trends within templates in a relative way rather than absolute magnitudes. Template T_4 (yellow) has the highest increase, beginning close to S_1 (about 0.15), peaking at S_2 (about

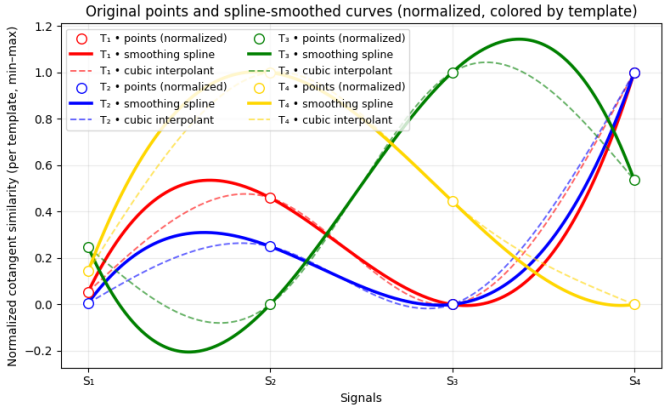

Figure 10. Spline-smoothed functional curves (normalized).

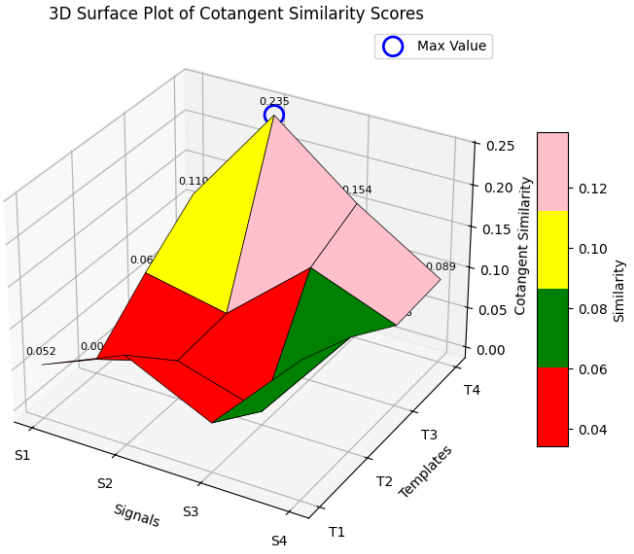

Figure 11. 3D surface plot.

1.0), and then gradually declining throughout S_3 (about 0.45), ending at S_4 (about 0.0). This vertical curve shows that T_4 is the most decisive of that signal since it applies its greatest force in the vicinity of S_2.

With an initial moderate value at S_1 (about 0.25), a value below zero at S_2 (about -0.2), a peak value at S_3 (about 1.15), and a fall to the value at S_4 (about 0.6), Template T_3 (in green) displays a sinusoidal kind of journey. This pattern of alternating indicates that T_3 is significantly associated with S_3 and mildly or even anti-correlated with S_2. A wave-like trajectory is depicted in Template T_1(red): starting low at S_1(0.1), it rises gradually to S_2(0.45), falls to S_3(0.0), and then rises to S_4(0.9). This pattern suggests that T_1 makes a variable and balanced contribution, with S_2 and S_4 receiving the largest contributions. Low to medium values are found throughout Template T_2 (blue): low (nearing zero) at S_1, higher at S_2 (around 0.8), lower near S_3, and highest at S_4 (1.0). It ends with a peak at S_4, indicating particular significance to that region, although it is not intrusive at any of the intermediate signals. Generally speaking, the normalized curves show the existence of particular behavioral characteristics:

1. The most noticeable single alignment at S_2 is T_4, which is also the most dominant.
2. With selective matching, T_3 is strongest at S_3.
3. Although T_1 is notable at S_2 and S_4, its contributions are equal.
4. T_2 has a last peak at S_4 and is often weak.

Relative within-template variation is increased by the normalization process, which also enhances the complimentary features of template involvement in different signals and visually accentuates peaks ($T_4 - S_2$, $T_3 - S_3$) and troughs ($T_3 - S_2$). A surface plot of signals ($S_1 - S_4$) against templates ($T_1 - T_4$) in three dimensions using cotangent similarity scores is shown in Figure 11. Additionally, the surface is color-coded according to the degree of resemblance: poor correlation is shown by red patches (= -0.00–0.06), medium similarity is indicated by yellow and green areas (= -0.06–0.15), and deeper similarity is indicated by pink areas (= -0.15–0.23). The world's maximum is encircled by blue, and the numerical values are indicated at significant spots. The most important match takes place at T_4S_2 (0.235), the surface's highest point and the worldwide maximum. This clearly demonstrates that, in accordance with earlier Heatmaps and bar chart assessments, S_2 would be best represented by T_4. Localized peaks that enhance classification reliability are shown by the second elevations, $T_4 - S_3$ (0.154) and $T_1 - S_4$ (0.153). Yellow-green regions on the surface indicate moderate increases in T_4S_1 (0.110) and T_3S_3 (0.126). In the case that dominant peaks are absent, these alignments which are supporting but less definitive play a significant role. The most important match takes place at T_4S_2 (0.235), the surface's highest point and the worldwide maximum. This clearly demonstrates that, in accordance with earlier Heatmaps and bar chart assessments, S_2 would be best represented by T_4. Localized peaks that enhance classification reliability are shown by the second elevations, $T_4 - S_3$ (0.154) and $T_1 - S_4$ (0.153). Yellow-green regions on the surface indicate moderate increases in T_4S_1 (0.110) and T_3S_3 (0.126). In the case that dominant peaks are absent, these alignments which are supporting but less definitive play a significant role.

In order to illustrate the relative amplitude of the signals ($S_1 - S_4$) and templates ($T_1 - T_4$), Figure 12 displays a surface plot of the normalized cotangent similarity in 3D with vivid colors.

The color map contrasts the magenta/green/yellow (moderate resemblance, 0.3, 0.5) and cyan/blue (highest similarity, 0.55, 1.0) with the reds (low similarity, 0.1, 0.2). The world's maximum has been represented with a blue circle. At T_1S_2 (1.00), the largest point in the whole data set and the tallest cyan peak on the surface, the most conclusive pairing is observed. In contrast to the earlier unaffinity raw similarity graphs where T_4 predominated, this suggests that S_2 will have the highest correlation with T_1 upon normalization. Bright yellow patches at $T_3 - S_3$ (0.652) and $T_1 - S_4$ (0.466) represent secondary peaks. Categorization relationships can be extended outside the dominant peak; there are a few moderate-similarity matches. Mod-

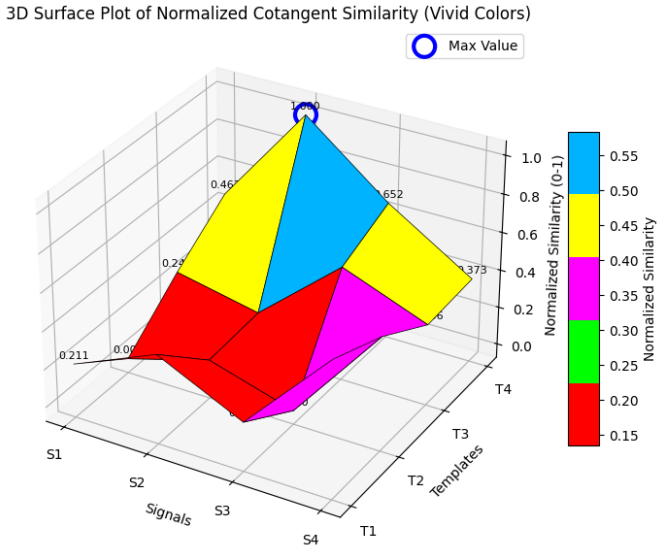

Figure 12. Normalized 3D surface plot.

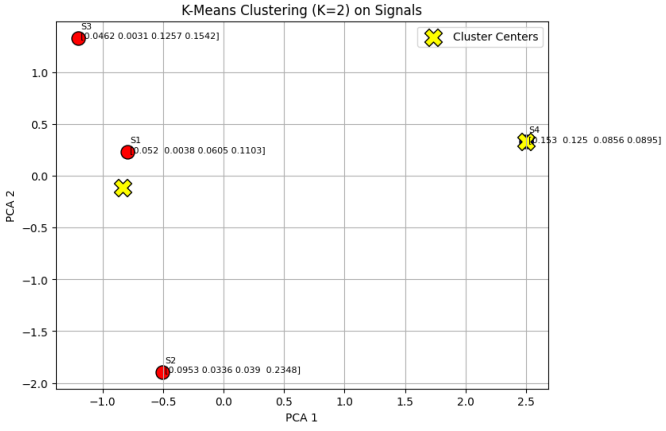

Figure 13. K-means clustering.

erate similarities show as magenta regions at T_4S_4 (0.373) and T_4S_1 (0.211), respectively. These values are very low and show a partial match between the signal and template, but are not as high as the principal peak, and so are secondary matching regions. Although useful, these numbers exhibit some partial coincidence and are not as significant as the dominating peaks. Weak areas predominate on the lower surface, particularly in the vicinity of T_2S_1 (= 0.00) and T_2S_3 (= 0.00), and low similarity is shown by flat depressions in red. This confirms the poor template performance of T_2, which was corroborated by further visualizations. The surface topology demonstrates that the highest peak in raw scores (T_4) is converted to the highest peak in normalized scores (T_1) as a result of the normalizing of template dominance. This demonstrates how scaling can alter how significance is perceived: normalization makes cross-template comparison more balanced while placing greater emphasis on T_1's relative peak, even though T_4 has high absolute scores. Signals $S_1 - S_4$ are shown in two principal component axes (PCA 1 and PCA 2) in a K-means cluster output ($K = 2$) in Figure 13. Each signal is depicted as a red point with yellow X markers denoting the cluster centers and cotangent similarity values to the templates ($T_1 - T_4$). Through the discovery of latent structure in the data, this technique is utilized to group signals according to similarity patterns. The signals are separated into two groups by the clustering process (Cluster 1 (left cluster)) has S_1, S_2, and S_3, but the PCA map shows that these are all more closely clustered. Comparable cotangent similarity profiles are displayed by their coordinates, particularly moderate-to-strong matches with many templates. For instance, S_3 is most connected with T_4 (0.1542) and T_3 (0.1257), while the highest value of S_2 is seen with T_4 (0.2348). This grouping demonstrates how T_3 and T_4 share the $S_1 - S_3$ capture. S_4, which is isolated and aligned with another centroid, is found in Cluster 2 (right cluster). In contrast to the robust T_4-based matches of S_2 and S_3, the similarity distribution (particularly $T_1 = 0.153$, $T_2 = 0.125$, $T_3 = 0.0856$, and $T_4 = 0.0895$) shows a more balanced but weaker profile. S_4 factors this out as functioning independently of the other signals. Centroid positions support this structure: S_4 is characterized by a more flattened distribution (the left centroid), whereas S_1 is less dominating and T_4 dominance is equalized (via S_2 and S_3). This clustering, in summary, suggests that these signals are divided into two groups: $S_1 - S_2 - S_3$-into a coherent cluster that shares a dependency on T_4 / T_3, and S_4-into an independent signal that forms its own cluster. This outcome is in line with earlier correlation heatmaps (Figures 8 and 9), which showed that S_2 had weak or negative associations while S_1, S_3, and S_4 had high positive correlations. Plotting the results of K-Means clustering on the Iris dataset in two-dimensional PCA space (PC1 vs. PC2) is shown in Figure 14. Depending on which cluster it belongs to, each point represents a sample of a flower and is colored differently (blue = cluster 0, orange = cluster 1, green = cluster 2). Additionally, the markers encode the names of the species: Setosa is denoted by circles, Versicolor by crosses, and Virginica by squares. The combination of those representations enables one to compare directly K-Means partitions with biological classes of species. The clustering shows three clusters: Cluster 1 (orange, left), Cluster 0 (blue, right), and Cluster 2 (green, lower-left). This cluster contains nearly all circular markers, demonstrating that K-Means has successfully identified this species' uniqueness. The tiny size of this group indicates that within-cluster similarity is considerable. Virginica and Versicolor dominate Cluster 0 (blue, right group). In this case, crosses and squares mix, indicating that K-Means is not very effective at distinguishing between these two species because their feature distributions overlap. Nonetheless, the cluster illustrates how Setosa differs greatly from the other two species. A smaller split, Cluster 2 (green, lower-left group) has a subgroup of Virginica and maybe confused Versicolor samples. It is believed to be a transitional group that captures edge cases when feature distributions overlap because it is situated between the orange and blue clusters. Overall, the PCA projection demonstrates that Setosa is easily differentiated from the other species and that Versicolor and Virginica share many

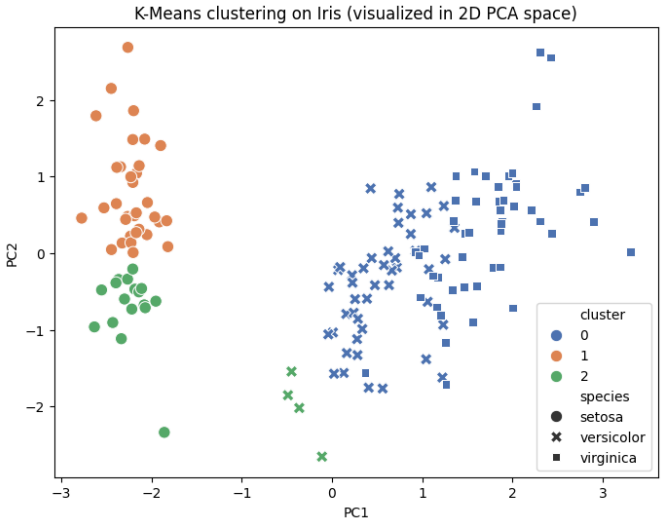

Figure 14. *K*-means clustering on the Iris dataset.

characteristics, which is also in line with the findings found in the Iris dataset. While K-Means successfully isolates Setosa, it only partially separates the other two, demonstrating the advantages and disadvantages of unsupervised clustering on mixed-class data.

8. Aspect-method hybrid analysis of signal-template correlation patterns

By combining aspect-related output with method-related analysis, this section's hybrid model of analysis allows it to provide a thorough explanation of the signal-template interaction. The most significant correspondences are identified by the aspect-based approach, which also assigns varying degrees of similarity strength and identifies which signal-template alignments are most important and which are merely incidental. On the other hand, the method-based analysis illustrates how these relationships are emphasized, normalized, or compared with the several potential viewpoints using a collection of visualization tools, including Heatmaps, bar plots, 3D surfaces, and spline-based curves. When combined, these viewpoints provide a more comprehensive image that combines statistical accuracy with visual clarity, enabling both quantification and interpretation of the analysis.

8.1. Aspect-based analysis

The amount of the data and the way the data is presented using the given readings and visuals allow for two levels of analysis of the correlation/similarity between the four signal samples (S_1–S_4) and the four class templates (T_1–T_4). The most important findings and patterns are highlighted by the aspect-based analysis. As the most definitive mapping that can be accomplished, the most important pairing is the T_4S_2 (0.235; the normalized views always enhance its counterpart peak), which is present throughout. S_4 matches well with T_1 (0.153) and S_3 fits well with T_4 (0.154), indicating that it can be reliably matched out of the primary maximum. This is another secondary but constant pattern. A weak band (= about 0.00–0.06; for example, T_2S_1=0.004, T_2S_3=0.003), a moderate band (= approximately 0.06–0.13; for example, T_1S_2=0.095, T_3S_1=0.060, T_2S_4=0.125, T_3S_3=0.126), and a strong band (= approximately 0.13–0.24; for example, T_4S_2=0.235, T_4S_3=0.154, and T_1S_4=0.153). The categorization importance of weak linkages is negligible, especially when T_2 is involved. Furthermore, inter-signal structure shows that S_4 is widely distributed (weak/negative correlations), while $S_1 - S_3$ is a close-knit cluster. In other words, T_4 (and T_4S in particular) dominance, T_1S_4 and T_4S_3, and T_2's sub par performance are all common.

8.2. Method-based analysis

Each method has its own advantages and disadvantages, and the method-based analysis is a mechanism to examine how these characteristics are visualized. (Figures 1, 2) Heatmaps: Color gradients instantly provide overviews. Global severity (T_4S_2 pop) is shown in Figure 1 (absolute), whereas the most typical template for each signal is highlighted in Figure 2 (row/normalized fast color map). 2D Grouped Bars (Figures 3, 4): These make it possible to precisely compare the severity of toxins side by side. Strong pairings, such $S_2 - T_4$, are highlighted in the normalized chart, which also clarifies the template rankings in raw or normalized signal, like $T_4 - S_2$ in raw and $T_1 - S_2$ in normalized signal. (Figures 5, 6) 3D Bars: Allow peaks (such as $T_4 - S_2$ in raw; $T_1 - S_2$ in normalized signal) to have depth and visual emphasis. Dominant and 3D Surfaces (Figures 11, 12): These provide a topographical picture with identifiable ridges/peaks in raw and a normalized reshaping where the tallest peak is placed on T_1S_2. Topographies can interfere with precise precision. Excellent reading of a complete landscape. Functional and Spline Curves (Figures 9, 10): Where each template performs best is indicated by smooth trends: T_1 achieves its maximum values at S_2 and S_4, T_2 tends to be weaker except for increasing to high levels in S_4, T_4 reaches its highest value at S_2, T_3 at S_3, and T_4 at S_4. They emphasize trends rather than values. *K*-means (Figure 13) and correlation maps (Figures 7, 8): Illuminate the latent structure between signals and confirm the isolation of S_1, S_3, and S_4, which template-centric plots are unable to disclose on their own. The set of visuals' complementary activity in producing a quick reconnaissance map and a more comprehensive comparison analysis is indicated by the combination of an absolute and normalized scale: Splines, surfaces, bars, and Heatmaps.

9. Five-dimensional evaluation of analytical techniques

A five-factor model correlation, visibility, associativity, dynamicity, and scalability is used to assess each technique. Adherence to numerical relations, interpretability, the ability to identify relationships or groups, the capacity to follow changes or trends, and the capacity to extend to greater or denser data are all represented by these dimensions, respectively. When taken as a whole, they offer a fair basis for assessing not only the pattern capture but also its interpretability and usefulness.

Table 4. Factor-based comparison of analytical techniques.

Factors	Heat Map	Grouped Bar	Normalized Bar	3D Plot	Normalized 3D	Surface Plot	Normalized Surface	Spline	Normalized Spline	Correlation Map	K-Means Clustering
Correlation	Strong	Strong	Very Strong	Strong	Very Strong	Strong	Very Strong	Strong	Very Strong	Strong	Strong
Visibility	Strong	Strong	Strong	Strong	Strong	Strong	Strong	Strong	Very Strong	Strong	Strong
Associativity	Medium	Medium	Strong	Strong	Very Strong	Strong	Very Strong	Strong	Very Strong	Very Strong	Very Strong
Dynamicity	Medium	Medium	Strong	Medium	Strong	Strong	Very Strong	Strong	Very Strong	Strong	Strong
Scalability	Medium	Strong	Very Strong	Medium	Very Strong	Very Strong	N/A	N/A	N/A	N/A	N/A

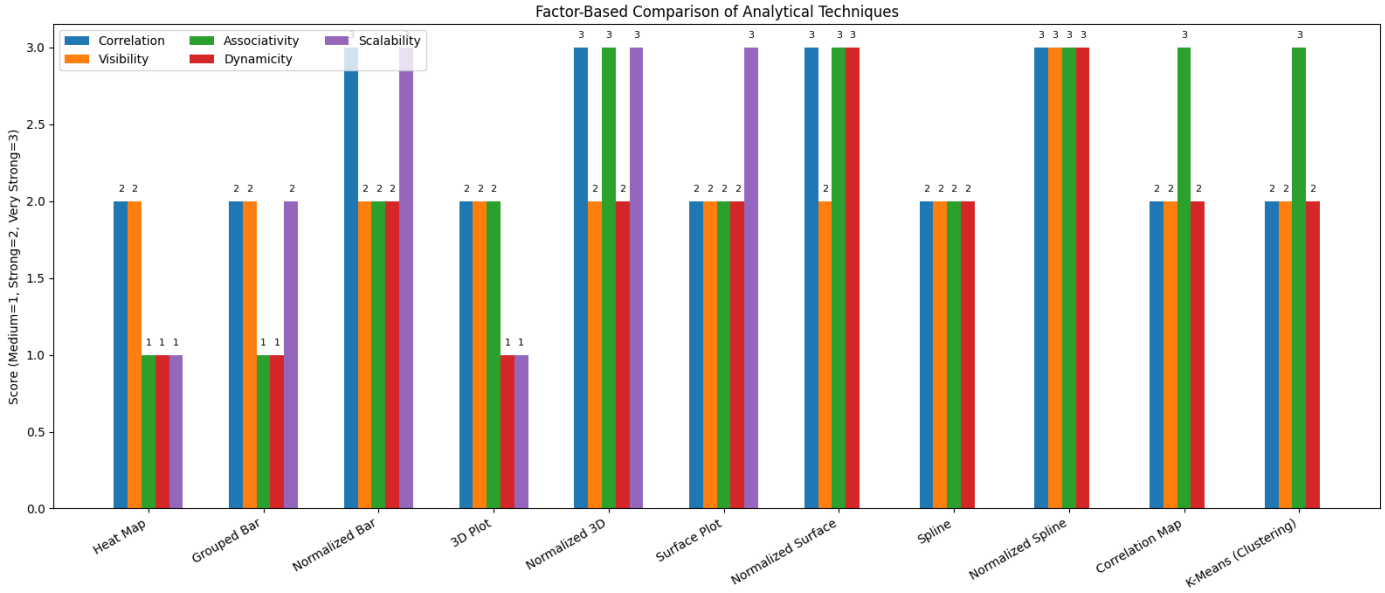

Figure 15. Factor-based comparison of analytical techniques.

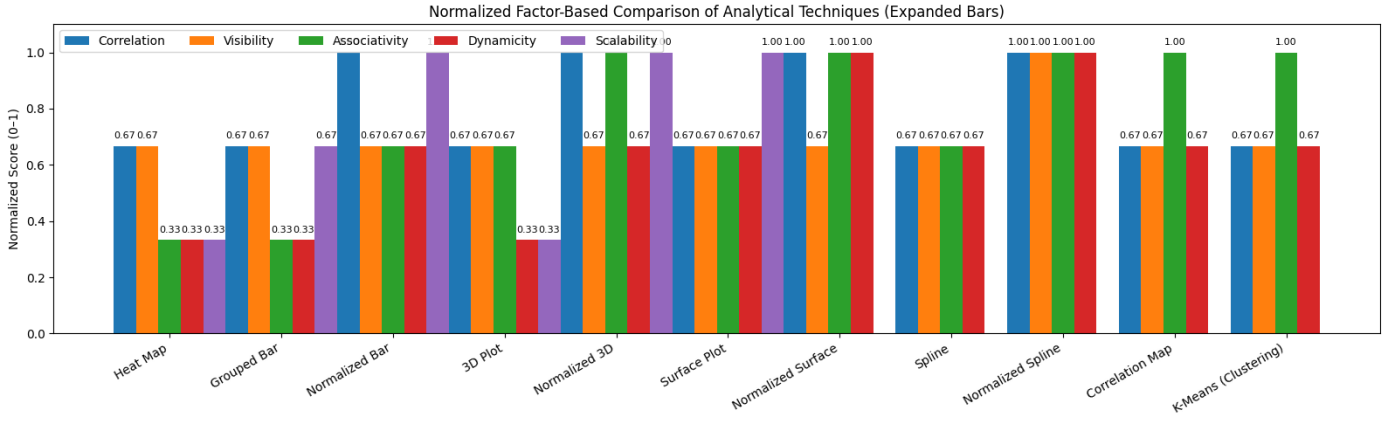

Figure 16. Normalized factor-based comparison of analytical techniques.

10. Conclusion

This work provides a stringent Complex Triple-Valued Neutrosophic Soft Set (CTVNSS) framework and invests the latter with the basic set of operations (union, intersection, complement) and a neutrosophic soft topology (interior/closure) that can collectively yield a stable foundation to the analysis of uncertainty through complex, triple-valued memberships. Combining this base with a Cotangent Similarity Measure (Cot SM) provides a feasible pipeline of signal classification and pattern recognition with hybrid visualization of data (2D Heatmaps, grouped bars, 3D surfaces, spline curves, clustering). Experimentally, Cot SM reveals a prevailing $S_2 - T_4$ interaction, secondary pairing ($S_3 - T_4, S_4 - T_1$), and a uniformly minor position of T_2. Dimensionality reduction and clustering also indicate an intrinsic structure where S_1, S_2, and S_3 compose a coherent group and S_4 is more distinct. Combined, these findings suggest that the suggested topology-conscious, similarity-oriented solution not only measures match strengths but also gives ex-

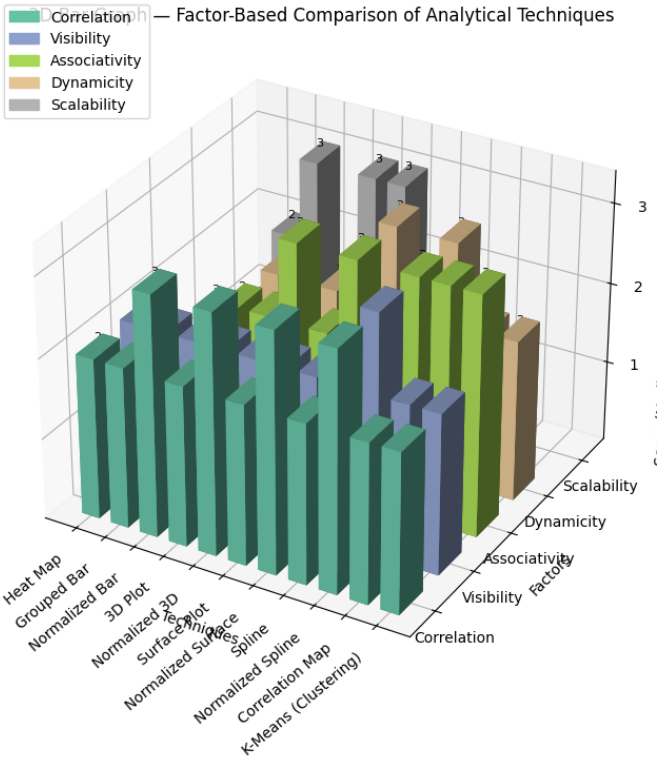

Figure 17. 3D bar graph.

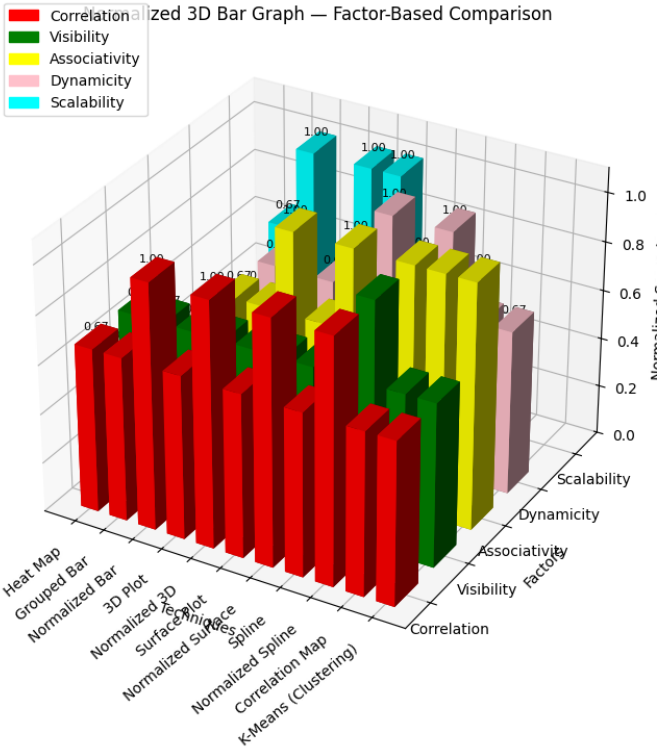

Figure 18. Normalized 3D bar graph.

plicable, multi-view information on reliability of classification.

10.1. Limitations

The study, while providing a rigorous development of operations and topological structures for Complex Triple-Valued Neutrosophic Soft Sets (CTVNS), remains largely theoretical, with limited validation on real-world datasets or practical applications. The signal-template analysis is conducted on a small and controlled dataset consisting of only four signals and four templates, which may not adequately represent the complexity of larger, real-world problems. Furthermore, the analysis relies primarily on the cotangent similarity measure, and the absence of comparisons with alternative similarity or distance metrics may restrict the generalizability of the results. The findings also reveal sensitivity to normalization techniques, as scaling significantly alters template dominance, which may affect consistency and interpretability. In addition, the computational complexity associated with complex-valued triple neutrosophic structures and their associated operations could pose challenges when extending the framework to large-scale datasets. The study does not extensively explore the impact of parameter selection, such as spline smoothing, interpolation methods, or clustering configurations, which may influence the robustness and reproducibility of the results. The use of K-means clustering with a fixed number of clusters may oversimplify the underlying data structure, potentially overlooking more nuanced patterns. Moreover, the reliance on max-min rules for defining neutrosophic components may not fully capture all forms of uncertainty present in complex systems. Finally, although the study employs various visualization techniques for interpretation, it leans more toward qualitative insights rather than comprehensive quantitative validation, and its applicability across diverse domains remains to be empirically established.

10.2. Future work

The results of the construction of Complex Triple Valued Neutrosophic Soft Sets (CTVNS) and the corresponding topological framework (CTVN-STS), together with the application of an AI approach to signal-template analysis, raise several lines of promising research for uncertainty modelling and intelligent decision systems. The algebraic structure of CTVNS could be further extended by considering higher order uncertainty parameters and more generalized neutrosophic representations based on the recent developments in neutrosophic theory, fuzzy systems, topology, fixed point theory, fractional calculus, and soft computing [61-85]. These upgrades would enable the framework to model complex, dynamic, and real-world environments. At the same time, it is necessary to analyze in greater depth the topological characteristics of CTVN-STS, especially continuity, compactness, connectedness, separation axioms. Improving these properties will give a more solid mathematical basis and a greater scope of application of the framework in mathematical analysis and uncertainty-based decision making. In addition, based on recent developments in artificial intelligence and soft computing applications, future research could include the incorporation of AI in signal-template analysis with the CTVNS framework. Such an integration would

allow an adaptive learning-based modeling, in which uncertain signals can be modeled, matched, classified and interpreted by neutrosophic soft topological structures in an efficient manner. Such a hybrid strategy is predicted to be very effective in fields like Biomedical signal processing, pattern recognition, fault diagnosis and communication systems. Besides, the proposed cotangent similarity measure can be further compared with some existing similarity and distance measures in various uncertainty contexts to examine its robustness, sensitivity and computation efficiency. It would be even more relevant if it could be validated on a large scale with complex datasets. Last, but not least, the marriage between machine learning and deep learning techniques with CTVNS is a promising future approach. This integration will facilitate the creation of models for intelligent decision-making that are driven by data and more accurate and interpretable when dealing with high-dimensional and uncertain data. Based on the above, the following directions are suggested for future research on Complex Triple-Valued Neutrosophic Soft Sets and its topological framework for improving its theory and effectiveness in the field of signal-template analysis in artificial intelligence and its applications in the real world.

Acknowledgement

We wish to express our sincere appreciation to the Principal Investigator of our collaborative project, Professor Dr. Arif Mehmood, whose intellectual leadership and visionary guidance were the driving forces behind this work. He consistently motivated, guided, and encouraged us to maintain professionalism and pursue the highest standards, even when the research process became challenging. Without his persistent support and invaluable insights, the successful completion of this project would not have been possible. Currently, he is actively leading a research group comprising 179 researchers, reflecting his remarkable academic leadership and commitment to collaborative research.

Data availability

The dataset used in this study is available upon request to the corresponding author.

Declaration of competing interest

The authors declare that they have no competing interests.

Funding

The authors received no specific funding for this work.

References

[1] L. A. Zadeh, “Fuzzy sets”, Information and Control **8** (1965) 338. https://doi.org/10.1016/S0019-9958(65)90241-X.

[2] I. B. Turksen, “Interval valued fuzzy sets based on normal forms”, Fuzzy Sets Syst. **20** (1986) 191. https://doi.org/10.1016/0165-0114(86)90077-1.

[3] K. Atanassov, “Intuitionistic fuzzy sets”, Fuzzy Sets Syst. **20** (1986) 87. https://doi.org/10.1016/S0165-0114(86)80034-3.

[4] K. Atanassov & G. Gargov, “Interval-valued intuitionistic fuzzy sets”, Fuzzy Sets Syst. **31** (1989) 343. https://doi.org/10.1016/0165-0114(89)90205-4.

[5] F. Smarandache, *A unifying field in logics: Neutrosophy and neutrosophic logic*, American Research Press, Rehoboth, NM, USA, 1998. https://doi.org/10.5281/zenodo.49174.

[6] F. G. Lupianez, “On neutrosophic topology”, Kybernetes **37** (2008) 797. https://doi.org/10.1108/03684920810876990.

[7] H. Wang, F. Smarandache, Y. Zhang & R. Sunderraman, “Single-valued neutrosophic sets”, Multispace & Multistructure. Neutrosophic Transdisciplinarity **4** (2010) 410. Available online: https://fs.unm.edu/SingleValuedNeutrosophicSets.pdf.

[8] H. Wang, F. Smarandache, Y. Q. Zhang & R. Sunderraman, *Interval neutrosophic sets and logic: Theory and applications in computing*, Hexis, Phoenix, AZ, USA, 2005. https://doi.org/10.5281/zenodo.8818.

[9] S. Broumi & F. Smarandache, “Cosine similarity measure of interval valued neutrosophic sets”, Neutrosophic Sets and Systems **5** (2014) 15. https://doi.org/10.6084/M9.FIGSHARE.1502645.

[10] S. Broumi & F. Smarandache, “New distance and similarity measures of interval neutrosophic sets”, 17th International Conference on Information Fusion, Salamanca, Spain, 2014, p. 249. Available online: https://digitalrepository.unm.edu/math_fsp/487.

[11] J. Ye, “Similarity measures between interval neutrosophic sets and their applications in multicriteria decision-making”, J. Intell. Fuzzy Syst. **26** (2014) 165. https://doi.org/10.3233/IFS-120724.

[12] S. Broumi & F. Smarandache, “Correlation coefficient of interval neutrosophic set”, Int. Conf. ICMERA, Bucharest, Romania, 2013. https://doi.org/10.5281/zenodo.48908.

[13] P. Majumdar & S. K. Samanta, “On similarity and entropy of neutrosophic sets”, J. Intell. Fuzzy Syst. **26** (2014) 1245. https://doi.org/10.3233/IFS-130810.

[14] S. M. Chen, “A new approach to handling fuzzy decision making problems”, IEEE Trans. Syst., Man, Cybern. **18** (1988) 1012. https://doi.org/10.1109/21.23100.

[15] S. M. Chen, S. M. Yeh & P. H. Hsiao, “A comparison of similarity measures of fuzzy values”, Fuzzy Sets Syst. **72** (1995) 79. https://doi.org/10.1016/0165-0114(94)00284-E.

[16] D. Molodtsov, “Soft set theory: First results”, Comput. Math. Appl. **37** (1999) 19. https://doi.org/10.1016/S0898-1221(99)00056-5.

[17] H. Aktas & N. Cagman, “Soft sets and soft groups”, Inf. Sci. **177** (2007) 2726. https://doi.org/10.1016/j.ins.2006.12.008.

[18] K. V. Babitha & J. J. Sunil, “Soft set relations and functions”, Comput. Math. Appl. **60** (2010) 1840. https://doi.org/10.1016/j.camwa.2010.07.014.

[19] D. Chen, E. C. C. Tsang & D. S. Yeung, “Some notes on the parameterization reduction of soft sets”, Int. Conf. Mach. Learn. Cybern., 2003, p. 1442. https://doi.org/10.1109/ICMLC.2003.1259720.

[20] D. Chen, E. C. C. Tsang, D. S. Yeung & X. Wang, “The parameterization reduction of soft sets and its applications”, Comput. Math. Appl. **49** (2005) 757. https://doi.org/10.1016/j.camwa.2004.10.036.

[21] N. Cagman & S. Enginoglu, “Soft set theory and uni-int decision making”, Eur. J. Oper. Res. **207** (2010) 848. https://doi.org/10.1016/j.ejor.2010.05.004.

[22] F. Feng, Y. B. Jun, X. Liu & L. Li, “An adjustable approach to fuzzy soft set based decision making”, J. Comput. Appl. Math. **234** (2010) 10. https://doi.org/10.1016/j.cam.2009.11.055.

[23] A. R. Roy & P. K. Maji, “A fuzzy soft set theoretic approach to decision making problems”, J. Comput. Appl. Math. **203** (2007) 412. https://doi.org/10.1016/j.cam.2006.04.008.

[24] K. N. Singh & J. K. Mantri, “A clinical decision support system using rough set theory and machine learning for disease prediction”, Intelligent Medicine **4** (2024) 200. https://doi.org/10.1016/j.imed.2023.08.002.

[25] B. Ahmad & A. Kharal, "On fuzzy soft sets", Adv. Fuzzy Syst. **2009** (2009) 586507. https://doi.org/10.1155/2009/586507.

[26] B. K. Tripathy, R. K. Mohanty & T. R. Sooraj, "On intuitionistic fuzzy soft set and its application in group decision making", Proc. 2016 Int. Conf. Emerging Trends in Engineering, Technology and Science (ICETETS), Pudukkottai, 2016, p. 1. https://doi.org/10.1109/ICETETS.2016.7603002.

[27] P. K. Maji, R. Biswas & A. R. Roy, "Soft set theory", Comput. Math. Appl. **45** (2003) 555. https://doi.org/10.1016/S0898-1221(03)00016-6.

[28] N. Cagman & I. Deli, "Means of FP-soft sets and its applications", Hacet. J. Math. Stat. **41** (2012) 615. Available online: https://dergipark.org.tr/tr/download/article-file/86337.

[29] N. Cagman & I. Deli, "Product of FP-soft sets and its applications", Hacet. J. Math. Stat. **41** (2012) 365.

[30] I. Deli, "Interval-valued neutrosophic soft sets and its decision making", arXiv:1402.3130 (2014). https://doi.org/10.48550/arXiv.1402.3130.

[31] P. Majumdar & S. K. Samanta, "Similarity measure of soft sets", New Math. Nat. Comput. **4** (2008) 1. https://doi.org/10.1142/S1793005708000908.

[32] A. Kharal, "Distance and similarity measures for soft sets", New Math. Nat. Comput. **6** (2010) 321. https://doi.org/10.1142/S1793005710001724.

[33] P. Grzegorzewski, "Distances between intuitionistic fuzzy sets and/or interval-valued fuzzy sets based on the Hausdorff metric", Fuzzy Sets Syst. **148** (2004) 319. https://doi.org/10.1016/j.fss.2003.08.005.

[34] M. Arora, R. Biswas & U. S. Pandy, "Neutrosophic relational database decomposition", Int. J. Adv. Comput. Sci. Appl. **2** (2011) 121. https://doi.org/10.14569/IJACSA.2011.020822.

[35] M. Arora & R. Biswas, "Deployment of neutrosophic technology to retrieve answers for queries posed in natural language", 3rd IEEE Int. Conf. Comput. Sci. Inf. Technol. (ICCSIT), Chengdu, China, 2010, p. 435. https://doi.org/10.1109/ICCSIT.2010.5564125.

[36] S. Aggarwal, R. Biswas & A. Q. Ansari, "Neutrosophic modeling and control", IEEE Int. Conf., 2010, p. 718. https://doi.org/10.1109/ICCCT.2010.5640435.

[37] H. D. Cheng & Y. Guo, "A new neutrosophic approach to image thresholding", New Math. Nat. Comput. **4** (2008) 291. https://doi.org/10.1142/S1793005708001082.

[38] Y. Guo & H. D. Cheng, "New neutrosophic approach to image segmentation", Pattern Recognit. **42** (2009) 587. https://doi.org/10.1016/j.patcog.2008.10.002.

[39] M. Zhang, L. Zhang & H. D. Cheng, "A neutrosophic approach to image segmentation based on watershed method", Signal Process. **90** (2010) 1510. https://doi.org/10.1016/j.sigpro.2009.10.021.

[40] A. Q. Ansari, R. Biswas & S. Aggarwal, "Proposal for applicability of neutrosophic set theory in medical AI", Int. J. Comput. Appl. **27** (2011) 5. https://doi.org/10.5120/3299-4505.

[41] M. I. Ali, F. Feng, X. Liu, W. K. Min & M. Shabir, "On some new operations in soft set theory", Comput. Math. Appl. **57** (2009) 1547. https://doi.org/10.1016/j.camwa.2008.11.009.

[42] M. I. Ali, "A note on soft sets, rough soft sets and fuzzy soft sets", Appl. Soft Comput. **11** (2011) 3329. https://doi.org/10.1016/j.asoc.2011.01.003.

[43] U. Acar, F. Koyuncu & B. Tanay, "Soft sets and soft rings", Comput. Math. Appl. **59** (2010) 3458. https://doi.org/10.1016/j.camwa.2010.03.034.

[44] Y. Jiang, Y. Tang, Q. Chen, H. Liu & J. Tang, "Interval-valued intuitionistic fuzzy soft sets and their properties", Comput. Math. Appl. **60** (2010) 906. https://doi.org/10.1016/j.camwa.2010.05.036.

[45] N. Cagman, "Similarity measures of intuitionistic fuzzy soft sets and their decision making", arXiv:1301.0456 (2013). https://doi.org/10.48550/arXiv.1301.0456.

[46] S. Broumi, "Generalized neutrosophic soft set", Int. J. Comput. Sci., Eng. Inf. Technol. **3** (2013) 17. https://doi.org/10.5121/ijcseit.2013.3202.

[47] S. Broumi & F. Smarandache, "Several similarity measures of neutrosophic sets", Neutrosophic Sets Syst. **1** (2013) 54. Available online: https://digitalrepository.unm.edu/nss_journal/vol1/iss1/10.

[48] T. Bera & N. K. Mahapatra, "Introduction to neutrosophic soft topological space", Opsearch **54** (2017) 841. https://doi.org/10.1007/s12597-017-0308-7.

[49] P. K. Maji, "Neutrosophic soft set", Ann. Fuzzy Math. Inform. **5** (2013) 157. Available online: http://www.afmi.or.kr/papers/2013/Vol-05_No-01/PDF/AFMI-5-1(157-168)-J-111216R1.pdf.

[50] I. Deli & S. Broumi, "Neutrosophic soft relations and some properties", Ann. Fuzzy Math. Inform. **9** (2015) 169. https://doi.org/10.5281/zenodo.23153.

[51] F. Smarandache, *Neutrosophic set - a generalization of the intuitionistic fuzzy set*, 2006 IEEE International Conference on Granular Computing, Atlanta, GA, USA, 2006, p. 38. https://doi.org/10.1109/GRC.2006.1635754.

[52] C. D. Manning, P. Raghavan & H. Schutze, *Introduction to information retrieval*, Cambridge University Press, Cambridge, United Kingdom, 2008. https://doi.org/10.1017/CBO9780511809071.

[53] L. Wilkinson, *The grammar of graphics*, Springer, New York, NY, USA, 2005. https://doi.org/10.1007/0-387-28695-0.

[54] J. Han, M. Kamber & J. Pei, *Data mining: Concepts and techniques*, 3rd ed., Elsevier, Amsterdam, Netherlands, 2011. https://doi.org/10.1016/C2009-0-61819-5.

[55] E. R. Tufte, *The visual display of quantitative information*, Graphics Press, Cheshire, CT, USA, 2001.

[56] K. Pearson, "On lines and planes of closest fit to systems of points in space", Philosophical Magazine **2** (1901) 559. https://doi.org/10.1080/14786440109462720.

[57] C. de Boor, *A practical guide to splines*, Springer, New York, NY, USA, 1978. https://doi.org/10.2307/2006241.

[58] MathWorks, "MATLAB documentation", The MathWorks, Inc., Natick, MA, USA. Accessed 20 June 2026. Available online: https://www.mathworks.com/help/matlab/.

[59] S. Lloyd, "Least squares quantization in PCM", IEEE Transactions on Information Theory **28** (1982) 129. https://doi.org/10.1109/TIT.1982.1056489.

[60] R. A. Fisher, "The use of multiple measurements in taxonomic problems", Annals of Eugenics **7** (1936) 179. https://doi.org/10.1111/j.1469-1809.1936.tb02137.x.

[61] M. M. Saeed, R. Hatamleh, A. M. Abd El-latif, A. Alhusban, H. M. Attaalfadeel, T. Fujita, K. A. Aldwoah & A. Mehmood, "A breakthrough approach to quadri-partitioned neutrosophic soft topological spaces", Eur. J. Pure Appl. Math. **18** (2025) 5845. https://doi.org/10.29020/nybg.ejpam.v18i2.5845.

[62] A. A. Abubaker, R. Hatamleh, K. Matarneh & A. Al-Husban, "On the numerical solutions for some neutrosophic singular boundary value problems by using (LPM) polynomials", International Journal of Neutrosophic Science **25** (2024) 197. https://doi.org/10.54216/IJNS.250217.

[63] A. A. Abubaker, R. Hatamleh, K. Matarneh & A. Al-Husban, "On the irreversible k-threshold conversion number for some graph products and neutrosophic graphs", International Journal of Neutrosophic Science **25** (2025) 183. https://doi.org/10.54216/IJNS.250216.

[64] R. Hatamleh, A. Al-Husban, K. Sundareswari, G. Balaj & M. Palanikumar, "Complex tangent trigonometric approach applied to (γ, τ)-rung fuzzy set using weighted averaging, geometric operators and its extension", Communications on Applied Nonlinear Analysis **32** (2025) 133. https://doi.org/10.52783/cana.v32.2978.

[65] R. Hatamleh & A. Hazaymeh, "On some topological spaces based on symbolic n-plithogenic intervals", International Journal of Neutrosophic Science **25** (2025) 23. https://doi.org/10.54216/IJNS.250102.

[66] H. Qawaqneh, "Fractional analytic solutions and fixed point results with some applications", Advances in Fixed Point Theory **14** (2024) 1. https://doi.org/10.28919/afpt/8279.

[67] H. Qawaqneh, M. S. Noorani, W. Shatanawi & H. Aydi, "On fixed point results in partial b-metric spaces", Journal of Function Spaces **2021** (2021) 8769190. https://doi.org/10.1155/2021/8769190.

[68] H. Qawaqneh, M. S. Noorani & H. Aydi, "Some new characterizations and results for fuzzy contractions in fuzzy b-metric spaces and applications", AIMS Mathematics **8** (2023) 6682. https://doi.org/10.3934/math.2023338.

[69] H. Qawaqneh, J. Manafian, M. Alharthi & Y. Alrashedi, "Stability analysis, modulation instability, and beta-time fractional exact soliton solutions to the van der Waals equation", Mathematics **12** (2024) 2257. https://doi.org/10.3390/math12142257.

[70] M. Elbes, A. Alkhateeb, T. Kanan, A. Al-Momani & M. Alia, "COVID-19 detection platform from X-ray images using deep learning", International Journal of Advances in Soft Computing and its Applications **14** (2022)

197. https://doi.org/10.15849/IJASCA.220328.13.

[71] T. Kanan, M. Elbes, K. Abu Maria & M. Alia, "Exploring the potential of IoT-based learning environments in education", International Journal of Advances in Soft Computing and its Applications **15** (2023) 167. https://www.i-csrs.org/Volumes/ijasca/IJASCA.230720.11.pdf.

[72] I. M. Batiha, S. A. Njadat, R. M. Batyha, A. Zraiqat, A. Dababneh & S. Momani, "Design fractional-order PID controllers for single-joint robot arm model", International Journal of Advances in Soft Computing and its Applications **14** (2022) 96. https://doi.org/10.15849/IJASCA.220720.07.

[73] A. M. Abd El-latif & M. H. Alqahtani, "Novel categories of supra soft continuous maps via new soft operators", AIMS Mathematics **9** (2024) 7449. https://doi.org/10.3934/math.2024361.

[74] A. M. Abd El-latif, M. H. Alqahtani & F. A. Gharib, "Strictly wider class of soft sets via supra soft δ-closure operator", International Journal of Analysis and Applications **22** (2024) 47. https://doi.org/10.28924/2291-8639-22-2024-47.

[75] A. Al-Omari & M. H. Alqahtani, "Some operators in soft primal spaces", AIMS Mathematics **9** (2024) 10756. https://doi.org/10.3934/math.2024525.

[76] A. M. Abd El-latif, A. A. Azzam, A. Al-Omari & M. H. Alqahtani, "New versions of maps and connected spaces via supra soft sd-operators", PLOS ONE **19** (2024) e0304042. https://doi.org/10.1371/journal.pone.0304042.

[77] A. M. Abd El-latif, A. Al-Omari & M. H. Alqahtani, "Applications on soft somewhere dense sets", Journal of Interdisciplinary Mathematics **27** (2024) 1679. https://doi.org/10.47974/JIM-2007.

[78] M. H. Alqahtani, "Neutrosophic primal structure with closure and proximity operators", AIMS Mathematics **11** (2026) 644. https://doi.org/10.3934/math.2026028.

[79] M. H. Alqahtani, "Operators and separation axioms within the framework of diving topological spaces", AIMS Mathematics **10** (2025) 25253. https://doi.org/10.3934/math.20251118.

[80] I. Ibedou, S. E. Abbas & M. H. Alqahtani, "Defining new structures on a universal set: Diving structures and floating structures", Mathematics **13** (2025) 1859. https://doi.org/10.3390/math13111859.

[81] M. H. Alqahtani & M. Tkachenko, "Normality and N-factorizable topological groups", Topology and its Applications **373** (2025) 109497. https://doi.org/10.1016/j.topol.2025.109497.

[82] S. A. El-Sheikh & A. M. Abd El-latif, "Decompositions of some types of supra soft sets and soft continuity", International Journal of Mathematics Trends and Technology **9** (2014) 37. https://doi.org/10.14445/22315373/IJMTT-V9P504.

[83] A. M. Abd El-latif, "Specific types of Lindelöfness and compactness based on novel supra soft operator", AIMS Mathematics **10** (2025) 8144. https://doi.org/10.3934/math.2025374.

[84] A. M. Abd El-latif & M. H. Alqahtani, "New soft operators related to supra soft δ_i-open sets and applications", AIMS Mathematics **9** (2024) 3076. https://doi.org/10.3934/math.2024150.

[85] M. H. Alqahtani & A. M. Abd El-latif, "Separation axioms via novel operators in topological spaces and applications", AIMS Mathematics **9** (2024) 14213. https://doi.org/10.3934/math.2024690.